Università Degli Studi Di Napoli
Federico II

Scuola Politecnica e delle Scienze di Base
Area Didattica di Scienze Matematiche Fisiche e Naturali
Corso di Dottorato in Matematica e Applicazioni
XXXV Ciclo

PhD thesis by
Jacopo Alfonso Gianfrani

Convection problems in porous media: the effect of vertical throughflow and local thermal nonequilibrium

Contents

Introduction

The phenomenon of thermal convection in a fluid saturating a porous medium has been widely studied throughout last decades by many researchers because of several applications in geophysical and engineering context. Most important applications can be found in geothermal energy utilization, underground contaminant transport, nuclear waste disposal, heat exchangers, thermal insulation and, more in general, in problems on removal and storage of heat [1].

By porous medium we intend a material composed by a rigid solid matrix with interconnected empty spaces (pores) through which the fluid flows. At microscopic scale, because of the random pores' distribution and dimension, the flow quantities (velocity, pressure...) are strongly irregular. On the other hand, at macroscopic scale, these quantities become regular functions in space and time. Therefore, a macroscopic approach seems to be more convenient. In this respect, we will employ the Continuum Mechanics approach. According to this approach, the fluid along with the solid is defined as a continuum whose properties are defined as appropriate means over a volume, called representative elementary volume, such that it is sufficiently large to include a significant number of pores and considerably smaller than the macroscopic flow domain.

Thermal convection problems usually involve a horizontal porous layer saturated by an incompressible fluid at rest and uniformly heated from below. A uniform temperature gradient is imposed and maintained constant across the layer. Hence, let $S = \mathbb{R}^2 \times [0, d]$ be the porous layer confined between the planes $z = 0$ and $z = d$, and let T_L and T_U be the temperatures on the lower and upper plane, respectively. When the fluid is at rest, heat spreads by conduction, i.e. without involving the motion of matter. Because of heating from below, particles that are close to the lower hotter plane expand and get lighter. Their density decreases and the volume increases, so the module of the buoyancy force of Archimede grows and these particles are pushed upward. But, the buoyancy force is initially balanced by viscosity of the fluid and the gravitational force. Consequently, the fluid keeps staying at rest and heat spreads by conduction. Nevertheless, this situation is potentially unstable because of the mean temperature gradient $\beta = \frac{T_L - T_U}{d}$. Once β overcomes a critical value, the force of Archimede wins over the opposite forces, the fluid motion begins and thermal convection occurs. Experiments show that,

as soon as convection takes place, fluid organises himself in cells, called convective cells, that are repeated periodically within the layer. Most importantly, the fluid motion is the same in each cell. As a result, from a mathematical point of view, it will be sufficient to analyse the fluid motion within a single cell.

If the regime where the fluid is motionless and heat propagates by conduction is defined as basic steady solution, then the onset of convection is referred to as the moment when the basic solution becomes unstable. A mathematical analysis suggests that the onset of instability is related to a dimensionless number, called Rayleigh number R. This number gives a measure of the destabilising effect of the buoyancy over the stabilising effect of molecular diffusion of momentum. Then, particularly, thermal convection occurs once the Rayleigh number overcomes a critical value. Hence, the aim is to determine the critical threshold of the Rayleigh number beyond which instability occurs. Specifically, the study of thermal convection problems is devoted to determine necessary and sufficient conditions ensuring the stability of the basic steady solution. To this aim, linear and nonlinear stability analyses are performed. Nonlinear analysis provides a sufficient condition for the stability of the basic solution, while linear analysis provides a sufficient condition for instability to occur. The optimal result that one can get is the coincidence between the critical threshold R_L for the linear instability and the critical threshold R_E for the nonlinear stability. Of course, this result is not granted and trivial. The main limitation of the linear analysis is that it provides only information about the fate of small perturbations to the basic state. Small-amplitude disturbances will grow in time when $R > R_L$, while they decay when $R < R_L$. But this does not necessarily mean that before the critical threshold there is no other configuration, other than the basic state, where the amplitude of a generic disturbance grows in time. When the coincidence between results from linear and nonlinear analyses is obtained, we are sure that $R < R_E = R_L$ is a necessary and sufficient condition for the stability of the basic steady solution. Otherwise, a so-called subcritical instability region exists, where we do not know what the fate of a perturbation is.

The first to study a thermal convection problem in porous media were Horton and Rogers [2], followed independently by Lapwood [3]. In their papers, in order to describe the fluid motion in presence of the porous medium, they considered the model proposed by the engineer Henry Darcy in 1856. Experiments led on the water supply in the Dijon fountain brought Darcy to formulate the following relationship of proportionality between the gradient of pressure p and the so-called seepage velocity $\mathbf{v}$, namely the fluid velocity in presence of a porous medium:

$$\mathbf{v} = -\frac{K}{\mu}\nabla p \tag{1}$$

where K is the permeability of the medium and depends only on its geometry, while μ is the dynamic viscosity of the fluid. Let us remark that in (1) body forces, such as gravity, are neglected. In this thesis problems, gravity acts on the layer, so (1)

will become:

$$\frac{\mu}{K}\mathbf{v} = -\nabla p + \rho_f \mathbf{g} \tag{2}$$

where ρ_f is the fluid density and $\mathbf{g}$ the gravity acceleration. Moreover, in chapters 5 and 7, the following extension of (2) will be employed:

$$\rho_f c_\alpha \frac{\partial \mathbf{v}}{\partial t} = -\nabla p - \frac{\mu}{K}\mathbf{v} + \rho_f \mathbf{g} \tag{3}$$

where c_α is the acceleration coefficient.

In 1947, Brinkman proposed an alternative to the Darcy's law, for cases where the medium porosity is high. Mathematically, porosity ε is defined as the ratio between the volume occupied by the empty space and the total volume of the medium. Hence, for the Brinkman's law to hold, one needs $\varepsilon > 0.6$. According to this law, the constitutive equation is

$$\nabla p = -\frac{\mu}{K}\mathbf{v} + \tilde{\mu}\Delta \mathbf{v} \tag{4}$$

where $\tilde{\mu}$ is the effective viscosity, different from the dynamic viscosity μ. The introduction of the effective viscosity $\tilde{\mu}$ leads to completely different results in terms of the onset of thermal convection. An illuminating analysis in this respect has been carried out by Rees in 2002 [4].

So far, we have described only equations to model the fluid motion in porous media. To make a step towards the modelling of thermal convection problems studied in the thesis, we need to add an equation both for the conservation of mass and for the conservation of energy. The former reduces to

$$\nabla \cdot \mathbf{v} = 0 \tag{5}$$

because of the hypothesis of incompressible fluid, which will be employed in each problem tackled in the thesis. While, defined T as the temperature of both fluid and solid phases, the energy balance equation is

$$(\rho c)_m \frac{\partial T}{\partial t} + (\rho c)_f \mathbf{v} \cdot \nabla T = k_m \Delta T \tag{6}$$

with

$$\begin{aligned} (\rho c)_m &= (1-\varepsilon)(\rho c)_s + \varepsilon(\rho c_p)_f \\ k_m &= (1-\varepsilon)k_s + \varepsilon k_f \end{aligned} \tag{7}$$

where ρ_i is the density, c_i the specific heat, k_i the thermal conductivity, for $i = f, s, m$. Subscripts f, s and m refer to fluid, solid and medium, respectively, while $(\rho c)_m$ and k_m are the overall heat capacity and the overall thermal conductivity per unit volume of the medium, respectively. The assumptions that bring to formulate Eq. (6) are the following:

- the medium is isotropic
- heat conduction in solid and fluid takes place in parallel
- there is no net heat flux from one phase to the other, i.e. the phases are in Local Thermal Equilibrium (LTE) (i.e. $T_f = T_s = T$)

Eq. (6) represents the first law of thermodynamics, which states, under appropriate restrictions of small deformations, that the variation of internal energy of a thermodynamic system is the sum of two contributions: internal heat sources and heat flux across the boundary. Hence,

$$\frac{dE}{dt} = Q_1 + Q_2 \tag{8}$$

where

$$\begin{aligned} E &= \int_C \rho c_p T \, dC \qquad \text{internal energy} \\ Q_1 &= \int_C q' \, dC \qquad \text{heat source} \\ Q_2 &= \int_{\partial C} \mathbf{q} \cdot \mathbf{n} \, d\sigma \qquad \text{flux across the boundary} \end{aligned} \tag{9}$$

where $\mathbf{q}$ is the heat flux and $\mathbf{n}$ is the outward normal versor to the surface ∂C. Specifically, Eq. (6) is obtained by neglecting heat source term (i.e. $Q_1 = 0$) and by assuming that the expression for the heat flux $\mathbf{q}$ is given by the Fourier's law, i.e.

$$\mathbf{q} = -k_m \nabla T \tag{10}$$

We refer to the problem modelled by Eqs. (2)-(5)-(6) as the Darcy-Bénard convection problem (or equivalently the Horton-Rogers-Lapwood problem). This problem involves impermeable planes delimiting the porous layer and deals with the stability of the steady conduction solution for which the fluid is at rest. On the other hand, if those planes are permeable, under appropriate boundary conditions, this problem admits a steady solution where the fluid moves with constant vertical velocity Q. This motion is usually caused by a suction from the external of the layer, which then leads to a net mass flow across the layer (throughflow). In this respect, we are going to investigate the type of instability occurring in a horizontal fluid-saturated porous layer uniformly heated from below and subject to a downward vertical throughflow. The strength of the flow in the dimensionless problem is modelled by the Péclet number

$$\mathrm{Pe} = \frac{Qd}{\kappa} \tag{11}$$

where d is the depth of the layer and κ is the thermal diffusivity. When Pe is large, the effect of the throughflow is to confine a significant thermal gradient in a boundary layer close to the boundary towards which the throughflow is directed.

Hence, the layer becomes isothermal almost everywhere except for in the boundary layer whose thickness will be of order Pe^{-1}. As consequence, the characteristic length will be the thickness of the boundary layer rather than the depth of the porous layer and the rescaled Rayleigh number will be smaller. Thus, the effect of a large throughflow is stabilising. Hence, in the large-Pe limit, the layer appears to mimic a region of infinite height and the problem becomes independent on the upper boundary conditions. In this limit, we recover the problem studied by Wooding in 1960 [5], who was the first to study the stability of a vertical throughflow in a porous medium. Later, Sutton in 1970 [6] studied the effect of throughflow with finite Péclet number in a finite box and provided the variation of the Rayleigh number with respect to the aspect ratio of the box. The analysis we performed was motivated by the comparison between results obtained in [5] and the ones obtained in the Darcy-Bénard problem. It is well known that in the Darcy-Bénard problem subcritical instabilities are not possible. On the other hand, in [5] it has been proved that subcritical instability may occur. Hence, we considered a problem with a finite Péclet number, which approximates both the Darcy problem and the Wooding problem in the limit cases, and decided to investigate for which value of Pe the transition from supercritical to subcritical instability happens.

The assumption of LTE works very well in many physical situations, and in particular in geophysical problems since usually, for that kind of problems, fluid and rocks are involved and their thermal conductivities are pretty similar. Nevertheless, there exist many practical industrial situations where LTE is not properly realistic. Specifically, once the fluid velocity is sufficiently high, or as long as the solid thermal conductivity is much different from the fluid one, the assumption of LTE is no longer suitable to describe the physical phenomenon [7]. Applications are numerous and can be found in processes involving quick heat transfer [8], metal foams and in everyday technology such as microwave heating [9], heat exchangers [10] and tube refrigerators (see [11] for more details). As a result, the hypothesis of Local Thermal Non Equilibrium (LTNE) is employed to obtain more accurate results. This assumption involves two different temperatures (one for the solid, one for the fluid) so as to take into account heat exchanges between the phases. Hence, let T_f be the fluid temperature and T_s the solid one, such that $T_f \neq T_s$. Two energy balance equations are needed:

$$\begin{aligned} (\rho c)_f \left[\varepsilon \frac{\partial T_f}{\partial t} + \mathbf{v} \cdot \nabla T_f \right] &= \varepsilon k_f \Delta T_f + h(T_s - T_f) \\ (1-\varepsilon)(\rho c)_s \frac{\partial T_s}{\partial t} &= (1-\varepsilon) k_s \Delta T_s - h(T_s - T_f) \end{aligned} \tag{12}$$

where h is interfacial convective heat transfer coefficient. The problem of thermal convection in porous media in LTNE has been widely studied over the last years, starting from [12, 13]. In [12], a linear analysis to determine the critical Rayleigh

number and an asymptotic analysis to study the case of $h \to \infty$ are performed. In [13], instead, a nonlinear analysis is performed to show the coincidence between the global nonlinear critical threshold and the linear one. Many authors studied the LTNE effect in rotating and/or anisotropic porous media [14, 15, 16, 17, 18], or when the porous medium is subject to a vertical throughflow [19, 20], and also in non-horizontal porous layer [21, 22, 23, 24, 25].

What would change if we relaxed the hypothesis of isotropic medium? In nature, real porous media are inevitably anisotropic at some scale. In some cases, the anisotropy is noticeable only at microscopic scale, in some others it is visible at macroscopic scale and it can affect significantly the fluid motion. Permeability is the characteristic of a porous medium to be permeated by a fluid. Low permeability would imply that the fluid struggles to permeate the porous medium. Such a characteristic may vary depending on the direction. It may be greater in some directions than in others. That is the case of sedimentary porous rocks, which exhibit a higher permeability in the horizontal direction than in the vertical one, because of their layered configuration [26]. Moreover, in industrial field, many porous media are usually man-made so that they exhibit anisotropy not only in their mechanical features, such as permeability, but also in thermal ones, such as thermal conductivity. This is because these characteristics may be tuned in order to suppress or promote the fluid motion and heat propagation across the medium [27, 28, 29, 30, 31, 32]. Mathematically, when permeability is anisotropic, we need to generalise the Darcy Eq. (1) in the following way:

$$\mu \mathbf{v} = -\mathcal{K} \cdot \nabla p \tag{13}$$

where $\mathcal{K}$ is the permeability tensor, which is required to be invertible. On the other hand, we need to generalise also the Fourier's law (10) as long as thermal conductivity is anisotropic. Coefficient k_m will be replaced by an invertible tensor. In the following, anisotropy tensors will be diagonal and we refer to horizontal isotropy (or light anisotropy) when values do not change on the horizontal plane; to full anisotropy when values change depending on the three directions. Castinel and Combarnous were the first to study the onset of convection in a porous layer with anisotropic permeability in 1975 [33], followed by Epherre [34] in 1975, who allowed for thermal conductivity to be anisotropic as well. In 1979, Kvernold and Tyvand [35] extended these analyses by considering full anisotropic permeability and thermal conductivity.

As far as the temperature propagation is concerned, so far we have employed the constitutive Fourier's law (10) both in (6) and in (12). The classical theory of heat propagation is based on Eq. (10) which has been widely employed over the years to model heat transport. By assuming that heat propagates by conduction in (6), namely fluid is at rest ($\mathbf{v} = \mathbf{0}$), we get a parabolic differential equation

$$(\rho c)_m \frac{\partial T}{\partial t} = k_m \Delta T \tag{14}$$

Looking at the solution of Eq. (14) an unpleasant behaviour arises: the so-called "Fourier Heat Paradox". According to this paradox, a disturbance in temperature in a bounded domain is felt instantly in the whole domain, namely heat spreads with infinite velocity. In order to overcome this paradox, in 1948, Cattaneo proposed the following alternative equation [36]:

$$\tau \frac{\partial \mathbf{q}}{\partial t} + \mathbf{q} = -k\nabla T \tag{15}$$

where τ is the time lag required to establish steady heat conduction in a volume element once a temperature gradient has been imposed across it. By employing law (15), one gets the following hyperbolic heat equation:

$$\tau \frac{\partial^2 T}{\partial t^2} + \frac{\partial T}{\partial t} = \frac{k_m}{(\rho c)_m} \Delta T \tag{16}$$

for which heat propagates with finite velocity $c^2 = \frac{k_m}{(\rho c)_m \tau}$. As a result, the concept of heat waves is introduced [37]. The phenomenon of heat propagation by a wave-like motion is called “second sound“, recalling the propagation of pressure waves in air (sound), and it becomes relevant once microscopic dimensions are taken into account. That is why the second sound mechanism is considered in many application fields, such as in modern technology, where much small devices (metallic-like solids) are involved. According to Pilgrim [38], the “hyperbolic description will become increasingly important as device dimensions move even further into the deep submicron regime”. For more details we refer to [39, 40, 41]. Straughan and Franchi [42] in 1984 were the first to study the Bénard problem coupled to a hyperbolic heat equation and analyse the effect of second sound on the onset of convection. More recently, Straughan in [43] first studied the problem of convection in a porous medium when Cattaneo’s law is employed to model heat propagation. Interesting results are obtained once the assumption of LTNE is combined with the Cattaneo’s law for heat conduction in the solid matrix, since in such a case convection by means of oscillatory motions can occur [44, 45, 46, 47, 48, 49]. Specifically, in [46] it has been first performed a nonlinear analysis for the onset of convection in a model with LTNE. In this paper, second sound is considered only in the solid phase, while Fourier’s law is retained in the fluid phase. This choice is motivated by experimental results. It has been proved with good approximation that the wave-like motion of heat appears greater in solids, especially in those involved in porous metallic foams. We will follow the same assumption in chapter 6.

In this thesis, we are going to take into account the effect of rotation on the onset of convection. Understanding thermal convection in rotating porous media is a physical problem that finds many applications in industrial and engineering field, specifically in centrifugal casting of metals or rotating machinery [50, 51, 52]. When the porous layer rotates about the vertical axis, fluid particles are subject to the

centrifugal and the Coriolis forces. Hence, the Darcy's law needs to be modified. The strong idea which allows to study the fluid motion in this configuration involves a change of reference in order to study the problem in the rotating frame. As a result, an additional term needs to added in the Darcy equation and a new pressure needs to be defined, resulting in

$$-\nabla p = \frac{\mu}{K}\mathbf{v} + \frac{2\Omega\rho}{\varepsilon}\mathbf{k}\times\mathbf{v} \tag{17}$$

where $\Omega\mathbf{k}$ is the constant angular velocity and p is called reduced pressure. In 1984, Palm and Tyvand [53] studied the problem of thermal convection in a porous layer which rotates uniformly about the vertical axis with constant angular velocity. They employed the Darcy model as in (17) to include the Coriolis term. They discovered an important analogy showing that the onset of steady convection in a rotating system is equivalent to the case of convection in an anisotropic stratified porous layer. As pointed out in the remarkable paper [54], the analysis performed in [53] excludes the possibility of overstability because a time-derivative term is not considered in the Darcy's law, as in (3). Such observation led Vadasz to study the Coriolis effect coupled to the time-derivative term (see [54, 55, 56, 57]). In these papers, the author proved that the presence of inertia term in a model for a rotating porous medium leads to the occurrence of convection through oscillatory motions, which are not allowed when the inertia term is neglected. Following the idea in the papers mentioned above, we are going to investigate in this thesis the occurrence of oscillatory convection in porous media in local thermal nonequilibrium. The relevance of oscillating convective motions lies in cooling systems when, for example, one is interested in a time modulated cooling down.

Another topic that caught our attention is the effect of depth-dependent viscosity on the onset of convection in a fluid-saturated porous medium. What motivated this study is the strong viscosity dependence on temperature and/or depth, for many fluids [58, 59]. In several industrial problems, variations of viscosity with temperature cannot be neglected. Main examples of such problems can be found in geophysical context and in engineering field [58, 60, 61, 62, 63]. Actually, the correlation between viscosity and temperature deeply depends on which fluid is taken into account. In fact, viscosity of gases increases with temperature, while viscosity of liquids shows the opposite behaviour [1, p. 253]. For example, viscosity of glycerin decreases by three orders of magnitude for a $10°C$ rise in temperature [9], while viscosity of water changes more than 1 order of magnitude between $25°C$ and $350°C$ [64]. Over the same temperature interval, water thermal conductivity exhibits only a 1% change [65]. Actually, as stated in [66], for most Newtonian liquids thermal conductivity is essentially constant over the temperature range in which viscosity shows remarkable variations. For this reason, we are going to take into account only viscosity variations. Over the years, thermal convection in variable viscosity fluids has represented a topic of great interest for many researchers. Early studies on

thermal convection in clear fluids with temperature-dependent viscosity are those of Torrance and Turcotte in 1970 [58] and Palm et al. in 1967 [67]. Since then, such a problem has been extensively investigated (see [59, 68, 69, 70, 71, 72, 73]). In [58], the influence of strongly temperature- and/or depth-dependent viscosity has been studied, with particular attention to convection in Earth's mantle. In [59], the conditional nonlinear stability is performed for a clear fluid whose viscosity decreases linearly with temperature. While in [70], a global nonlinear stability result is obtained when viscosity shows a maximum. Nonlinear stability results have been obtained also in [71], where viscosity shows exponential dependence on temperature, and in [72] where viscosity is a convex function of temperature. The problem of thermal convection in variable viscosity fluids saturating a porous medium has been widely investigated, as well (see [60, 64]). Nonlinear stability results have been determined in [74] and [75]. While in [61] linear stability analysis of convection in water-saturated porous medium is performed. At the best of our knowledge, natural convection in depth-dependent viscosity fluids in porous media in LTNE has not received a proper attention so far, that is why we decided to undertake the study shown in chapter 7. The LTNE model has been employed in [9], where the onset of Darcy-Bénard convection is investigated for a temperature-dependent viscosity fluid with quadratic density constitutive equation.

The outline of the thesis is the following: chapter 1 provides tools to study the stability in the Lyapunov sense. The Lyapunov Direct Method is explained and the connection between linear and nonlinear stability is pointed out. In chapter 2, the type of instability that occurs for a vertical downward throughflow in a horizontal porous layer uniformly heated from below is studied. The validity of the principle of exchange of stabilities implies that only steady convection can occur. Particular attention is devoted to determine the critical value of the Péclet number for which the transition from supercritical to subcritical instability occurs. To this aim, weakly nonlinear analysis is performed and an original shooting method coupled to the Newton-Raphson scheme is employed. Chapter 3 is devoted to study the linear and nonlinear stability of the conduction solution in a rotating fully anisotropic porous medium in LTNE. The strong form of the principle of exchange of stabilities holds and the coincidence between linear and nonlinear results is proved. In chapter 4, the effect of horizontal isotropy on the onset of convection in a rotating porous medium in LTNE is studied. The fluid motion is described by the Brinkman law. Nevertheless, we obtained the optimal result of coincidence between the linear instability threshold and the global nonlinear one. Instead, in chapter 5, the effect of Vadasz inertia term on the onset of convection in a rotating porous medium in LTNE is studied. It is proved that the presence of this term may cause the onset of oscillatory convection. Chapter 6 is devoted to analyse the effect of second sound, modelled by the Cattaneo's law, in a LTNE Darcy-Brinkman anisotropic porous medium. The usage of hyperbolic temperature equation for the solid phase leads to the possibility for oscillatory convection to occur. The nonlinear stability analysis

is performed by employing the coupling parameter method. Finally, chapter 7 involves the onset of natural thermal convection in an anisotropic porous layer in LTNE saturated by a fluid whose viscosity depends on the depth of the layer. For this problem, we managed to obtain coincidence between linear and nonlinear results, and, in order to determine the critical threshold for the Rayleigh number, we implemented and employed the Chebyshev-tau method, which is able to solve differential eigenvalue problems.

Chapter 1

Stability Preliminaries

Let $\mathcal{F}$ be a physical phenomenon that one aims to describe and let $D \subset \mathbb{R}^3$ the domain in which this phenomenon takes place. If $\mathbf{u}(\mathbf{x}, t)$ is the vector that describes the state of the phenomenon $\mathcal{F}$, then one can model the physical phenomenon by the following system of partial differential equations

$$\frac{\partial \mathbf{u}}{\partial t} = \mathbf{F} \qquad \forall (\mathbf{x}, t) \in D \times (0, T) \tag{1.1}$$

where $\mathbf{F} = \mathbf{F}\left(\mathbf{x}, t, \mathbf{u}, \dfrac{\partial u_i}{\partial x_r}, \dfrac{\partial^2 u_i}{\partial x_r \partial x_s}, \dots\right)$ is a vectorial function that describes the behaviour of the time derivative of the state vector $\mathbf{u}(\mathbf{x}, t)$. To system (1.1), the following boundary and initial conditions are appended

$$\begin{cases} \mathbf{u}(\mathbf{x}, 0) = \mathbf{u}_0 & \forall \mathbf{x} \in D \\ G(\mathbf{u}, \nabla \mathbf{u}) = \hat{\mathbf{u}} & \forall (\mathbf{x}, t) \in \delta D \times [0, T] \end{cases} \tag{1.2}$$

where G is a given operator, $\hat{\mathbf{u}}$ an assigned vector and T a positive constant. The boundary value problem (1.1)-(1.2) is the mathematical model describing the evolution of $\mathcal{F}$.

Now, the problem of finding a solution to the boundary value problem (1.1)-(1.2) arises. The existence of a solution is assured, but determining explicitly such a solution is not trivial. Hence, a qualitative analysis of the model is required in order to get information on the behaviour of a solution.

During the second half of XIX century, Poincaré developed a qualitative study for dynamical systems with the aim of providing estimates and highlight properties of the state vector relative to the physical phenomenon in question. A key role in this kind of study is played by the stability analysis. The major contribution to this kind of analysis was given by the Russian mathematician Aleksandr Mikhailovich Lyapunov who developed a pioneering approach to the stability analysis for non-linear dynamical systems, in a period where the linearization method was widely employed.

In the present chapter, we will discuss the notion of stability in the sense of Lyapunov, looking at both linear and nonlinear stability analyses.

1.1 Some definitions

Let (X, d) be a metric space where $S_r(\mathbf{x})$ is a sphere with centre $\mathbf{x}$ and radius r and let f be a dynamical system, i.e. the application

$$f \,:\, (\mathbf{v}_0, t) \in (X, \mathbb{R}) \longrightarrow f(\mathbf{v}_0, t) \in X \tag{1.3}$$

such that $f(\mathbf{v}_0, 0) = \mathbf{v}_0$. The following definitions hold:

Definition 1. A motion with initial data $\mathbf{v}_0$ is defined as the application:

$$\mathbf{v}(\mathbf{v}_0, \cdot) \,:\, t \in \mathbb{R}^+ \longrightarrow \mathbf{v}(\mathbf{v}_0, t) \in X \tag{1.4}$$

where $\mathbf{v}(\mathbf{v}_0, 0) = \mathbf{v}_0$.

If $\mathbf{v}(\mathbf{v}_0, t) = \mathbf{v}_0 \ \forall t \in \mathbb{R}^+$, then the motion is stationary and $\mathbf{v}_0$ is called equilibrium.

Definition 2. A motion $\mathbf{v}(\mathbf{v}_0, \cdot)$ depends continuously on initial data if and only if $\forall \varepsilon > 0$, $\forall T > 0$, $\exists \delta(\varepsilon, T) > 0$ such that

$$\mathbf{v}_1 \in S_\delta(\mathbf{v}_0) \Longrightarrow \mathbf{v}(\mathbf{v}_1, t) \in S_\varepsilon(\, \mathbf{v}(\mathbf{v}_0, t)\,) \quad \forall t \in [0, T] \tag{1.5}$$

Stability in the Lyapunov sense extends to an upper unbounded interval the previous concept.

Definition 3. A motion $\mathbf{v}(\mathbf{v}_0, \cdot)$ is stable in the sense of Lyapunov if and only if:

$$\forall \varepsilon > 0,\, \exists \delta(\varepsilon) > 0 \,:\, \mathbf{v}_1 \in S_\delta(\mathbf{v}_0) \Longrightarrow \mathbf{v}(\mathbf{v}_1, t) \in S_\varepsilon(\, \mathbf{v}(\mathbf{v}_0, t)\,) \quad \forall t > 0$$

Definition 4. A motion $\mathbf{v}(\mathbf{v}_0, \cdot)$ is unstable in the sense of Lyapunov if and only if:

$$\exists \varepsilon > 0 \,:\, \forall \delta(\varepsilon) > 0,\, \exists t_1 > 0 \,:\, \mathbf{v}_1 \in S_\delta(\mathbf{v}_0) \Longrightarrow \mathbf{v}(\mathbf{v}_1, t_1) \notin S_\varepsilon(\, \mathbf{v}(\mathbf{v}_0, t_1)\,)$$

Hence, stability with respect to perturbations on initial data is stronger than continuous dependence on initial data.

Definition 5. A motion $\mathbf{v}(\mathbf{v}_0, \cdot)$ is called an attractor over a set Y if

$$\mathbf{v}_1 \in Y \Longrightarrow \lim_{t \to \infty} d[\mathbf{v}(\mathbf{v}_0, t),\, \mathbf{v}(\mathbf{v}_1, t)] = 0 \tag{1.6}$$

Definition 6. A motion $\mathbf{v}(\mathbf{v}_0, \cdot)$ is said to be asymptotically stable if it is stable and, moreover, there exists $\delta_1 > 0$ such that $\mathbf{v}(\mathbf{v}_0, \cdot)$ is an attractor over $S_{\delta_1}(\mathbf{v}_0)$. Moreover, $\mathbf{v}(\mathbf{v}_0, \cdot)$ is said to be exponentially stable if there exist $\delta_1 > 0$, $\lambda(\delta_1) > 0$, $M(\delta_1) > 0$ such that:

$$\mathbf{v}_1 \in S_{\delta_1}(\mathbf{v}_0) \Longrightarrow d[\mathbf{v}(\mathbf{v}_1, t),\, \mathbf{v}(\mathbf{v}_0, t)] \leq M e^{-\lambda t}\, d[\mathbf{v}_1,\, \mathbf{v}_0], \qquad \forall t \in \mathbb{R}^+.$$

In particular, if $\delta_1 = \infty$, then $\mathbf{v}(\mathbf{v}_0, \cdot)$ is asymptotically exponentially globally stable.

Given a basic motion $\mathbf{v}^*(\mathbf{v}_0, t)$, whose stability one wants to investigate, the stability of $\mathbf{v}^*(\mathbf{v}_0, t)$ may be expressed in terms of the perturbation $\mathbf{u}(\mathbf{u}_0, t) = \mathbf{v}(\mathbf{v}_1, t) - \mathbf{v}^*(\mathbf{v}_0, t)$ $(\mathbf{u}_0 = \mathbf{v}_1 - \mathbf{v}_0)$. Then,

Definition 7. A basic motion $\mathbf{v}^*(\mathbf{v}_0, t)$ is said to be stable in the Lyapunov sense if and only if:

$$\forall \varepsilon > 0,\, \exists \delta(\varepsilon) > 0 \,:\, \mathbf{u}_0 \in S_\delta(\mathbf{0}) \Longrightarrow \mathbf{u}(\mathbf{u}_0, t) \in S_\varepsilon(\mathbf{0}) \quad \forall t > 0. \tag{1.7}$$

where $\mathbf{0}$ is the origin of X.

As a result, in plain words, a given basic motion is stable if all perturbations that are small initially remain small for all time, and it is unstable if at least one small perturbation grows so much that it ceases to be small after some time.

From previous definitions, it emerges that the notion of stability in the Lyapunov sense is related to the definition of distance and, as a consequence, in a normed vector space, to the definition of norm. Specifically, when studying problems with a finite number of degree of freedom, embedded in finite-dimensional spaces, the concept of stability is independent on the chosen norm as in $\mathbb{R}^n$ all the norms are equivalent.

On the other hand, for phenomena with infinite number of degree of freedom, which are usually described by partial differential equations in infinite-dimensional spaces, stability will depend on the chosen norm. For example, one could choose $\|\mathbf{u}\| = \sup_{\mathbf{u}\in X} |\mathbf{u}|$ even though it is usually preferred the energy norm $\|\mathbf{u}\| = \left(\int_X |\mathbf{u}|^2 dX\right)^{1/2}$. In this case, stability depends on the topology of the space X. For a discussion about topology dependent stability see [76].

1.2 Lyapunov Direct Method

In 1893, Lyapunov developed a method, called direct method, to determine conditions ensuring the stability of a solution of a nonlinear system of ordinary differential equations. This method allows to get important information of solutions, although they are not obtained explicitly. The basic idea on which the method is built involves determining the sign of the time derivative of an auxiliary function (called

Lyapunov function) evaluated along solutions of the differential system studied. This method was recognized to be very powerful and it has been employed in the qualitative theory for many years. Later, the idea of Lyapunov was applied successfully to systems of partial differential equations. We introduce the fundamental ideas of the direct method.

Definition 8. Let (1.3) be a dynamical system on the metric space (X, d). A function $V : X \to \mathbb{R}$ is said Lyapunov function on $I \subset X$ if $V \in C^1(I)$ and V is a nonincreasing function in time along the solutions of (1.3) with initial data in I.

By virtue of (1.7), the stability of a given basic motion can be studied through the stability of the zero solution of the perturbed dynamical system. As a consequence, we introduce the direct method to investigate the stability of the null solution as basic state.

Let X be a normed linear space and let $\mathcal{F}_r$, $r = cost > 0$, the set of functions $\varphi : [0, r) \to \mathbb{R}^+$ that are continuous, strictly increasing and such that $\varphi(0) = 0$. Hence, the Lyapunov direct method is summarized by the following theorems:

Theorem 1. *Let $\boldsymbol{u}$ be a dynamical system on a normed space X and let $\boldsymbol{O}$ be an equilibrium point. If V is a Lyapunov function on the open set $S_r(\boldsymbol{O})$ with $r > 0$ such that*

i) $V(\boldsymbol{O}) = 0$;

ii) $\exists f \in \mathcal{F}_r : V(\boldsymbol{u}) \geq f(\|\boldsymbol{u}\|), \forall \boldsymbol{u} \in S_r(\boldsymbol{O})$

then $\boldsymbol{O}$ is stable. In addition, if

iii) $\exists g \in \mathcal{F}_r : \dot{V}(\boldsymbol{u}) \leq -g(\|\boldsymbol{u}\|), \forall \boldsymbol{u} \in S_r(\boldsymbol{O})$

then $\boldsymbol{O}$ is asymptotically stable.

Proof. See [76] □

The following theorem holds as particular case of Theorem 1.

Theorem 2 (Lyapunov Lemma)**.** *Let $\boldsymbol{u}$ be a dynamical system on X and let $\boldsymbol{O}$ be an equilibrium point. If V is the Lyapunov function on $S_r(\mathbf{O})$ such that*

$$V(\mathbf{O}) = 0, \qquad V(\boldsymbol{u}) > 0 \quad \forall \boldsymbol{u} \neq \mathbf{O} \tag{1.8}$$

then the stability with respect to the measure V of perturbation is obtained. Plus, if there exists a positive constant c such that the following inequality holds along the solutions

$$\dot{V} \leq cV \tag{1.9}$$

then

$$V \leq V(\boldsymbol{u}_0)e^{-ct} \tag{1.10}$$

i.e. the asymptotic exponential stability with respect to the measure V is obtained.

Setting $\Sigma(X,\alpha) = \{x \in X : V(x) < \alpha\}$, the following theorem holds:

Theorem 3. *Let $\boldsymbol{u}$ be a dynamical system on $X \times \mathbb{R}^+$ and let $\boldsymbol{O}$ be an equilibrium point. If V is the Lyapunov function on the open set $A_r = S_r(\boldsymbol{O}) \cap \Sigma(X,0)$, with $r > 0$, and*

i) $V(\boldsymbol{O}) = 0$;

ii) $\exists g \in \mathcal{F}_r : \widehat{V}(\boldsymbol{u}) \leq -g[-V(\boldsymbol{u})],\ \boldsymbol{u} \in A_r$;

iii) $A_r \neq \emptyset, \quad \forall \epsilon > 0$

then $\boldsymbol{O}$ is unstable.

Proof. See [76] □

1.3 Stability Analysis

1.3.1 Linear Stability

Let $\mathcal{H}$ be a Hilbert space endowed with scalar product $(\cdot,\cdot)$ and associated norm $\|\cdot\|$. Let $\mathbf{v}^*(\mathbf{v}_0,t)$ be the basic motion and let $\mathbf{u}(\mathbf{u}_0,t) = \mathbf{v}(\mathbf{v}_1,t) - \mathbf{v}^*(\mathbf{v}_0,t)$ be the perturbation arising after perturbing the basic motion at initial time. Let us consider the following initial value problem

$$\begin{cases} \dfrac{\partial \mathbf{u}}{\partial t} + L\mathbf{u} + N(\mathbf{u}) = 0 \\ \mathbf{u}(\mathbf{x},0) = \mathbf{u}_0(\mathbf{x}) \end{cases} \tag{1.11}$$

L being a linear operator, N a nonlinear one with $N(\mathbf{0}) = 0$ so that (1.11) admits the null solution. Let us assume that

i) L is a densely defined (i.e. $D(L)$ dense in $\mathcal{H}$), closed, with compact resolvent, i.e. such that $\{\lambda \in \mathbb{C} : \exists (L - \lambda I)^{-1}\}$ is compact;

ii) the bilinear form associated with L is defined and bounded on a space $\mathcal{H}^*$, which is compactly embedded in $\mathcal{H}$;

iii) the nonlinear operator N verifies the condition:

$$(N(\mathbf{u}),\mathbf{u}) \geq 0 \qquad \forall \mathbf{u} \in D(N) \tag{1.12}$$

where $D(N)$ is the domain of the operator N.

To study the linear stability of the basic state, nonlinear terms are neglected in (1.11), i.e. terms included in $N(\mathbf{u})$. Hence, one obtains

$$\begin{cases} \dfrac{\partial \mathbf{u}}{\partial t} + L\mathbf{u} = 0 \\ \mathbf{u}(\mathbf{x}, 0) = \mathbf{u}_0(\mathbf{x}). \end{cases} \tag{1.13}$$

Under the hypotheses in (i), the following result holds

Theorem 4 (Kato 1976)**.** *The spectrum of the operator L consists entirely of an at most denumerable number of eigenvalues $\{\sigma_n\}_{n\in\mathbb{N}}$ with finite (both algebraic and geometric) multiplicities and, moreover, such eigenvalues can cluster only at infinity.*

Since the operator L is autonomous, solutions are of this kind: $\mathbf{u}(\mathbf{x}, t) = \varphi(\mathbf{x})e^{-\sigma t}$. As a result, the behaviour in time of perturbations $\mathbf{u}(\mathbf{x}, t)$ is governed by the sign of the real part of σ. In particular, if $Re(\sigma) > 0$ for all σ then the zero solution is linearly stable; if $Re(\sigma) < 0$ for some σ then the solution is linearly unstable. The eigenvalues, which satisfy the equation

$$L\varphi = \sigma\varphi \tag{1.14}$$

are not necessarily real as the operator L is in general non-symmetric. Nevertheless, the eigenvalues may be ordered in the following way:

$$Re(\sigma_1) \leq Re(\sigma_2) \leq \cdots \leq Re(\sigma_n) \leq \ldots \tag{1.15}$$

Hence, since for the linear stability we need all the eigenvalues to be with positive real part, the linear stability analysis reduces to studying the sign of $Re(\sigma_1)$. Hence,

Definition 9. The zero solution of (1.11) is linearly stable if and only if

$$Re(\sigma_1) > 0 \tag{1.16}$$

In problems that we are going to study in this thesis, σ_1 will depend on the dimensionless Rayleigh number R. Our aim is to determine the least value R_c for which $Re(\sigma_1) = 0$, namely, for which instability sets in. One also expects that $Re(\sigma_1) > 0$ if $R < R_c$ and $Re(\sigma_1) < 0$ if $R > R_c$.

Now, the aim is to investigate the connection between linear stability results and nonlinear stability ones. We will see that a strong connection is obtained not only when the operator L is symmetric but also when it is not. In the latter case, the main contribution is to show that when the principle of exchange of stabilities holds in a well defined sense, then the link between linear and nonlinear stability is provided.

Definition 10. The principle of exchange of stabilities holds if

$$Im(\sigma_1) \neq 0 \Longrightarrow Re(\sigma_1) < 0 \tag{1.17}$$

The weak form of the principle is the following

Definition 11. The principle of exchange of stabilities is said to hold in the weak sense if

$$Re(\sigma_1) = 0 \Longrightarrow Im(\sigma_1) = 0 \tag{1.18}$$

Finally, the strong form

Definition 12. The principle of exchange of stabilities holds in the strong form if the spectrum of the linear operator L is subset of $\mathbb{R}$.

Conditions in the previous definitions certainly happen when the operator L is symmetric or symmetrizable.

In all these cases, at the criticality, σ_1 is real and equal to zero. We say that instability sets in as a secondary steady motion when $\sigma_1 = 0$ at the criticality. On the other hand, if σ_1 is a pure imaginary number at the criticality, instability sets in as an oscillatory motion. In this case, the principle of exchange of stabilities does not hold and overstability is possible.

1.3.2 Nonlinear Stability

The aim of this section is to investigate the connection between the linear stability results and the nonlinear stability ones. Let us recall the definition of nonlinear stability:

Definition 13. The null solution of (1.11) is nonlinearly stable if and only if for each $\varepsilon > 0$, there exists a $\delta = \delta(\varepsilon)$ such that

$$\|\mathbf{u}_0\| < \delta \Rightarrow \|\mathbf{u}(t)\| < \varepsilon \tag{1.19}$$

and there exists $\gamma \in (0, +\infty]$ such that

$$\|\mathbf{u}_0\| < \gamma \Rightarrow \lim_{t\to\infty} \|\mathbf{u}(t)\| = 0. \tag{1.20}$$

If $\gamma = \infty$, the zero solution of (1.11) is said to be unconditionally nonlinearly stable, otherwise, if $\gamma < \infty$, the solution is conditionally stable.

The operator L is in general non-symmetric, but the following decomposition is possible:

$$L = L_1 + L_2 \tag{1.21}$$

where L_1 is a symmetric operator with compact resolvent and L_2 is a skew-symmetric operator bounded in $\mathcal{H}^*$. These two operators are such that $D(L_2) \supset D(L_1) = D(L)$.

It turns out that L_1 satisfies the hypotheses of Theorem 4. Moreover, because of symmetry, eigenvalues $\{\lambda_n\}_{n\in\mathbb{N}}$ associated with L_1 are all real and may be ordered as follows:

$$\lambda_1 \leq \lambda_2 \leq \cdots \leq \lambda_n \leq \ldots \tag{1.22}$$

Let $L_1[\varphi,\varphi]$, with $\varphi \in \mathcal{H}^*$, be the bilinear form associated with the operator L_1, i.e.

$$(L_1\varphi,\varphi) = L_1[\varphi,\varphi] \qquad \forall\varphi \in D(L_1) \tag{1.23}$$

then the following remark holds:

Remark 1. *Let φ be an eigenfunction related to the eigenvalue λ_1. Then*

$$\lambda_1 = \min_{\varphi\in\mathcal{H}^*} \frac{L_1[\varphi,\varphi]}{\|\varphi\|^2}. \tag{1.24}$$

As a consequence, the following theorem holds:

Theorem 5. *If $\lambda_1 > 0$ then the zero zolution of (1.11) is unconditionally nonlinearly stable.*

Proof. See [65]. □

From previous arguments it follows that while the linear stability reduces to studying the sign of eigenvalues related to the linear operator L, the nonlinear stability involves the eigenvalues of the symmetric part L_1 only.

Remark 2. *If the skew-symmetric part L_2 of L is zero, i.e. $L = L_1$, then the linear stability implies the nonlinear one and vice versa.*

Let us assume that the strong form of the principle of exchange of stabilities 12 holds and the operator L is not symmetric. Moreover, let us assume that we are able to provide a new scalar product $<\cdot,\cdot>$ for which L is symmetric and that the bilinear form associated with L in the new scalar product admits the decomposition

$$L'[\varphi,\psi] = I(\varphi,\psi) + D(\psi,\psi) \tag{1.25}$$

where I and D are symmetric, bounded bilinear forms in $\mathcal{H}^*$,

$$\begin{aligned} &I(\varphi,\varphi) \leq C_1|\varphi||\varphi|^* \quad \forall\varphi \in \mathcal{H}^* \\ &D(\varphi,\varphi) \geq C|\varphi|^*|\varphi|^* \end{aligned} \tag{1.26}$$

where C, C_1 are positive constants. Although (1.12) is satisfied in the "old" scalar product, it is not granted that it is satisfied also in the "new" one. In general, we shall assume

$$\forall\varepsilon > 0\ \exists c = c(\varepsilon)\ :\ |<N(\mathbf{u}),\mathbf{u}>| \leq \varepsilon D(\mathbf{u},\mathbf{u}) + c\|\mathbf{u}\|^\alpha \quad \forall\mathbf{u} \in D(N),\ \alpha > 2 \tag{1.27}$$

or

$$|<N(\mathbf{u}),\mathbf{u}>| \leq k\|\mathbf{u}\|^\beta D(\mathbf{u},\mathbf{u}) \quad \forall\mathbf{u} \in D(N) \text{ and } k,\beta > 0 \tag{1.28}$$

Hence the following main result holds [77]:

Theorem 6. *Suppose definition 12 holds and* (1.25)-(1.26) *and either* (1.27) *or* (1.28) *are satisfied. Then, if the null solution of* (1.11) *is linearly stable, it is also asymptotically nonlinearly stable. In particular, there exist computable constants* $A, \gamma, \delta > 0$ *such that*

$$\|\boldsymbol{u}_0\|^2 < \gamma \Longrightarrow \|\boldsymbol{u}(t)\|^2 \leq A\|\boldsymbol{u}_0\|^2 e^{-\delta t} \quad \forall t \geq 0 \tag{1.29}$$

Chapter 2

A weakly nonlinear analysis of vertical throughflow on Darcy-Bénard convection

2.1 Introduction

In the present chapter, it is shown the first part of a joint work, soon to be published, in collaboration with Prof. F. Capone, G. Massa and Dr. D. A. S. Rees. It is investigated the type of instability occurring in a fluid-saturated horizontal porous layer heated from below and subject to a downward vertical throughflow. The main aim of the work is to determine conditions such that the onset of instability is subcritical. Linear instability analysis is performed to set the context for the subsequent weakly nonlinear analysis. It turns out that subcriticality may be expected once the Péclet number overcomes 3.1617. Moreover, subcritical instability always occurs over ranges of wavenumber that do not contain the critical value, for $\mathrm{Pe} \neq 0$.

The chapter is organised as follows. In section 2.2 the mathematical model is described and the dimensionless form of the system is determined. Section 2.3 is devoted to the basic stationary solution and its behaviour in the small-Pe and large-Pe limits. In section 2.4 the instability of the basic flow is analysed via linear analysis. We proved the principle of exchange of stabilities and provide and discuss the tenth order system of ODEs to determine the critical Rayleigh number for the onset of instability. In section 2.5 the weakly nonlinear analysis is performed in order to determine the Landau equation. From that equation, we are able to determine conditions on the Péclet number and the wavenumber that may lead to the onset of subcritical instability.

2.2 Mathematical model

Let us consider a fluid-saturated horizontal planar porous layer $L = \mathbb{R} \times [0, d]$ uniformly heated from below and let Ox^*z^* be the reference frame. Let T_L be the fixed temperature at $z^* = 0$ and let T_U be the fixed temperature at $z^* = d$ where $T_L > T_U$. The temperature, T_U, is also regarded as being the reference temperature. The two bounding surfaces are permeable and admit a constant downward vertical throughflow of magnitude Q across the layer.

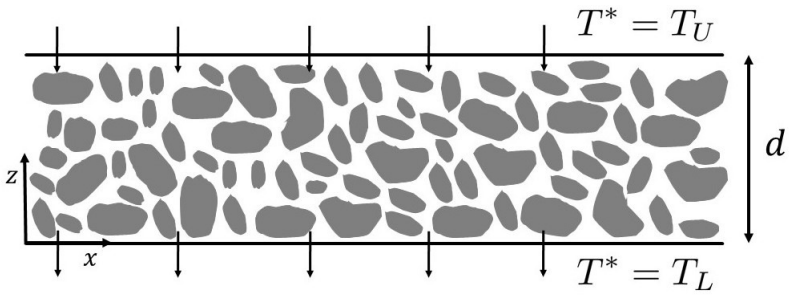

Figure 2.1: Depicting a horizontal porous layer

Let $\mathbf{v}^*, T^*, p^*$ be the velocity, temperature and pressure fields, respectively. The governing system is derived by employing the Boussinesq approximation, i.e. the fluid density ρ is constant in all terms of the governing equations, except for in the buoyancy term. In this paper, we shall assume that ρ is linearly dependent on temperature T^*:

$$\rho(T^*) = \rho_0[1 - \alpha(T^* - T_U)], \tag{2.1}$$

where α is the thermal expansion coefficient and ρ_0 is the fluid density at the reference temperature T_U.

Therefore, the governing equations, according to the Darcy's model, are well known to be, cf. [1],

$$\begin{cases} \dfrac{\mu}{K}\mathbf{v}^* = -\nabla^* p^* + \rho_0 \alpha g T^* \mathbf{k}, \\ \nabla^* \cdot \mathbf{v}^* = 0, \\ (\rho c)_m T^*_{,t^*} + (\rho c)_f \mathbf{v}^* \cdot \nabla^* T^* = k \nabla^{*2} T^*, \end{cases} \tag{2.2}$$

where k is the overall thermal conductivity, K the permeability, μ the viscosity of the fluid, $\mathbf{g} = -g\mathbf{k}$ the gravitational acceleration, and c the specific heat. The subscripts m and f refer to the porous medium and the fluid, respectively. The

system (2.2) is completed by the following boundary conditions:

$$\begin{aligned} \mathbf{v}^* &= -Q\mathbf{k} \quad \text{on} \quad z^* = 0, d, \\ T^* &= T_L \quad \text{on} \quad z^* = 0, \\ T^* &= T_U \quad \text{on} \quad z^* = d. \end{aligned} \tag{2.3}$$

In order to write the non-dimensional versions of (2.2) and (2.3), we introduce the following non-dimensional parameters:

$$\mathbf{x}^* = d\mathbf{x}, \quad \mathbf{v}^* = U\mathbf{u}, \quad p^* + \rho_0 \alpha g T_U z^* = Pp, \quad T^* = \theta(T_L - T_U) + T_U, \quad t^* = \hat{\tau} t, \tag{2.4}$$

where typical velocity, pressure and time scales are given by,

$$U = \frac{k}{d(\rho c)_f}, \quad P = \frac{k\mu}{K(\rho c)_f}, \quad \hat{\tau} = \frac{(\rho c)_m d^2}{k}. \tag{2.5}$$

In the above, the values, $\mathbf{u} = (u, w)$, θ and p are the dimensionless velocity, temperature and pressure fields, respectively. The governing non-dimensional system is,

$$\begin{cases} \mathbf{u} = -\nabla p + \mathrm{Ra}\theta\, \mathbf{k}, \\ \nabla \cdot \mathbf{u} = 0, \\ \theta_{,t} + \mathbf{u} \cdot \nabla\theta = \nabla^2\theta, \end{cases} \tag{2.6}$$

with the boundary conditions

$$\begin{aligned} w &= -\mathrm{Pe} \quad \text{on} \quad z = 0,1, \\ \theta &= 1 \quad \text{on} \quad z = 0, \\ \theta &= 0 \quad \text{on} \quad z = 1, \end{aligned} \tag{2.7}$$

where

$$\mathrm{Ra} = \frac{d\rho_0 \alpha g (T_L - T_U) K(\rho c)_F}{\mu k} \tag{2.8}$$

is the Darcy-Rayleigh number (hereinafter called the Rayleigh number), and

$$\mathrm{Pe} = \frac{Q(\rho c)_F d}{k} \tag{2.9}$$

is the Péclet number.

2.3 The basic state

The basic dimensionless solution of (2.6)-(2.7) is

$$\mathbf{u}_b = -\mathrm{Pe}\, \mathbf{k}, \qquad \theta_b = g(z), \qquad p_b = \bar{p}(z). \tag{2.10}$$

where

$$g(z) = \frac{e^{-\mathrm{Pe}z} - e^{-\mathrm{Pe}}}{1 - e^{-\mathrm{Pe}}} \quad \text{and} \quad \bar{p}(z) = -\frac{\mathrm{Ra}}{1 - e^{-\mathrm{Pe}}} \left(\frac{e^{-\mathrm{Pe}z}}{\mathrm{Pe}} + e^{-\mathrm{Pe}} z - \frac{1}{\mathrm{Pe}} \right) + p_b(0). \tag{2.11}$$

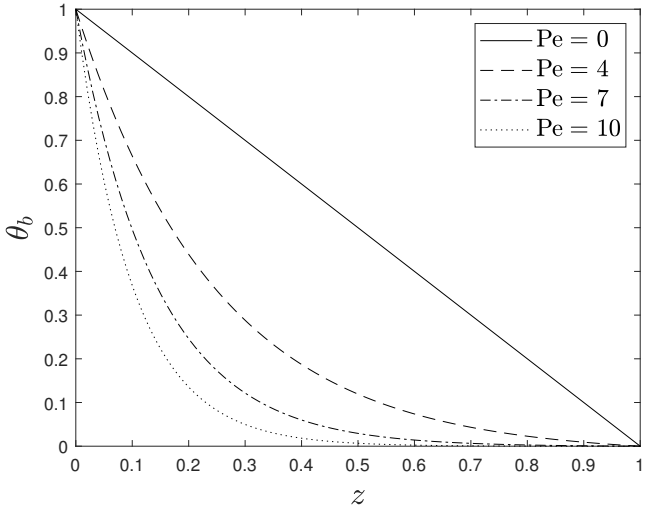

Figure 2.2: Basic temperature profiles for the the quoted values of the Péclet number, Pe.

We may begin our discussion of the basic state with the following remarks.

Remark 2.3.1. When the limit as $\mathrm{Pe} \to 0$ is taken of the basic temperature profile, θ_b, the well-known Darcy linear profile is recovered:

$$\lim_{\mathrm{Pe}\to 0} \theta_b(z) = 1 - z. \tag{2.12}$$

Remark 2.3.2. When the large-Pe limit is taken then

$$\theta_b(z) \sim e^{-\mathrm{Pe}\, z}. \tag{2.13}$$

This means that the temperature field is confined to region of thickness of $O(\mathrm{Pe}^{-1})$ at the lower surface.

Both of these extreme cases may be demonstrated easily from Eqs. (2.11), and are confirmed in Figure 2.2, which also shows the detailed manner in which the basic temperature profile varies with the magnitude the Péclet number, Pe.

As Pe increases from zero the upward conduction of heat from the lower surface is counteracted increasingly by the externally-imposed downward advection.

Therefore, for very large values of Pe, the layer appears to mimic a region of infinite height because most of the layer is uniformly cold apart from the narrow thermal boundary layer near $z = 0$. Therefore, for $\mathrm{Pe} \gg 1$, we have an *a priori* expectation that instabilities will be confined to this boundary layer which is where the basic temperature gradient is destabilising. In the large-Pe limit, then, the problem essentially becomes independent of the depth of the layer should $1/\mathrm{Pe}$ be used as an alternative characteristic nondimensional length. With such an approximation we recover the Wooding problem [5]. Hence, if we wished to compare our large-Pe results with those of Wooding, we should rescale the Rayleigh number to the appropriate one for the Wooding problem, namely,

$$\mathrm{Ra}_w = \mathrm{RaPe}^{-1}. \tag{2.14}$$

2.4 Linear Instability Analysis

We shall now consider the onset of convection. Squire's theorem may be shown easily to hold, and therefore we may confine ourselves to the analysis of two-dimensional perturbations. Let us introduce the stream function ψ such that $u = -\psi_{,z}$ and $w = \psi_{,x}$. Hence, system (2.6) becomes:

$$\begin{cases} \nabla^2\psi = \mathrm{Ra}\,\theta_{,x}, \\ \theta_{,t} + \psi_{,x}\theta_{,z} - \psi_{,z}\theta_{,x} = \nabla^2\theta, \end{cases} \tag{2.15}$$

and the basic solution now takes the form,

$$\psi_b = -\mathrm{Pe}\,x, \qquad \theta_b = g(z). \tag{2.16}$$

By introducing a perturbation $\hat{\psi}, \hat{\theta}$ to (2.16) the non-dimensional system arising from (2.15) is

$$\begin{cases} \nabla^2\psi = \mathrm{Ra}\,\theta_{,x}, \\ \theta_{,t} - \mathrm{Pe}\,\theta_{,z} + g'(z)\psi_{,x} + \psi_{,x}\theta_{,z} - \psi_{,z}\theta_{,x} = \nabla^2\theta, \end{cases} \tag{2.17}$$

where the circumflexes have been dropped for notational convenience and where primes denote ordinary derivatives with respect to z. System (2.17) will be solved subject to the following boundary conditions:

$$\psi = \theta = 0, \quad \text{on } z = 0,1. \tag{2.18}$$

Let us underline that the perturbation fields are Sobolev functions in $W^{2,2}(V)$ $\forall t \in \mathbb{R}^+$, V being the periodicity cell, and they are periodic in the horizontal direction with period $2\pi/k$.

The determination of the critical threshold for the Rayleigh number begins with a linear stability analysis. The linear system associated with (2.17) is

$$\begin{cases} \nabla^2\psi = \mathrm{Ra}\theta_{,x}, \\ \theta_{,t} - \mathrm{Pe}\,\theta_{,z} + g'(z)\psi_{,x} = \nabla^2\theta. \end{cases} \tag{2.19}$$

Since this system and its boundary conditions are homogeneous with coefficients that are independent of time, it is possible to look for solutions where the spatial dependence may be separated from an exponential time-dependence. Let

$$\varphi(\mathbf{x}, t) = \bar{\varphi}(\mathbf{x})e^{\sigma t} \quad \forall\varphi \in \{\psi, \theta\} \tag{2.20}$$

where σ is the exponential growth rate, so system (2.19) becomes:

$$\begin{cases} \nabla^2\psi = \mathrm{Ra}\theta_{,x}, \\ \sigma\theta - \mathrm{Pe}\,\theta_{,z} + g'(z)\psi_{,x} = \nabla^2\theta. \end{cases} \tag{2.21}$$

Theorem 2.4.1. The strong form of the principle of exchange of stabilties holds for system (2.21)-(2.18), hence convection can occur only via steady motions.

Proof. Since the perturbation fields are periodic in the horizontal direction x, (2.21)-(2.18) admits solution of the form:

$$\psi = -i\ \bar{\psi}\ e^{ikx} + c.c., \qquad \theta = \bar{\theta}\ e^{ikx} + c.c., \tag{2.22}$$

where k is the wavenumber and $\bar{\psi}$, $\bar{\theta}$ are complex functions. Hence, system (2.21) becomes (dropping the bars)

$$\begin{cases} (D^2 - k^2)\psi = -\mathrm{Ra}\ k\theta, \\ \sigma\theta = \mathrm{Pe}\ D\theta - g'(z)k\psi + (D^2 - k^2)\theta, \end{cases} \tag{2.23}$$

Equation $(2.23)_1$ is equivalent to

$$\mathrm{Ra}\theta = \frac{D^2 - k^2}{-k}\psi := B^{-1}(\psi) \tag{2.24}$$

i.e.

$$\psi = \mathrm{Ra}B(\theta) \tag{2.25}$$

Using the above, system (2.23) becomes

$$\begin{cases} \psi = \mathrm{Ra}B(\theta), \\ \sigma\theta = \mathrm{Pe}\ D\theta - g'(z)k\mathrm{Ra}B(\theta) + (D^2 - k^2)\theta, \end{cases} \tag{2.26}$$

under the following boundary conditions:

$$\theta(0) = \theta(1) = \psi(0) = \psi(1) = 0. \tag{2.27}$$

The linear operator associated to (2.26) is

$$\mathcal{L} = D^2 - k^2 + \mathrm{Pe}D - g'k\mathrm{Ra}B(\cdot) \tag{2.28}$$

that is not symmetric with respect to the scalar product in $L^2(0,1)$. Therefore, by virtue of a similarity transformation which symmetrizes the operator $\mathcal{L}$, we will show that the principle of exchange of stabilities holds. Let us employ the following transformation

$$\theta = M(z)\varphi := e^{-\frac{\mathrm{Pe}}{2}z}\varphi \tag{2.29}$$

hence,

$$\mathcal{L}\theta = e^{-\frac{\mathrm{Pe}}{2}z}\left[D^2\varphi - \left(\frac{\mathrm{Pe}^2}{2} + k^2\right)\varphi - e^{\frac{\mathrm{Pe}}{2}z}g'k\mathrm{Ra}B(e^{-\frac{\mathrm{Pe}}{2}z}\varphi)\right] := M\hat{\mathcal{L}}M^{-1}\theta, \tag{2.30}$$

where the operator $\hat{\mathcal{L}}$ is defined as

$$\hat{\mathcal{L}} = D^2 - k^2 - \frac{\mathrm{Pe}^2}{2} - e^{\frac{\mathrm{Pe}}{2}z}g'k\mathrm{Ra}B(\cdot) \tag{2.31}$$

Via the transformation (2.29), we can now focus our attention on the following problem

$$\begin{cases} \psi = \mathrm{Ra}B(e^{-\frac{\mathrm{Pe}}{2}z}\varphi), \\ \sigma\varphi = \hat{\mathcal{L}}\varphi, \end{cases} \tag{2.32}$$

with associated boundary conditions

$$\varphi(0) = \varphi(1) = \psi(0) = \psi(1) = 0. \tag{2.33}$$

The operator $\hat{\mathcal{L}}$ is symmetric - hence its eingenvalues are all real - and the spectrum of $\hat{\mathcal{L}}$ is contained in the spectrum of $\mathcal{L}$ [78]. Moreover, part of the spectrum of $\mathcal{L}$ for which the eigenfunctions are in

$$\{\theta \in L^2(0,1) \mid e^{\frac{\mathrm{Pe}}{2}z}\theta \in L^2(0,1)\}$$

coincides with the spectrum of $\hat{\mathcal{L}}$ with respect to $L^2(0,1)$. Let us consider $\varphi = e^{\frac{\mathrm{Pe}}{2}z}\theta$, with $\theta \in L^2(0,1)$ therefore

$$\|\varphi\|^2_{L^2(0,1)} \leq \|e^{\mathrm{Pe}z}\|_{L^\infty(0,1)}\|\theta\|^2_{L^2(0,1)} < +\infty \tag{2.34}$$

so

$$\varphi \in L^2(0,1),\ \forall\ \theta \in L^2(0,1),$$

this means the spectra of $\mathcal{L}$ and $\hat{\mathcal{L}}$ coincide and the principle of exchange of stabilities holds, i.e. convection can arise only via stationary motions.

□

By virtue of theorem 2.4.1, let us assume $\sigma = 0$ at the criticality. Therefore, system (2.21) becomes

$$\begin{cases} \nabla^2\psi - \mathrm{Ra}\theta_{,x} = 0, \\ \nabla^2\theta + \mathrm{Pe}\,\theta_{,z} - g'(z)\psi_{,x} = 0, \end{cases} \tag{2.35}$$

Consequence of theorem 2.4.1 is that $\bar{\psi}$ and $\bar{\theta}$ in (2.22) are real functions. Hence, solutions in (2.22) reduce to

$$\psi = A\ F(z)\sin kx, \qquad \theta = A\ G(z)\cos kx, \tag{2.36}$$

where A is an arbitrary amplitude. Hence, from (2.35) we obtain a boundary value problem consisting of two second order ODEs in z:

$$\begin{cases} F'' - k^2F + \mathrm{Ra}\,kG = 0, \\ G'' - k^2G + \mathrm{Pe}\,G' - kg'F = 0, \end{cases} \tag{2.37}$$

with the boundary conditions:

$$F(0) = 0,\ F(1) = 0,\ G(0) = 0,\ G(1) = 0. \tag{2.38}$$

Nonzero solutions of this ordinary differential eigenvalue problem for Ra were guaranteed by the use of the fifth boundary condition,

$$G'(0) = \text{nonzero constant}, \tag{2.39}$$

which is one of various ways of normalising the eigensolution. This extra condition requires one further ordinary differential equation and, given that Ra is a constant, we may supplement Eqs. (2.37) with

$$\mathrm{Ra}' = 0. \tag{2.40}$$

The fifth order system, (2.37)-(2.40), was solved using the shooting method as described in [79, 80, 12]. To summarise: the system was first reduced to first order form consisting of five ODEs. However, only three initial conditions are given and therefore the values of the two remaining ones ($F'(0)$ and Ra) were found by using a Newton-Raphson iteration scheme which ensures that both the known boundary conditions at $z = 1$ ($F(1) = 0$ and $G(1) = 0$) are satisfied. The classical fourth

order Runge-Kutta method was used as the basic solver, and it was found that solutions were generally correct to between five and six decimal places.

The system (2.37)-(2.40) was found to provide a unimodal neutral curve, $\mathrm{Ra}(k)$, with a unique minimum for all values of the Péclet number. The critical Rayleigh number, Ra_c, is defined as being that value which corresponds to the minimum of the neutral curve while the critical wavenumber, k_c, is the corresponding wavenumber where,

$$\mathrm{Ra}_c = \min_{k\in\mathbb{R}^+} \mathrm{Ra}(k) = \mathrm{Ra}(k_c). \tag{2.41}$$

Accurate numerical values of Ra_c and k_c need the system (2.37) to be replaced by a suitable extended system that will fulfil Eq. (2.41). Therefore we solved the following system:

$$\begin{cases} F'' - k^2 F + \mathrm{Ra}\, kG = 0, \\ G'' - k^2 G + \mathrm{Pe}\, G' - kg'F = 0 \\ \mathrm{Ra}' = 0, \\ F_1'' - k^2 F_1 - 2kF + \mathrm{Ra}(G + kG_1) = 0, \\ G_1'' - k^2 G_1 - 2kG + \mathrm{Pe}\, G_1' - g'(F + kF_1) = 0, \\ k' = 0, \end{cases} \tag{2.42}$$

where $F_1 = F_{,k}$, $G_1 = G_{,k}$. The full set of boundary conditions is,

$$F = G = F_1 = G_1 = 0 \quad \text{for } z = 0{,}1 \qquad \text{and} \qquad G'(0) = 1/\pi,\ G_1'(0) = 0, \tag{2.43}$$

where the specific value used here for $G'(0)$ will be discussed in the following section, while $G_1'(0)$ may take any value.

Figure 2.3 shows the neutral curves for values of the Péclet number varying between $\mathrm{Pe} = 0$ and $\mathrm{Pe} = 10$ with unit increments. These were obtained by solving the system (2.37)-(2.40). Also shown as small disks are the critical points (k_c, Ra_c), which were obtained by solving the system (2.42)-(2.43).

When Pe increases from zero, it is immediately apparent that Ra_c increases and thus the system is stabilised increasingly. The corresponding critical wavenumber also increases which means that the wavelength of the convecting pattern decreases. As has already been mentioned, the basic temperature field becomes increasingly confined to the lower part of the layer as Pe increases, and therefore disturbances will be increasingly concentrated there. This is confirmed in Figure 2.4 where we see that locations of the extreme values of both the streamfunction and the isotherms descend as Pe increases. At the moderate value, $\mathrm{Pe} = 3$, the cells still occupy the full cavity but have clearly lost the up/down symmetry that is present when $\mathrm{Pe} = 0$. But when $\mathrm{Pe} = 10$ both the flow and temperature fields are essentially detached from the upper surface, and this becomes increasingly so as Pe increases still further. The width of the convecting cells has now become proportional to the

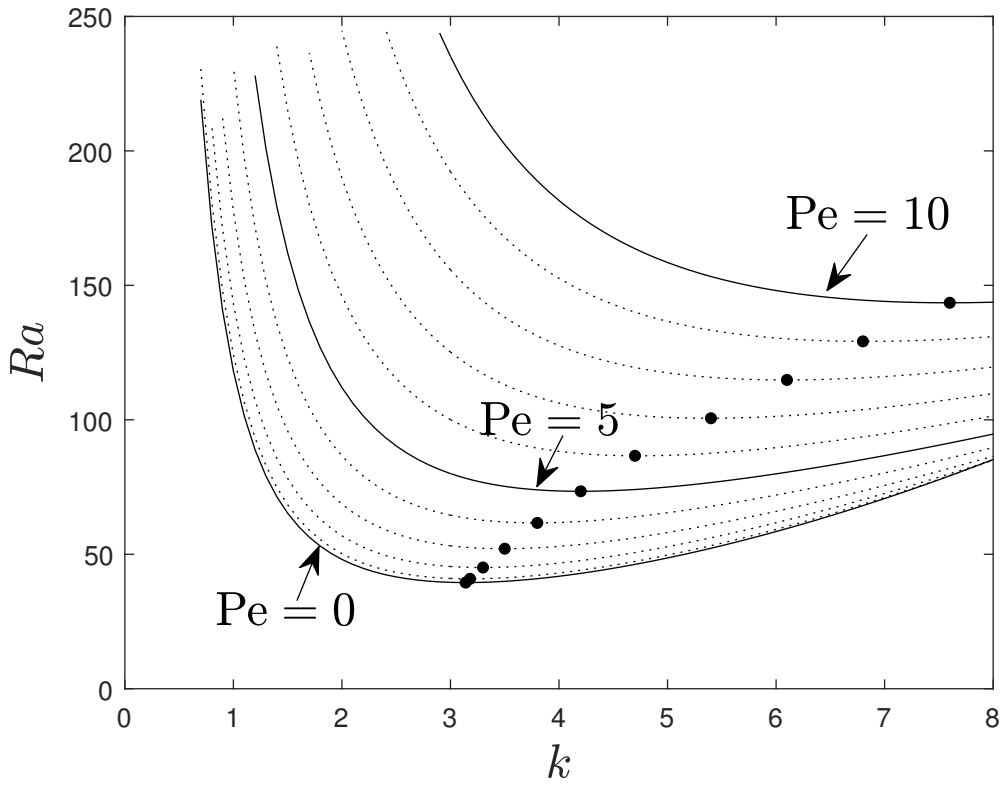

Figure 2.3: Neutral curves $\mathrm{Ra}(k)$ for increasing values of Pe. The circles show the location of the minimum, $\mathrm{Ra_c}$ of each curve.

height of the thinning basic thermal boundary layer as we approach the large-Pe asymptotic regime that is the Wooding problem.

Figures 2.5a and 2.5b show how the critical values of Ra_c and k_c vary as Pe increases. The respective values for the Darcy-Bénard problem are recovered when $\mathrm{Pe} = 0$, while the red dashes show the approach to the Wooding problem as Pe increases for which

$$(k_w, \mathrm{Ra}_w) = (0.7589, 14.3522) \qquad \Rightarrow \qquad (k_c, \mathrm{Ra}_c) \sim (0.7589{,}14.3522)\mathrm{Pe}, \quad (2.44)$$

where the numerical data was taken from [81] and confirmed by the present authors.

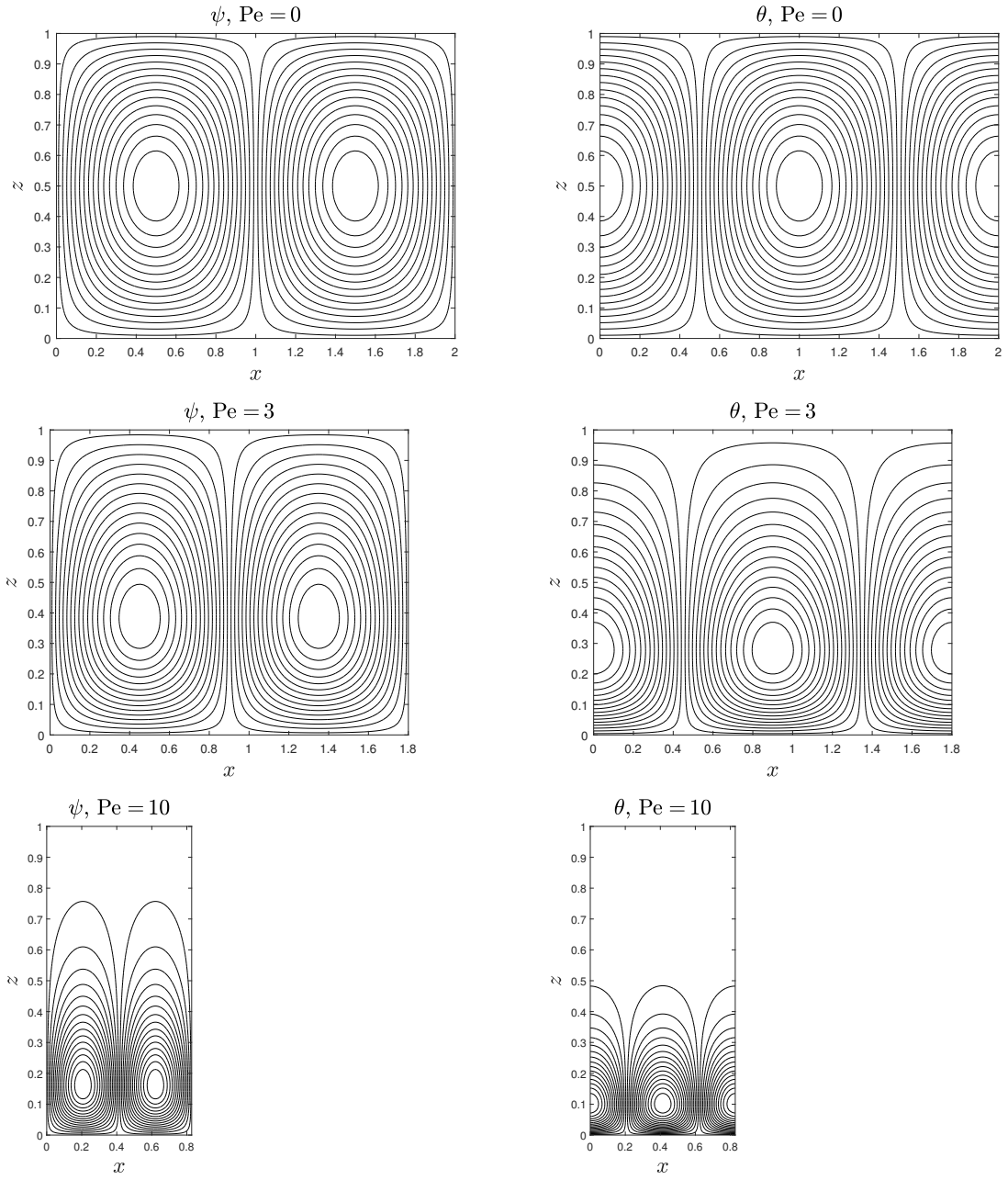

Figure 2.4: Streamlines and isothermal for the quoted values of the Péclet number.

2.5 Weakly nonlinear analysis

It is well-known that the onset of convection for the Darcy-Bénard problem (Pe = 0) is supercritical for all wavenumbers ([82]) and so the primary aim here is to determine whether or not this remains true in the presence of a vertical throughflow.

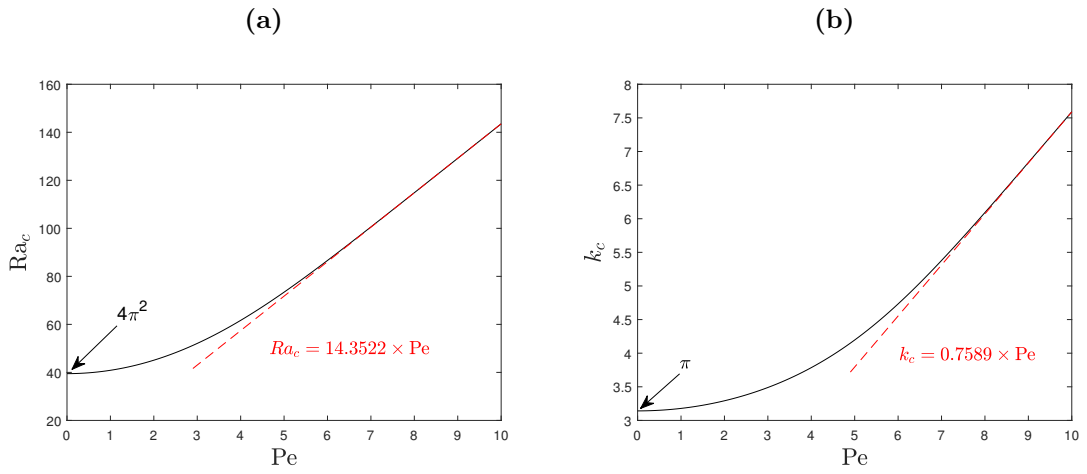

Figure 2.5: The variation of (a) Ra_c and (b) k_c with the Péclet number. In both cases the dashed red line corresponds to the Wooding problem.

Therefore we shall undertake a weakly nonlinear analysis of the basic steady solution (2.16) close to the onset of convection. Such an analysis allows us to determine the so-called Landau equation which relates the amplitude of the most unstable mode to the deviation of the Rayleigh number from its critical value. The coefficients of the Landau equation will determine whether or not the onset of convection is supercritical or subcritical.

Let us introduce a small parameter $\epsilon \ll 1$ and perturb the critical Rayleigh number by an $O(\epsilon^2)$ amount [83], i.e. let

$$\mathrm{Ra} = \mathrm{Ra}_0 + \epsilon^2 \mathrm{Ra}_2 + \dots \tag{2.45}$$

where Ra_0 is a neutral value of the Rayleigh number arising from the linear analysis. Given the proximity of the Rayleigh number to its critical value we will need to define τ to be a suitably slow time scale, as follows,

$$\tau = \tfrac{1}{2}\epsilon^2 t, \tag{2.46}$$

where the numerical factor was chosen so that the resulting Landau equation will have solely unit coefficients when $\mathrm{Pe} = 0$ and $k = \pi$. Hence system (2.17) becomes,

$$\begin{cases} \nabla^2\psi = (\mathrm{Ra}_0 + \epsilon^2 \mathrm{Ra}_2)\theta_{,x}, \\ \nabla^2\theta = \tfrac{1}{2}\epsilon^2\theta_{,\tau} - \mathrm{Pe}\,\theta_{,z} + g'(z)\psi_{,x} + \psi_{,x}\theta_{,z} - \psi_{,z}\theta_{,x}. \end{cases} \tag{2.47}$$

The weakly nonlinear analysis proceeds by expanding the solution of (2.47) as a power series in ϵ [79]:

$$\begin{pmatrix} \psi \\ \theta \end{pmatrix} = \sum_{n=1}^{\infty} \epsilon^n \begin{pmatrix} \psi_n \\ \theta_n \end{pmatrix}. \tag{2.48}$$

The following analysis focuses on the first three orders of approximation arising from the substitution of (2.48) into (2.47).

2.5.1 First order

At the first order of approximation, $O(\epsilon)$, the resulting equations coincide with the linear system (2.35), i.e.

$$\begin{cases} \nabla^2\psi_1 = \mathrm{Ra}_0\theta_{1,x}, \\ \nabla^2\theta_1 = -\mathrm{Pe}\,\theta_{1,z} + g'(z)\psi_{1,x}, \end{cases} \tag{2.49}$$

for which we may choose the following solution

$$\begin{cases} \psi_1 = A(\tau)f_1(z)\sin kx, \\ \theta_1 = A(\tau)g_1(z)\cos kx, \end{cases} \tag{2.50}$$

where $A(\tau)$ is the amplitude of the perturbation which evolves slowly in time. Hence, upon substituting (2.50) in (2.49), we obtain (2.37) which can be solved as already described in Section 2.4.

2.5.2 Second order

At the second order of approximation, $O(\epsilon^2)$, the first self-interaction of the perturbation occurs. System (2.47) reduces to

$$\begin{cases} \nabla^2\psi_2 - \mathrm{Ra}_0\theta_{2,x} = 0, \\ \nabla^2\theta_2 = -\mathrm{Pe}\,\theta_{2,z} + g'(z)\psi_{2,x} + \psi_{1,x}\theta_{1,z} - \psi_{1,z}\theta_{1,x}. \end{cases} \tag{2.51}$$

Since

$$\begin{aligned} \psi_{1,x}\theta_{1,z} - \psi_{1,z}\theta_{1,x} =& A^2k(f_1g_1'\cos^2 kx + f_1'g_1\sin^2 kx) \\ =& \tfrac{1}{2}A^2k\Big[f_1g_1' + f_1'g_1 + (f_1g_1' - f_1'g_1)\cos 2kx\Big] \end{aligned} \tag{2.52}$$

we choose the following form as the solutions for (2.51),

$$\begin{cases} \psi_2 = A^2(\tau)f_2(z)\sin 2kx, \\ \theta_2 = A^2(\tau)g_0(z) + A^2(\tau)g_2(z)\cos 2kx. \end{cases} \tag{2.53}$$

Hence, the resulting system of ODEs is

$$\begin{cases} f_2'' - 4k^2f_2 + \mathrm{Ra}_0 2kg_2 = 0, \\ g_2'' - 4k^2g_2 + \mathrm{Pe}g_2' - 2kg'f_2 = \tfrac{1}{2}k(f_1g_1' - f_1'g_1), \\ g_0'' + \mathrm{Pe}\,g_0' = \tfrac{1}{2}k(f_1g_1' + f_1'g_1), \end{cases} \tag{2.54}$$

where each of f_2, g_2 and g_0 are zero at $z = 0{,}1$. Generally these equations may be solved easily because the inhomogeneous terms are nonresonant.

2.5.3 Third order

A further self-interaction appears in the $O(\epsilon^3)$ system, which is

$$\begin{cases} \nabla^2\psi_3 = \mathrm{Ra}_0\theta_{3,x} + \mathrm{Ra}_2\theta_{1,x}, \\ \nabla^2\theta_3 = \frac{1}{2}\theta_{1,\tau} - \mathrm{Pe}\,\theta_{3,z} + g'(z)\psi_{3,x} + \psi_{1,x}\theta_{2,z} + \psi_{2,x}\theta_{1,z} - \psi_{1,z}\theta_{2,x} - \psi_{2,z}\theta_{1,x}. \end{cases} \tag{2.55}$$

By employing solutions (2.50) and (2.53) and defining the partial differential operators $\mathcal{L}_1$ and $\mathcal{L}_2$ to be such that

$$\begin{aligned} \mathcal{L}_1(\psi_3, \theta_3) &= \nabla^2\psi_3 - \mathrm{Ra}_0\theta_{3,x}, \\ \mathcal{L}_2(\psi_3, \theta_3) &= \nabla^2\theta_3 + \mathrm{Pe}\theta_{3,z} - g'(z)\psi_{3,x}, \end{aligned} \tag{2.56}$$

the resulting system is

$$\begin{cases} \mathcal{L}_1(\psi_3, \theta_3) = & -\mathrm{Ra}_2 A k g_1 \sin kx, \\ \mathcal{L}_2(\psi_3, \theta_3) = & \frac{1}{2}A_\tau g_1 \cos kx \\ & + A^3\Big\{\Big[f_1 g_0' + \frac{1}{2}(f_1 g_2' + 2f_2 g_1' + 2f_1' g_2 + f_2' g_1)\Big] k\cos kx \\ & \qquad + \frac{1}{2}\Big[f_1 g_2' + 2f_2 g_1' - 2f_1' g_2 - f_2' g_1\Big] k\cos 3kx\Big\} \end{cases} \tag{2.57}$$

Many of the inhomogeneous terms in (2.57) have the wavenumber, k, in the x-direction and are therefore resonant because the partial differential operators on the left hand side have eigensolutions with the same the same horizontal wavenumber. This means that (2.57) cannot be solved unless a solvability condition involving A, A_τ and Ra_2 can be found. In many problems, particularly those which are self-adjoint, it is usually quite straightforward to write down an integral solvability condition for this purpose. The present system is not self-adjoint, but it remains possible to obtain a solvability condition using numerical means. The manner in which we accomplished this may be found in the Appendix, and it means that the quantities $\mathrm{Ra}_2 A$, $A_{,\tau}$ and A^3 need to balance in such a way that they satisfy the Landau equation,

$$c_1 A_{,\tau} = \mathrm{Ra}_2 A - c_2 A^3, \tag{2.58}$$

where the values of c_1 and c_2 are obtained numerically. As a partial check on the accuracy of the present analysis, the value $G'(0) = 1/\pi$ in (2.43) and the $1/2$ using for the definition of τ in (2.46) yield $c_1 = c_2 = 1$ when $\mathrm{Pe} = 0$, $k = \pi$ and $\mathrm{Ra} = 4\pi^2$, a result that may be shown analytically. The value, c_1, is found always to be positive; we shall not discuss its value but we note that it is related to the speed at which A varies and it may even be scaled out of Eq. (2.58) by a suitable redefinition of τ.

Eq. (2.58) admits the steady solutions $A = 0$ and $A = \pm\sqrt{\mathrm{Ra}_2/c_2}$. The former is a stable state when $\mathrm{Ra}_2 < 0$ and an unstable one when $\mathrm{Ra}_2 > 0$; these conclusions

are consistent with the linear theory presented earlier. The nonzero solution exists when both Ra_2 and c_2 have the same sign. Therefore positive values of c_2 mean that nonzero solutions arise when $\mathrm{Ra}_2 > 0$ and therefore the onset of convection is supercritical in such cases. This property is shared with the Darcy-Bénard problem. On the other hand, negative values of c_2 means that steady nonzero solutions exist only when $\mathrm{Ra}_2 < 0$, and so the bifurcation is subcritical (see [84, p. 21]). It is already known that the onset of convection is subcritical for the Wooding problem, $\mathrm{Pe} \to \infty$ ([85]).

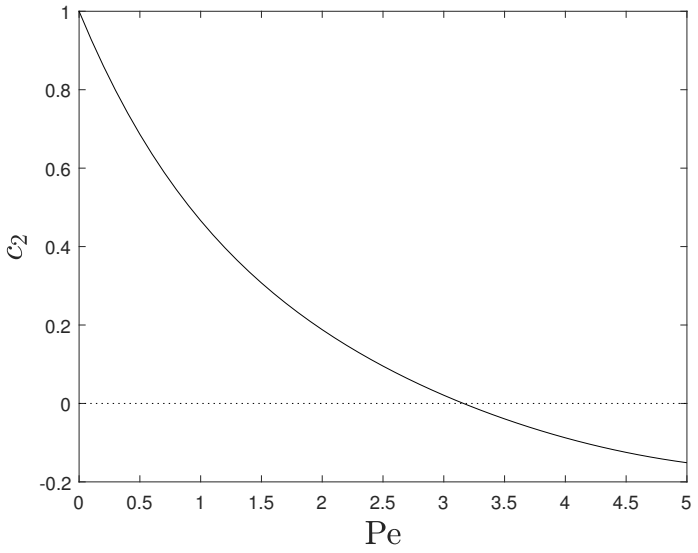

Figure 2.6: Variation of c_2 with Pe when $k = k_c(\mathrm{Pe})$.

Therefore the simplest *a priori* expectation is that the transition between a supercritical onset and a subcritical one will take place at an intermediate value of Pe, i.e. when the value of c_2 changes sign. The detailed dependence of c_2 on Pe is shown in Figure 2.6, where one may see that c_2 decreases from 1 as Pe increases from zero, and that it changes sign when $\mathrm{Pe} = 3.1617$. So far, we have been considering the weakly nonlinear theory at the minimum in the neutral curves, i.e. when $\mathrm{Ra} = \mathrm{Ra}_c$ and $k = k_c$, and therefore $\mathrm{Pe} = 3.1617$ marks the global transition between supercritical and subcritical onset subject to that restriction.

We shall now consider what happens at other points on the neutral curves by computing the variation of c_2 along each curve. Figure 2.7 shows a selection of neutral curves where those portions which correspond to a supercritical instability ($c_2 > 0$) are rendered in black, while those which are subcritical ($c_2 < 0$) are rendered in red. Also shown are the neutral pairs, (k_c, Ra_c), as the dotted line. In the figure there are two clear boundaries which demarkate the edge of the region of subcriticality at onset. For convenience we shall refer to these as the left and right

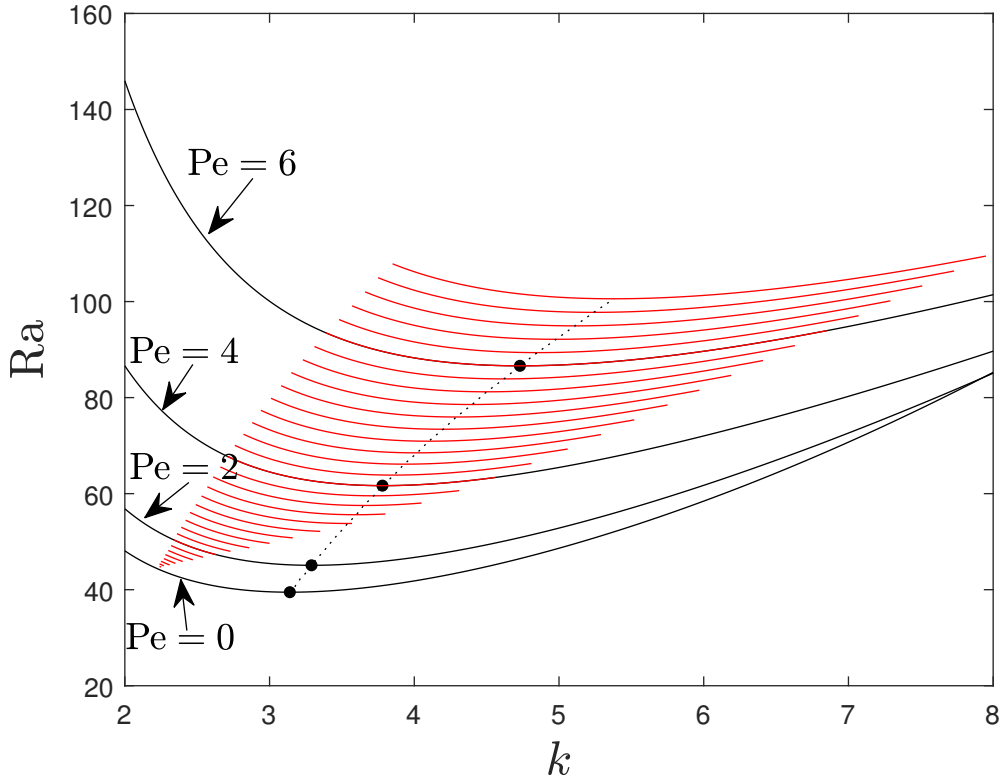

Figure 2.7: Region of subcritical instability as Pe increases.

transitional loci.

Immediately, it is clear that all neutral curves, with the exception of when $\mathrm{Pe} = 0$, have some portion which corresponds to subcritical instability. Whenever $\mathrm{Pe} < 3.1617$ these sections of the neutral curve do not include the minimum. Therefore the onset of convection in an unbounded domain will be supercritical. But once Pe rises above 3.1617 onset will be subcritical. Clearly, if the domain is bounded horizontally by insulated and impermeable boundaries, then the neutral values of Ra will correspond to a set of discrete values of k. Then the issue of whether onset is supercritical or subcritical will depend on which value of the Rayleigh number is the smallest.

The right hand transitional locus corresponds to when $c_2 = 0$ and this represents a transition from subcriticality to supercriticality as k increases. However, the left hand transitional locus marks the value of k where c_2 has a simple pole. So as the locus is approached from the left $c_2 \to \infty$ but as it is approached from the right then $c_2 \to -\infty$. A detailed examination of the intermediate solutions in the above weakly nonlinear theory shows that the solutions for f_2 and g_2 in (2.54) become infinite in magnitude as this boundary is approached. This marks a new resonance

but it is one which involves forcing terms with the wavenumber, $2k$. Indeed, this left hand boundary is precisely where $\mathrm{Ra}(k) = \mathrm{Ra}(2k)$ which is the source of the resonance. Our conclusion for now is that the Landau equation given above is inadequate in this isolated case and the nonlinear dynamics close to onset will involve both wavenumbers as competing solutions.

Finally, we note that the left and right transitional loci merge when $\mathrm{Pe} = 0$ which is where we recover the Darcy-Bénard problem. In this case there is no resonance at all because the inhomogeneous terms in (2.54) have an odd symmetry about $z = \frac{1}{2}$ whereas the $O(\epsilon)$ eigensolutions are even. However, it is our intention in a subsequent paper to break this symmetry weakly by allowing $\mathrm{Pe} = O(\epsilon)$ in magnitude; such a device will relegate the problematical resonance mentioned in the previous paragraph to the $O(\epsilon^3)$ equations and therefore it will be possible to obtain a pair of coupled Landau equations for the amplitudes of the k-mode and the $2k$-mode.

2.6 Conclusions

We have studied the onset of convection in a fluid-saturated horizontal porous layer heated from below and under the action of a uniform vertical throughflow. The principle of exchange of stabilities has been proved to hold and a linear instability analysis has been provided in order to set the context for the subsequent weakly nonlinear analysis. The main aim of the weakly nonlinear analysis was to establish whether or not the onset of convection is supercritical in all cases and, if not, to determine those circumstances when subcriticality may be expected. Figure 2.7 gives the locus within which the onset of convection is subcritical. We found that the onset of convection at the critical values will always be subcritical once the Péclet number exceeds 3.1617, but that a subcritical onset always arises when $\mathrm{Pe} \neq 0$ but only over ranges of wavenumber that do not contain the critical value.

We have already mentioned one possible extention to the present work where we will consider what happens when $\mathrm{Pe} = O(\epsilon)$. Another study which will supplement the present work involves undertaking strongly nonlinear computations, one aim for which will be to determine the depth of subcriticality of convective motion. This will enable us to provide a nonlinear stability curves to supplement the present linear stability curves and to compare with energy-based methods. Such an analysis already exists for the Wooding problem in [85] where that author found that nonlinear onset takes place when,

$$\mathrm{Ra}_w = 11.6132 \quad \text{and} \quad k_w = 0.2867, \tag{2.59}$$

which should be compared with the values given in (2.44).

Appendix

Since (2.58) holds also for the stationary case, we can suppress the time derivative term A_τ in system (2.57), obtaining

$$\begin{cases} \mathcal{L}_1(\psi_3,\theta_3) = \ -\mathrm{Ra}_2 A k g_1 \sin kx, \\ \mathcal{L}_2(\psi_3,\theta_3) = A^3\Big\{\Big[f_1 g_0' + \frac{1}{2}(f_1 g_2' + 2f_2 g_1' + 2f_1' g_2 + f_2' g_1)\Big] k\cos kx \\ \qquad\qquad + \frac{1}{2}\Big[f_1 g_2' + 2f_2 g_1' - 2f_1' g_2 - f_2' g_1\Big] k\cos 3kx\Big\} \end{cases} \tag{2.60}$$

The resulting system (2.60) admits the following solution

$$\psi_3 = A^3\ f_3(z)\sin kx, \qquad \theta_3 = A^3\ g_3(z)\cos kx, \tag{2.61}$$

Hence, substituting solution (2.61) in (2.60) and dividing both sides of the equations by A^3, we get

$$\begin{cases} f_3'' - k^2 f_3 + \mathrm{Ra}_0 k g_3 = \ -\left(\dfrac{\mathrm{Ra}_2}{A^2}\right) k g_1 \sin kx, \\ g_3'' - k^2 g_3 + \mathrm{Pe} g_3' - g'(z) k f_3 = \Big[f_1 g_0' + \frac{1}{2}(f_1 g_2' + 2f_2 g_1' + 2f_1' g_2 + f_2' g_1)\Big] k\cos kx \\ \qquad\qquad + \frac{1}{2}\Big[f_1 g_2' + 2f_2 g_1' - 2f_1' g_2 - f_2' g_1\Big] k\cos 3kx \end{cases} \tag{2.62}$$

We then solved system (2.62) as an eigenvalue problem for Ra_2/A^2 from which, and given the form of (2.58), we may now say that

$$c_2 = \frac{\mathrm{Ra}_2}{A^2}. \tag{2.63}$$

A similar device was used to compute c_1.

Chapter 3

Optimal stability thresholds in a rotating fully anisotropic porous medium with LTNE

3.1 Introduction

In the present chapter, it is analysed the onset of convection in a fully anisotropic porous medium in LTNE scheme, allowing for the Corolis force (see [86]). Linear and nonlinear stability analyses of the conduction solution are performed. In particular, the coincidence between the global nonlinear stability threshold and the linear instability threshold is proved. This means that a necessary and sufficient condition for global nonlinear stability of conduction solution is obtained.

In section 3.2, we introduce the mathematical model and the dimensionless evolution equations for perturbation fields to conduction solution in order to study the stability of the motionless state. Then, in section 3.3, a detailed proof of the strong form of the principle of exchange of stabilities is performed and the critical Rayleigh number for the onset of (stationary) convection is determined, in a closed algebraic form. Section 3.4 deals with the nonlinear stability analysis of the conduction solution, with respect to the L^2-norm. Finally, in section 3.5 numerical simulations concerning the influence of rotation and anisotropy on the stability/instability thresholds is analysed. We show that the increasing conductivity ratio γ has a destabilizing effect on conduction. Mechanical anisotropy ξ_i $(i = 1,2)$ has the same effect, for ξ_j small $(j \neq i)$, while a slightly different behaviour is obtained when ξ_j is high. Then we prove that increasing fluid and solid thermal conductivities delay the onset of convection, as well as rotation. Moreover, the presence of anisotropy forces the fluid in a two-dimensional motion. Convective cells are rolls aligned in x or y direction, depending on the ratios between anisotropy parameters.

3.2 Local thermal nonequilibrium model

Let us consider a horizontal porous layer of depth d, filled by an incompressible, homogeneous fluid at rest. We assume that the medium is uniformly heated from below and uniformly rotating about the vertical axis z (upward vertical) with constant angular velocity Ω. Let T_L be the temperature of the lower plane $z = 0$ and let T_U be the temperature of the upper plane $z = d$. In the local thermal non equilibrium scheme (LTNE), denoting by T_f and T_s the fluid temperature and the solid skeleton temperature, respectively, it turns out that

$$T_s = T_f = T_L \quad \text{on } z = 0, \qquad T_s = T_f = T_U \quad \text{on } z = d \quad (T_L > T_U)\,. \tag{3.1}$$

Moreover, we assume that the layer is anisotropic and we denote by $\mathcal{K}$ the permeability tensor, and let $\mathcal{D}_s$, $\mathcal{D}_f$ be the thermal conductivity tensors of solid phase and fluid phase, respectively. Assume that the principal axis (x, y, z) of the permeability tensor are the same as the ones of conductivity tensor, one obtains

$$\begin{aligned}
&\mathcal{K} = K_z\mathcal{K}^* \qquad \mathcal{K}^* = \begin{pmatrix} \xi_1 & 0 & 0 \\ 0 & \xi_2 & 0 \\ 0 & 0 & 1 \end{pmatrix} \qquad \xi_1 = \frac{K_x}{K_z} \quad \xi_2 = \frac{K_y}{K_z} \\
&\mathcal{D}_s = \kappa_z^s\mathcal{D}_s^* \qquad \mathcal{D}_s^* = \begin{pmatrix} \zeta_1 & 0 & 0 \\ 0 & \zeta_2 & 0 \\ 0 & 0 & 1 \end{pmatrix} \qquad \zeta_1 = \frac{\kappa_x^s}{\kappa_z^s} \quad \zeta_2 = \frac{\kappa_y^s}{\kappa_z^s} \\
&\mathcal{D}_f = \kappa_z^f\mathcal{D}_f^* \qquad \mathcal{D}_f^* = \begin{pmatrix} \eta & 0 & 0 \\ 0 & \eta & 0 \\ 0 & 0 & 1 \end{pmatrix} \qquad \eta = \frac{\kappa_h^f}{\kappa_z^f}
\end{aligned} \tag{3.2}$$

where, in particular, η is the thermal anisotropy parameter for the fluid phase.

The mathematical model, in the Oberbeck - Boussinesq approximation and accounting for the Coriolis force due to the uniform rotation of the layer about the vertical axis z is [11, 27, 17, 51]

$$\begin{cases}
\mathbf{v} = \mu^{-1}\mathcal{K}\left[-\nabla p + \rho_f g\alpha T_f\mathbf{k} - \dfrac{2\Omega\rho_f}{\varepsilon}\mathbf{k}\times\mathbf{v}\right] \\
\nabla\cdot\mathbf{v} = 0 \\
\varepsilon(\rho c)_f T_{,t}^f + (\rho c)_f\mathbf{v}\cdot\nabla T_f = \varepsilon\nabla\cdot(\mathcal{D}^f\cdot\nabla T_f) + h(T_s - T_f) \\
(1-\varepsilon)(\rho c)_s T_{,t}^s = (1-\varepsilon)\nabla\cdot(\mathcal{D}^s\cdot\nabla T_s) - h(T_s - T_f)
\end{cases} \tag{3.3}$$

where $\mathbf{v}$, p, T_s and T_f are (seepage) velocity, reduced pressure, solid phase temperature and fluid phase temperature, respectively; μ, ρ_f, ρ_s, g, α, Ω, ε, c, h are dynamic viscosity, fluid density, solid density, gravity acceleration, thermal expansion coefficient, angular velocity, porosity, specific heat and interaction coefficient, respectively.

To system (3.3) we append the following boundary conditions

$$\begin{aligned} &T_s = T_f = T_L \quad \text{on } z = 0, \qquad T_s = T_f = T_U \quad \text{on } z = d, \\ &\mathbf{v} \cdot \mathbf{n} = 0 \quad \text{on } z = 0, d \end{aligned} \tag{3.4}$$

being $\mathbf{n}$ the unit outward normal to planes $z = 0, d$.

The system (3.3) admits the conduction solution m_0:

$$m_0 = \left\{ \bar{\mathbf{v}} = \mathbf{0}\,, \quad \bar{T}_s = \bar{T}_f = -\beta z + T_L\,, \quad \bar{p} = -\rho_f g \alpha \beta \frac{z^2}{2} + \rho_f g \alpha T_L z \right\} \tag{3.5}$$

where $\beta = \dfrac{T_L - T_U}{d} (> 0)$ is the adverse temperature gradient.

In order to study the stability of the steady solution (3.5), let us introduce the following perturbation fields

$$v_i = u_i + \bar{v}_i \qquad T_s = \varphi + \bar{T}_s \qquad T_f = \theta + \bar{T}_f \qquad p = \pi + \bar{p} \tag{3.6}$$

and the dimensionless quantities

$$x_i = \tilde{x}_i d, \quad t = \tilde{t} \frac{\varepsilon d}{U}, \quad \pi = \tilde{\pi} P, \quad u_i = \tilde{u}_i U, \quad \theta = \tilde{\theta} T', \quad \varphi = \tilde{\varphi} T' \tag{3.7}$$

where

$$U = \frac{\varepsilon \kappa_z^f}{(\rho c)_f d}\,, \qquad P = \frac{U \mu d}{K_z}\,, \qquad T' = \beta d \sqrt{\frac{\kappa_z^f \varepsilon \mu}{\beta g \alpha K_z \rho_f^2 c_f d^2}}. \tag{3.8}$$

The dimensionless equations for the perturbation fields, omitting all the tilde, are

$$\begin{cases} \mathcal{K}^{-1} \mathbf{u} = -\nabla \pi + R \theta \mathbf{k} - \mathcal{T} \mathbf{k} \times \mathbf{u} \\ \nabla \cdot \mathbf{u} = 0 \\ \theta_{,t} + \mathbf{u} \cdot \nabla \theta = Rw + \eta \Delta_1 \theta + \theta_{,zz} + H(\varphi - \theta) \\ A \varphi_{,t} - \zeta_1 \varphi_{,xx} - \zeta_2 \varphi_{,yy} - \varphi_{,zz} + H \gamma (\varphi - \theta) = 0 \end{cases} \tag{3.9}$$

where $\Delta_1 = \partial_{,xx} + \partial_{,yy}$ and

$$\gamma = \frac{\varepsilon \kappa_z^f}{(1-\varepsilon)\kappa_z^s}\,, \qquad A = \frac{(\rho c)_s \kappa_z^f}{(\rho c)_f \kappa_z^s}\,, \qquad H = \frac{h d^2}{\varepsilon \kappa_z^f}$$

$$R^2 = \frac{K_z \rho_f^2 c_f d^2 \beta g \alpha}{\mu \varepsilon \kappa_z^f} \quad \text{Rayleigh number}\,, \quad \mathcal{T} = \frac{2 \Omega \rho_f K_z}{\varepsilon \mu} \quad \text{Taylor number.}$$

To system (3.9) we append the following initial conditions

$$\mathbf{u}(\mathbf{x},0) = \mathbf{u}_0(\mathbf{x})\,, \quad \pi(\mathbf{x},0) = \pi_0(\mathbf{x})\,, \quad \theta(\mathbf{x},0) = \theta_0(\mathbf{x})\,, \quad \varphi(\mathbf{x},0) = \varphi_0(\mathbf{x}) \tag{3.10}$$

where $\nabla \cdot \mathbf{u}_0 = 0$, and the following boundary conditions

$$w = \theta = \varphi = 0 \qquad \text{on } z = 0,1. \tag{3.11}$$

We assume that perturbation fields are periodic in x and y directions of periods $\frac{2\pi}{a_x}$ and $\frac{2\pi}{a_y}$, respectively, and they belong to $W^{2,2}(V)$, $\forall t \in \mathbb{R}^+$ where $V = \left[0, \frac{2\pi}{a_x}\right] \times \left[0, \frac{2\pi}{a_y}\right] \times [0,1]$ is the periodicity cell. Then we denote by $(\cdot,\cdot)$ and $\|\cdot\|$ the scalar product on the Hilbert space $L^2(V)$, and the related norm, respectively.

3.3 Principle of exchange of stabilities

In order to study the linear stability of m_0, let us consider the linear version of (3.9), i.e.

$$\begin{cases} \mathcal{K}^{-1}\mathbf{u} = -\nabla\pi + R\theta\mathbf{k} - \mathcal{T}\mathbf{k}\times\mathbf{u} \\ \nabla\cdot\mathbf{u} = 0 \\ \theta_{,t} = Rw + \eta\Delta_1\theta + \theta_{,zz} + H(\varphi-\theta) \\ A\varphi_{,t} - \zeta_1\varphi_{,xx} - \zeta_2\varphi_{,yy} - \varphi_{,zz} + H\gamma(\varphi-\theta) = 0 \end{cases} \tag{3.12}$$

under the boundary conditions (3.11). Applying the curl to $(3.12)_1$, one obtains

$$\begin{cases} w_{,y}\xi_2 - v_{,z} = R\theta_{,y}\xi_2 + \mathcal{T}u_{,z}\xi_2 \\ u_{,z} - w_{,x}\xi_1 = -R\theta_{,x}\xi_1 + \mathcal{T}v_{,z}\xi_1 \\ v_{,x}\xi_1 - u_{,y}\xi_2 = \mathcal{T}\xi_1\xi_2 w_{,z} \end{cases} \tag{3.13}$$

and deriving $(3.13)_1$ by y, $(3.13)_2$ by x and $(3.13)_3$ by z, one gets

$$\begin{cases} w_{,yy}\xi_2 - v_{,zy} = R\theta_{,yy}\xi_2 + \mathcal{T}u_{,zy}\xi_2 \\ u_{,zx} - w_{,xx}\xi_1 = -R\theta_{,xx}\xi_1 + \mathcal{T}v_{,zx}\xi_1 \\ v_{,xz}\xi_1 - u_{,yz}\xi_2 = \mathcal{T}\xi_1\xi_2 w_{,zz}. \end{cases} \tag{3.14}$$

Subtracting $(3.14)_2$ from $(3.14)_1$ and then substituting the result in $(3.14)_3$, it follows that

$$\xi_1 w_{,xx} + \xi_2 w_{,yy} + w_{,zz} = \xi_1 R\theta_{,xx} + \xi_2 R\theta_{,yy} - \mathcal{T}^2\xi_1\xi_2 w_{,zz}. \tag{3.15}$$

Let us consider now the autonomous system

$$\begin{cases} \xi_1 w_{,xx} + \xi_2 w_{,yy} + w_{,zz} + \mathcal{T}^2\xi_1\xi_2 w_{,zz} - \xi_1 R\theta_{,xx} - \xi_2 R\theta_{,yy} = 0 \\ \theta_{,t} - Rw - \eta\Delta_1\theta - \theta_{,zz} - H(\varphi-\theta) = 0 \\ A\varphi_{,t} - \zeta_1\varphi_{,xx} - \zeta_2\varphi_{,yy} - \varphi_{,zz} + H\gamma(\varphi-\theta) = 0 \end{cases} \tag{3.16}$$

and seek for solutions having the following time-dependence ([87]):
$\hat{\varphi}(t,\mathbf{x}) = \varphi(\mathbf{x})\, e^{\sigma t}$, $\forall \hat{\varphi} \in (w,\theta,\varphi)$, $\sigma \in \mathbb{C}$, (3.16) becomes

$$\begin{cases} \xi_1 w_{,xx} + \xi_2 w_{,yy} + w_{,zz} + \mathcal{T}^2 \xi_1 \xi_2 w_{,zz} - \xi_1 R\theta_{,xx} - \xi_2 R\theta_{,yy} = 0 \\ \sigma\theta - Rw - \eta\Delta_1\theta - \theta_{,zz} - H(\varphi - \theta) = 0 \\ A\sigma\varphi - \zeta_1\varphi_{,xx} - \zeta_2\varphi_{,yy} - \varphi_{,zz} + H\gamma(\varphi - \theta) = 0. \end{cases} \tag{3.17}$$

Let us multiply $(3.17)_1$ by w^*, $(3.17)_2$ once by $\xi_1\theta^*_{,xx}$ and once by $\xi_2\theta^*_{,yy}$, $(3.17)_3$ once by $\xi_1\varphi^*_{,xx}$ and once by $\xi_2\varphi^*_{,yy}$, where the asterisks denote the complex conjugate, accounting for the boundary conditions one obtains:

$$\begin{aligned} &\sigma\left[\xi_1\|\theta_{,x}\|^2 + \xi_2\|\theta_{,y}\|^2 + \frac{A\xi_1}{\gamma}\|\varphi_{,x}\|^2 + \frac{A\xi_2}{\gamma}\|\varphi_{,y}\|^2\right] = -\xi_1\|w_{,x}\|^2 \\ &- \xi_2\|w_{,y}\|^2 - (1 + \mathcal{T}^2\xi_1\xi_2)\|w_{,z}\|^2 - \xi_1 R\left[(\theta_{,xx}, w^*) + (w, \theta^*_{,xx})\right] \\ &- \xi_2 R\left[(\theta_{,yy}, w^*) + (w, \theta^*_{,yy})\right] - \xi_1\eta\|\theta_{,xx}\|^2 - \xi_1\eta\|\theta_{,xy}\|^2 - \xi_1\|\theta_{,xz}\|^2 \\ &- H\xi_1\left[(\varphi_{,xx}, \theta^*) + (\theta, \varphi^*_{,xx})\right] - H\xi_1\|\theta_{,x}\|^2 - \xi_2\eta\|\theta_{,xy}\|^2 - \xi_2\eta\|\theta_{,yy}\|^2 \\ &- \xi_2\|\theta_{,yz}\|^2 - H\xi_2\left[(\varphi_{,yy}, \theta^*) + (\theta, \varphi^*_{,yy})\right] - H\xi_2\|\theta_{,y}\|^2 - \frac{\zeta_1\xi_1}{\gamma}\|\varphi_{,xx}\|^2 \\ &- \frac{\zeta_2\xi_1}{\gamma}\|\varphi_{,xy}\|^2 - \frac{\xi_1}{\gamma}\|\varphi_{,xz}\|^2 - H\xi_1\|\varphi_{,x}\|^2 - \frac{\zeta_1\xi_2}{\gamma}\|\varphi_{,xy}\|^2 \\ &- \frac{\zeta_2\xi_2}{\gamma}\|\varphi_{,yy}\|^2 - \frac{\xi_2}{\gamma}\|\varphi_{,yz}\|^2 - H\xi_2\|\varphi_{,y}\|^2 \end{aligned} \tag{3.18}$$

and hence, since terms in (3.18) are real, then necessarily $\sigma \in \mathbb{R}$. Therefore, *the strong form of the principle of exchange of stabilities holds*, i.e. convection can occur only through a steady motion.

In order to determine the critical Rayleigh number for the onset of convection, by virtue of the principle of exchange of stabilities, setting $\sigma = 0$ in (3.17), one obtains

$$\begin{cases} \xi_1 w_{,xx} + \xi_2 w_{,yy} + w_{,zz} + \mathcal{T}^2\xi_1\xi_2 w_{,zz} = \xi_1 R\theta_{,xx} + \xi_2 R\theta_{,yy} \\ \eta\Delta_1\theta + \theta_{,zz} - H\theta = -Rw - H\varphi \\ \zeta_1\varphi_{,xx} + \zeta_2\varphi_{,yy} + \varphi_{,zz} - H\gamma\varphi = -H\gamma\theta. \end{cases} \tag{3.19}$$

Denoting

$$\begin{aligned} \mathcal{L} &\equiv \xi_1\partial_{,xx} + \xi_2\partial_{,yy} + \partial_{,zz} + \mathcal{T}^2\xi_1\xi_2\partial_{,zz} \\ \mathcal{L}_1 &\equiv \eta\Delta_1\theta + \partial_{,zz} - H \\ \mathcal{L}_2 &\equiv \zeta_1\partial_{,xx} + \zeta_2\partial_{,yy} + \partial_{,zz} - H\gamma \end{aligned} \tag{3.20}$$

(3.19) becomes

$$\begin{cases} \mathcal{L}w = \xi_1 R\theta_{,xx} + \xi_2 R\theta_{,yy} \\ \mathcal{L}_1\theta = -Rw - H\varphi \\ \mathcal{L}_2\varphi = -H\gamma\theta. \end{cases} \tag{3.21}$$

Now, applying the operators $\mathcal{L}$ and $\mathcal{L}_2$ to $(3.21)_2$ and substituting $(3.21)_1$ and $(3.21)_3$ in the resulting equation, one leads

$$\mathcal{L}\mathcal{L}_1\mathcal{L}_2\theta = -R^2\xi_1(\mathcal{L}_2\theta)_{,xx} - R^2\xi_2(\mathcal{L}_2\theta)_{,yy} + H^2\gamma\mathcal{L}\theta. \tag{3.22}$$

Splitting the operators $\mathcal{L}_1$ and $\mathcal{L}_2$, from (3.22) it follows that

$$\begin{aligned} &(\zeta_1\partial_{,xx} + \zeta_2\partial_{,yy} + \partial_{,zz} - H\gamma)(\eta\Delta_1 + \partial_{,zz})\mathcal{L}\theta = \\ &= (\zeta_1\partial_{,xx} + \zeta_2\partial_{,yy} + \partial_{,zz})H\mathcal{L}\theta \\ &- R^2(\xi_1\partial_{,xx} + \xi_2\partial_{,yy})(\zeta_1\partial_{,xx} + \zeta_2\partial_{,yy} + \partial_{,zz})\theta \\ &+ R^2(\xi_1\partial_{,xx} + \xi_2\partial_{,yy})H\gamma\theta. \end{aligned} \tag{3.23}$$

By virtue of the periodicity and of the boundary conditions $(3.11)_2$, since the sequence $\{\sin(n\pi z)\}_{n\in\mathbb{N}}$ is a complete orthogonal system for $L^2([0,1])$, accounting for solutions of the form $\theta = \Theta_0 \sin(n\pi z)e^{i(a_x x + a_y y)}$, (3.23) becomes

$$\begin{aligned} &(-\zeta_1 a_x^2 - \zeta_2 a_y^2 - n^2\pi^2 - H\gamma)(-\eta a_x^2 - \eta a_y^2 - n^2\pi^2) \\ &(-\xi_1 a_x^2 - \xi_2 a_y^2 - n^2\pi^2 - \mathcal{T}^2\xi_1\xi_2 n^2\pi^2) = \\ &= (-\zeta_1 a_x^2 - \zeta_2 a_y^2 - n^2\pi^2)H(-\xi_1 a_x^2 - \xi_2 a_y^2 - n^2\pi^2 - \mathcal{T}^2\xi_1\xi_2 n^2\pi^2) \\ &- R^2(-\xi_1 a_x^2 - \xi_2 a_y^2)(-\zeta_1 a_x^2 - \zeta_2 a_y^2 - n^2\pi^2 - H\gamma). \end{aligned} \tag{3.24}$$

Setting $A^* = 1 + \mathcal{T}^2\xi_1\xi_2$ and

$$\begin{aligned} f(a_x^2, a_y^2, n^2) =& \frac{\xi_1 a_x^2 + \xi_2 a_y^2 + n^2\pi^2 A^*}{\xi_1 a_x^2 + \xi_2 a_y^2} \\ &\cdot \left[\eta a_x^2 + \eta a_y^2 + n^2\pi^2 + \frac{H(\zeta_1 a_x^2 + \zeta_2 a_y^2 + n^2\pi^2)}{\zeta_1 a_x^2 + \zeta_2 a_y^2 + n^2\pi^2 + H\gamma}\right], \end{aligned} \tag{3.25}$$

from (3.24) it follows that the critical Rayleigh number R_L for the onset of convection is given by

$$R_L = \min_{(n^2, a_x^2, a_y^2)\in\mathbb{N}\times\mathbb{R}^+\times\mathbb{R}^+} f(a_x^2, a_y^2, n^2) \tag{3.26}$$

and since $f(a_x^2, a_y^2, n^2)$ is strictly increasing with n^2, this implies that the minimum is attained at $n^2 = 1$. Hence

$$R_L = \min_{(a_x^2, a_y^2)\in\mathbb{R}^+\times\mathbb{R}^+} f(a_x^2, a_y^2, 1). \tag{3.27}$$

Remark 3. *Define*

$$R_0 = \frac{R_L}{\pi^2} = \min_{(\bar{x},\bar{y})\in\mathbb{R}^+\times\mathbb{R}^+} f_1(\bar{x},\bar{y}), \tag{3.28}$$

where

$$\begin{aligned} f_1(\bar{x},\bar{y}) &= \frac{\xi_1\bar{x}+\xi_2\bar{y}+A^*}{\xi_1\bar{x}+\xi_2\bar{y}}\left[\eta\bar{x}+\eta\bar{y}+1+\frac{H_0(\zeta_1\bar{x}+\zeta_2\bar{y}+1)}{\zeta_1\bar{x}+\zeta_2\bar{y}+1+H_0\gamma}\right] \\ \bar{x} &= \frac{a_x^2}{\pi^2}, \qquad \bar{y} = \frac{a_y^2}{\pi^2}, \qquad H_0 = \frac{H}{\pi^2}\,. \end{aligned} \tag{3.29}$$

Let us observe that:

i) in the case of horizontal isotropy, i.e. $\xi_1 = \xi_2$ and $\zeta_1 = \zeta_2$, the critical Rayleigh number R_0 given by (3.28) coincides with that one obtained in [17];

ii) in the absence of rotation ($\mathcal{T}^2 = 0$) and if the porous medium is isotropic ($\xi_1 = \xi_2 = \zeta_1 = \zeta_2 = \eta = 1$), then the critical Rayleigh number R_0 coincides with that one obtained in [12]. Moreover, in the hypothesis of local thermal equilibrium ($H_0 \to \infty$), by simple calculations, the critical Rayleigh reverts to the classical Rayleigh number for the isotropic porous medium in the local thermal equilibrium ([27]);

iii) the stabilizing effect of fluid thermal conductivity on the onset of convection is evident since the partial derivative of (3.29) with respect to η is strictly positive.

3.4 Optimal stability result

In order to study the nonlinear stability of the conduction solution m_0, let us introduce the following Lyapunov functional

$$E(t) = \frac{\|\theta\|^2}{2} + \frac{A\|\varphi\|^2}{2\gamma} \tag{3.30}$$

and define

$$\begin{aligned} D(t) &= \eta\|\nabla_1\theta\|^2 + \|\theta_{,z}\|^2 + \frac{\zeta_1}{\gamma}\|\varphi_{,x}\|^2 + \frac{\zeta_2}{\gamma}\|\varphi_{,y}\|^2 + \frac{1}{\gamma}\|\varphi_{,z}\|^2 + H\|\theta-\varphi\|^2 \\ I(t) &= (\theta, w)\,. \end{aligned} \tag{3.31}$$

Multiplying $(3.9)_3$ by θ, $(3.16)_3$ by φ, integrating over V and then adding the resulting equations, we find out

$$\frac{dE}{dt} = -D\left(1 - R\frac{I}{D}\right). \tag{3.32}$$

In order to capture the influence of rotation on the nonlinear stability analysis of the conduction solution m_0, we shall apply the differential constraint approach [13, 22, 17]. To this end let us consider the following variational problem

$$\frac{1}{R_E} = \max_{\mathcal{H}^*} \frac{I}{D} \tag{3.33}$$

with

$$\begin{aligned} \mathcal{H}^* = \{(w,\theta,\varphi) \ : \ & w=\theta=\varphi=0 \text{ on } z=0,1; \text{ periodic in } x \text{ and } y \\ & \text{directions, with period } \frac{2\pi}{a_x}, \frac{2\pi}{a_y} \text{ respectively; } D<\infty; \text{ verifying } (3.16)_1\} \end{aligned} \tag{3.34}$$

the space of the kinematically admissible perturbations.

The variational problem (3.33) is equivalent to

$$\frac{1}{R_E} = \max_{\mathcal{H}} \frac{I + \int_V \lambda \ g \ dV}{D} \tag{3.35}$$

where $\lambda(\mathbf{x})$ is a Lagrange multiplier and

$$\begin{aligned} g(\mathbf{x}) &= \xi_1 w_{,xx} + \xi_2 w_{,yy} + w_{,zz} + T^2 \xi_1 \xi_2 w_{,zz} - \xi_1 R\theta_{,xx} - \xi_2 R\theta_{,yy} \\ \mathcal{H} &= \{(w,\theta,\varphi) \ : \ w=\theta=\varphi=0 \text{ on } z=0,1; \text{ periodic in } x \text{ and } y \\ &\qquad \text{directions, with period } \frac{2\pi}{a_x}, \frac{2\pi}{a_y} \text{ respectively; } D<\infty\}. \end{aligned} \tag{3.36}$$

By applying the Poincaré inequality in $(3.31)_1$, it turns out that

$$D(t) \geq \pi^2 a \|\theta\|^2 + b\frac{\pi^2}{\gamma}\|\varphi\|^2 \tag{3.37}$$

where

$$a = \min\{\eta, 1\} \qquad b = \min\{\zeta_1, \zeta_2, 1\}. \tag{3.38}$$

Then, from (3.32) by virtue of (3.37) , if $R < R_E$ one obtains:

$$\frac{dE}{dt} \leq \frac{\pi^2 (R - R_E) c}{R_E} E$$

where $c \leq \min\left\{2a, \frac{2b}{A}\right\}$. Hence the condition $R < R_E$ implies the nonlinear, global and exponential stability of m_0, according to the following inequality

$$E(t) \leq E(0) \exp\left[\frac{\pi^2 (R - R_E) c}{R_E} t\right]. \tag{3.39}$$

Remark 4. *Multiplying* $(3.9)_1$ *by* $\boldsymbol{u}$*, integrating over* V *and applying the Cauchy-Schwarz inequality, it turns out that*

$$\delta^{-1}\|\boldsymbol{u}\|^2 \leq \|\theta\|^2. \tag{3.40}$$

where $\delta = \dfrac{R^2}{2}\max\{\xi_1, \xi_2, 2\}$*. Therefore, the condition* $R < R_E$ *implies the decay of* $\|\boldsymbol{u}\|$*, as well.*

In order to determine the critical Rayleigh number R_E, we solve the variational problem (3.35). The Euler Lagrange equations are

$$\begin{cases} \theta + \xi_1\lambda_{,xx} + \xi_2\lambda_{,yy} + \lambda_{,zz} + \mathcal{T}^2\xi_1\xi_2\lambda_{,zz} = 0 \\ 2[\eta\Delta_1\theta + \theta_{,zz} - H(\theta - \varphi)] = \xi_1 R^2\lambda_{,xx} + \xi_2 R^2\lambda_{,yy} - Rw \\ \zeta_1\varphi_{,xx} + \zeta_2\varphi_{,yy} + \varphi_{,zz} + H\gamma(\theta - \varphi) = 0 \\ \xi_1 w_{,xx} + \xi_2 w_{,yy} + w_{,zz} + \mathcal{T}^2\xi_1\xi_2 w_{,zz} = \xi_1 R\theta_{,xx} + \xi_2 R\theta_{,yy}. \end{cases} \tag{3.41}$$

By virtue of (3.20), (3.41) becomes

$$\begin{cases} \mathcal{L}\mathcal{L}_1\theta = -H\mathcal{L}\varphi - R\mathcal{L}w \\ \mathcal{L}w = \xi_1 R\theta_{,xx} + \xi_2 R\theta_{,yy} \\ \mathcal{L}_2\varphi = -H\gamma\theta. \end{cases} \tag{3.42}$$

Applying $\mathcal{L}_2$ to $(3.42)_1$ and substituting $(3.42)_2$ and $(3.42)_3$ in the resulting equation, one obtains (3.22) and therefore $R_L = R_E$, i.e. the coincidence between the global nonlinear stability threshold and the linear instability threshold, implying the absence of subcritical instabilities. This is an optimal result since the condition $R < R_E = R_L$ is a necessary and sufficient condition to guarantee the stability of m_0.

3.5 Numerical results

This section will deal with the solution of Eq. (3.28). It will be analysed the influence of parameters on the critical Rayleigh number. First of all, we would like to point out the behaviour of function $f_1(\bar{x}, \bar{y})$ in (3.29). Fixed five parameters $(\xi_1, \xi_2, \zeta_1, \zeta_2, \eta)$ in $f_1(\bar{x}, \bar{y})$, once the following transformation is adopted

$$(\xi_1, \xi_2, \zeta_1, \zeta_2, \eta) \to (\xi_2, \xi_1, \zeta_2, \zeta_1, \eta), \tag{3.43}$$

values initially assumed by $\bar{x}$ are taken by $\bar{y}$ and vice versa. Moreover, function $f_1(\bar{x},0)$ will have the same graph as $f_1(0, \bar{y})$. This behaviour is important because by applying the previous transformation, the same results obtained for $\bar{x}$ hold for $\bar{y}$ and vice versa.

Figure 3.1 shows the stabilizing effect of rotation on the onset of convection, which is an expected physical behaviour. Moreover, taking into account (3.29), one immediately proves that $f_1(\bar{x}, \bar{y})$ is an increasing function of $\mathcal{T}^2$. In numerical analysis, for the sake of simplicity, we confine ourselves in considering the case of isotropic porous medium, i.e. $\xi_1 = \xi_2 = \zeta_1 = \zeta_2 = \eta = 1$. However, analogous results are obtained when another set of these parameters is fixed.

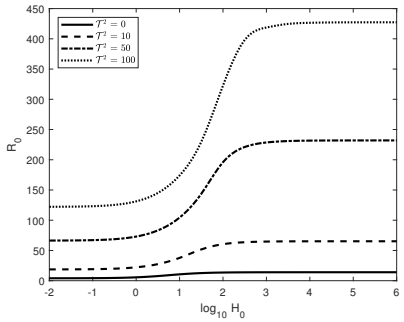

Figure 3.1: Critical Rayleigh number as function of the scaled inter-phase heat transfer coefficient H_0 for different values of Taylor number $\mathcal{T}$ with $\xi_1 = \xi_2 = \zeta_1 = \zeta_2 = \eta = 1$ and $\gamma = 0.4$

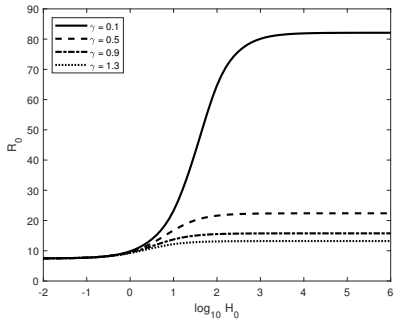

Figure 3.2: Critical Rayleigh number as function of the scaled inter-phase heat transfer coefficient H_0 for different values of γ with $\xi_1 = \zeta_1 = 0.1$, $\xi_2 = \zeta_2 = \eta = 1$ and $\mathcal{T}^2 = 20$

Note that in Figure 3.1 the critical Rayleigh number is taken as a function of the scaled inter-phase heat transfer coefficient H_0. As [27] pointed out, since this quantity is not easily measured, we need to determine a range in which this parameter can vary. Starting from its definition $H_0 = \dfrac{h^2 d}{\varepsilon \kappa_z^f \pi^2}$, for reasonable combinations of these parameters, H_0 is assumed to vary between 0.01 and 10^6. It is well known that rotation has a stabilizing effect on conduction. In particular, Figure 3.1 shows that this effect of Taylor number is very pronounced for large values of H_0, while it is less remarkable for $H_0 \sim 10^{-1}$. We would like to remark that for large values of

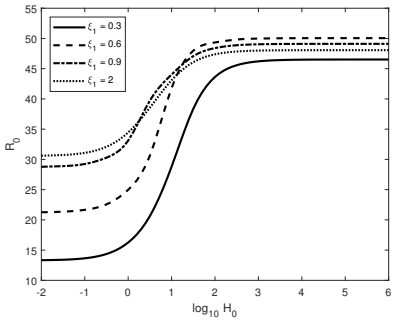

Figure 3.3: Critical Rayleigh number as function of the scaled inter-phase heat transfer coefficient H_0 for different values of ξ_1 with $\xi_2 = \zeta_2 = \eta = 1$, $\zeta_1 = 0.1$, $\gamma = 0.4$ and $\mathcal{T}^2 = 20$

(a) **(b)**

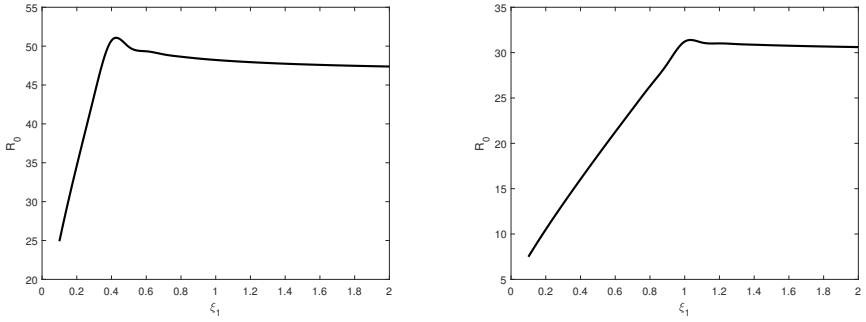

Figure 3.4: Critical Rayleigh number as function of ξ_1 with $\zeta_1 = 0.1$, $\zeta_2 = \xi_2 = \eta = 1$, $\mathcal{T}^2 = 20$, $\gamma = 0.4$, (a) $H_0 = 100$, (b) $H_0 = 0.01$

H_0, each curve tends to become parallel to x axis. As shown in [27], this behaviour represents the region of local thermodynamic equilibrium and it will characterize the following images, as well.

In Figure 3.2, the destabilizing effect of the parameter γ on the onset of convection is clear. For large values of H_0, R_0 is inversely proportional to γ, while for small values of H_0, the presence of γ is negligible. This kind of behaviour is evident in Eq. (3.28) and it is reported in [27], as well. Physically, if h is large, i.e. the heat exchange between the phases is high, increasing the fluid conductivity κ_z^f fosters the onset of convection.

Figures 3.3 shows the behaviour of the critical Rayleigh number as a function of H_0 for different values of ξ_1. The behaviour for low values of H_0 is similar to the one for large values. In particular, R_0 increases up to a certain value either for $H_0 = 0.01$ and $H_0 = 10^6$. After this point, it starts decreasing towards a limit value. The asymptotic trend is highlighted in Figures 3.4a-3.4b, where $H_0 = 100$ and $H_0 = 0.01$, respectively.

Table 3.1: Significant values of R_0, $\bar{x}$ and $\bar{y}$ depending on ξ_1, with $\xi_2 = \eta = \zeta_2 = 1$, $\zeta_1 = 0.1$

(a) $H_0 = 100$

ξ_1	R_0	$\bar{x}$	$\bar{y}$
0.20	34.6354	0	2.4519
0.30	43.6359	0	2.9776
0.39	51.3471	0	3.4167
0.40	50.7299	7.9758	0
0.41	50.6284	7.9648	0
0.45	50.2671	7.9257	0
0.50	49.8963	7.8854	0

(b) $H_0 = 0.01$

ξ_1	R_0	$\bar{x}$	$\bar{y}$
0.80	26.2973	0	4.1436
0.98	30.7327	0	4.5613
0.99	30.9769	0	4.5834
1	31.2207	4.6010	0.0043
1.01	31.2086	4.6043	0
1.05	31.1626	4.6001	0
1.10	31.1098	4.5954	0

Table 3.2: Significant values of R_0, $\bar{x}$ and $\bar{y}$ depending on ξ_2, with $\xi_1 = \eta = \zeta_1 = 1$, $\zeta_2 = 0.1$

(a) $H_0 = 100$

ξ_2	R_0	$\bar{x}$	$\bar{y}$
0.20	34.6354	2.4519	0
0.30	43.6359	2.9776	0
0.39	51.3471	3.4167	0
0.40	50.7299	0	7.9758
0.41	50.6284	0	7.9648
0.45	50.2671	0	7.9257
0.50	49.8963	0	7.8854

(b) $H_0 = 0.01$

ξ_2	R_0	$\bar{x}$	$\bar{y}$
0.80	26.2973	4.1436	0
0.98	30.7327	4.5613	0
0.99	30.9769	4.5834	0
1	31.2207	0.0043	4.6010
1.01	31.2086	0	4.6043
1.05	31.1626	0	4.6001
1.10	31.1098	0	4.5954

Furthermore, in Tables 3.1-3.2, some significant values of R_0 are reported in order to show which is the critical anisotropy parameter beyond which R_0 inverts its trend, both for $H_0 = 100$ and $H_0 = 0.01$. In addition, note that the moment in which R_0 starts decreasing coincides with the one in which the periodicity cells change their nature. Firstly, when ξ_2 is fixed and ξ_1 is increasing, they are rolls aligned along x axis. Then they turn into rolls aligned along y axis. The opposite transition occurs when transformation (3.43) is adopted, as shown in Table 3.2. This phenomenon is physically admissible, as pointed out by [88]. Small values of ξ_1 imply that the fluid struggles to move in the x direction therefore the motion has components along y and z axis. Whereas, greater values of ξ_1 allow the fluid to move easier in x direction, favouring the creation of rolls along y axis.

[35] found that the presence of anisotropic porous media yields a two-dimensional fluid motion. Convective cells are rolls aligned in x or y direction, depending on the ratios between anisotropy parameters. This fluid behaviour is preserved under

the hypothesis of local thermal non equilibrium.

Table 3.3: Significant values of R_0, $\bar{x}$ and $\bar{y}$ depending on ξ_1, with $\xi_2 = \eta = \zeta_1 = 1,\ \zeta_2 = 0.1$

(a) $H_0 = 100$

ξ_1	R_0	$\bar{x}$	$\bar{y}$
2.20	86.4714	0	11.3535
2.30	89.5334	0	11.6095
2.40	92.5822	0	11.8606
2.41	92.8864	0	11.8854
2.42	96.3788	6.0680	0
2.43	96.3726	6.0676	0
2.50	96.3307	6.0649	0

(b) $H_0 = 0.01$

ξ_1	R_0	$\bar{x}$	$\bar{y}$
0.80	26.2972	0	4.1436
0.98	30.7327	0	4.5613
0.99	30.9767	0	4.5834
1	31.2207	0.0043	4.6010
1.01	31.2088	4.6043	0
1.05	31.1628	4.6002	0
1.10	31.1100	4.5954	0

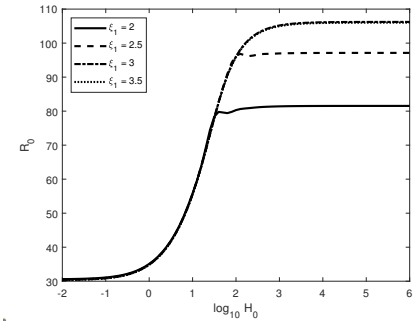

Figure 3.5: Critical Rayleigh number as function of the scaled inter-phase heat transfer coefficient H_0 for different values of ξ_1 with $\xi_2 = \eta = \zeta_1 = 1,\ \zeta_2 = 0.1,\ \gamma = 0.4$ and $\mathcal{T}^2 = 20$

The behaviour of critical Rayleigh number for different values of ξ_1 changes once the ratio $\frac{\zeta_1}{\zeta_2}$ is inverted. However, Figure 3.5 is similar to Figure 3.3.

Increasing ξ_1 makes R_0 grow up to a certain value, beyond which it starts decreasing. Moreover, for small values of H_0, inverting ζ_1 and ζ_2 affects neither the shape of periodicity cells, which are firstly still rolls aligned along x axis, nor the influence of ξ_1 on R_0. Table 3.3 shows what has been just pointed out.

Now, we decided to fix a direction in which the fluid fails to move easily. So we assumed $\xi_2 = 0.1$ and looked at the critical Rayleigh number as a function of ξ_1. In Figures 3.6a-3.6b the destabilizing effect of permeability is evident, for all H_0, both for $\zeta_1 < \zeta_2$ and $\zeta_1 > \zeta_2$. Recalling the definition of Rayleigh number, this kind of behaviour is expected. Fixed the horizontal permeability parameters K_x and K_y, decreasing values of vertical permeability K_z yield a decrease of Rayleigh number,

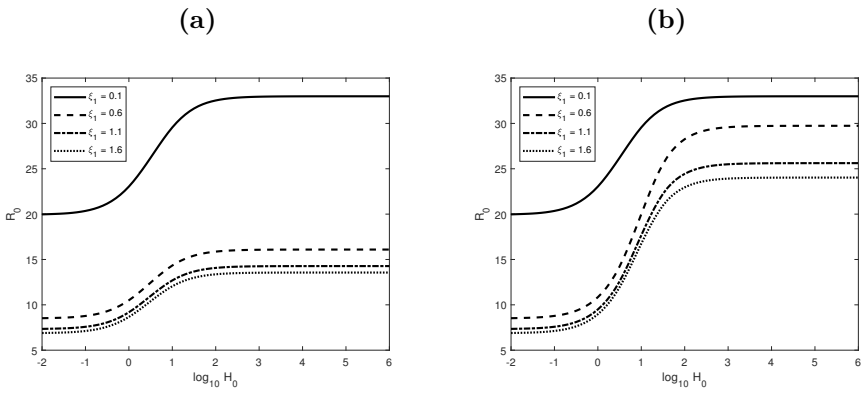

Figure 3.6: Critical Rayleigh number as function of H_0 for different values of ξ_1 with $\eta = 1,\ \mathcal{T}^2 = 20,\ \gamma = 0.4$ (a) $\xi_2 = \zeta_1 = 0.1,\ \zeta_2 = 1$, (b) $\xi_2 = \zeta_2 = 0.1,\ \zeta_1 = 1$

in agreement with findings of [27] in the case of horizontal isotropy. Furthermore, increasing K_x will promote the horizontal motion, which increases the preferred cells width and reduces the critical Rayleigh number, as also proposed by [89].

Now let us analyse how R_0 varies with respect to the thermal anisotropy. Figure 3.7 shows clearly that ζ_1 has a stabilizing effect on conduction if H_0 is large. A similar result is found by [27] in a simpler situation. Physically, increasing solid conductivity implies that the solid matrix absorbs heat from the fluid more easily. On the other hand, when $H_0 \sim 10^{-1}$, the effect of ζ_1 is negligible.

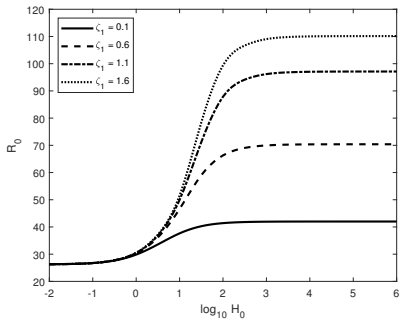

Figure 3.7: Critical Rayleigh number as function of the scaled inter-phase heat transfer coefficient H_0 for different values of ζ_1 with $\xi_1 = \eta = \zeta_2 = 1,\ \xi_2 = 0.8,\ \gamma = 0.4$ and $\mathcal{T}^2 = 20$

Tables 3.4a-3.4b represent a focus on the influence of solid thermal conductivity on the onset of convection. They are obtained when $H_0 = 100$, but however analogous results are valid for all large H_0.

Note that the stabilizing effect of ζ_1 is evident up to a certain value, beyond which R_0 is constant. This behaviour is direct consequence of the change of rolls direction. Once the fluid motion occurs on the plane yz, i.e. rolls are aligned along

x axis, modifying ζ_1 does not produce any effect on the motion. Furthermore, inverting the ratio $\frac{\xi_1}{\xi_2}$ does not modify the way ζ_1 affects R_0, as shown in Table 3.4b.

Table 3.4: (a) Significant values of R_0 as function of ζ_1 with $\xi_1 = \eta = \zeta_2 = 1$, $\xi_2 = 0.8$, $H_0 = 100$. (b) Significant values of R_0 as function of ζ_1 with $\xi_2 = \eta = \zeta_2 = 1$, $\xi_1 = 0.8$, $H_0 = 100$.

(a)

ζ_1	R_0	$\bar{x}$	$\bar{y}$
1.30	95.8271	5.3503	0
1.31	96.2154	5.3556	0
1.39	99.2900	5.4055	0
1.40	99.4132	0	6.2639
1.41	99.4132	0	6.2639
1.50	99.4132	0	6.2639
1.60	99.4132	0	6.2639

(b)

ζ_1	R_0	$\bar{x}$	$\bar{y}$
0.60	78.6021	6.3297	0
0.68	82.9496	6.2686	0
0.69	83.4862	6.2628	0
0.70	83.7592	0	5.2852
0.71	83.7592	0	5.2852
0.80	83.7592	0	5.2852
0.90	83.7592	0	5.2852

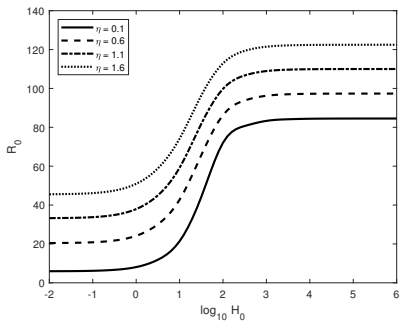

Figure 3.8: Critical Rayleigh number as function of the scaled inter-phase heat transfer coefficient H_0 for different values of η with $\xi_1 = 1.6$, $\xi_2 = \zeta_1 = \zeta_2 = 1$, $\gamma = 0.4$ and $\mathcal{T}^2 = 20$

In Figure 3.8 the stabilizing effect of fluid thermal conductivity η is highlighted for any H_0. This behaviour is expected since we have shown previously that increasing κ_z^f fosters the onset of convection. Moreover, looking at the definition of R_0 in (3.28), it is evident that the critical Rayleigh number is directly proportional to η.

3.6 Conclusions

Linear and nonlinear stability analyses of the conduction solution in a fluid saturating an anisotropic porous layer under the effect of rotation, in local thermal non

equilibrium, has been performed. In particular, the coincidence between the global nonlinear stability threshold and the linear instability threshold has been proved. Therefore, a necessary and sufficient condition for global nonlinear stability of conduction solution has been obtained. Moreover, we showed convection can occur only through a steady motion as the principle of exchange of stabilities has been proved to hold.

Given that the critical Rayleigh number is obtained in a closed form, we performed a numerical analysis to highlight influence of parameters of the onset of convection. We showed that the conductivity ratio γ destabilises the conduction. Mechanical anisotropy ξ_i ($i = 1,2$) has the same effect, for ξ_j small ($j \neq i$), while a slightly different behaviour is obtained when ξ_j is high. In addition, we proved that increasing values of fluid and solid thermal conductivities delay the onset of convection. The same consequence is obtained when increasing the strength of rotation.

Regarding the shape of cells arising with the onset of convection, we proved that anisotropy forces the fluid in a two-dimensional motion. Convective cells are rolls aligned in x or y direction, depending on the ratios between anisotropy parameters.

Chapter 4

Thermal convection for a Darcy-Brinkman rotating anisotropic porous layer in local thermal non-equilibrium

4.1 Introduction

This chapter is intended to investigate the onset of convection in a rotating high-porosity medium, whose mechanical and thermal properties are horizontally isotropic, under the LTNE assumption (see [90]). It is proved that only steady convection is allowed, since the strong form of the principle of exchanges of stability holds, via a linear instability analysis. The coincidence between the linear instability and the global nonlinear stability thresholds is obtained with respect to the L^2-norm. The presence of a high-porosity medium is modelled by the Darcy number Da in the dimensionless problem. It is proved that this number yields a delayed onset of convection.

In section 4.2 the Darcy-Brinkman model is introduced and the dimensionless system for perturbation fields is obtained. Section 4.3 is devoted to the proof of the strong form of the principle of exchange of stabilities. Consequently, the linear instability analysis is performed to determine the critical Rayleigh number for the onset of steady convection analytically. In section 4.4 the nonlinear stability analysis of the conduction solution is carried out to prove the coincidence between the linear instability threshold and the global nonlinear stability threshold, with respect to the L^2- norm. While, section 4.5 deals with numerical simulations that highlight the influence of rotation, anisotropy and the Da number on the critical Rayleigh number. Permeability turns out to have a destabilising effect on conduction. Whereas, thermal conductivities stabilise conduction, delaying the

onset of convection. Moreover, we prove that rotation has a stabilising effect on conduction, as well as the thermal conductivities' ratio γ.

4.2 Governing equations

Let us take into account a horizontal highly porous medium, whose depth is d, saturated by an incompressible, homogeneous fluid at rest. The medium is assumed evenly warmed up from below and rotating about the upward vertical axis z with constant angular velocity Ω. As consequence, in addition to the gravitational field, the Coriolis force acts on the medium. Moreover, we assume that the medium is in local thermal non-equilibrium so that the heat exchange between fluid and solid skeleton is allowed. We denote by T_L the temperature of the lower plane $z = 0$ and by T_U the temperature of the upper plane $z = d$, while we refer to the fluid temperature with T_f and to the solid temperature with T_s. Then

$$T_s = T_f = T_L \qquad \text{on } z = 0, \qquad T_s = T_f = T_U \qquad \text{on } z = d \tag{4.1}$$

with $T_L > T_U$.

Besides, we assume that the layer is lightly anisotropic, i.e. its features, such as thermal conductivity and permeability, are homogeneous in the horizontal direction. This assumption allows us to write the permeability tensor $\mathcal{K}^*$, the thermal conductivity tensors of solid phase and fluid phase, $\mathcal{D}_s^*$ and $\mathcal{D}_f^*$, respectively, in the following way

$$\begin{aligned}
&\mathcal{K}^* = K_z \mathcal{K} \qquad \mathcal{K} = \begin{pmatrix} \xi & 0 & 0 \\ 0 & \xi & 0 \\ 0 & 0 & 1 \end{pmatrix} \qquad \xi = \frac{K_H}{K_z} \\
&\mathcal{D}_s^* = \kappa_z^s \mathcal{D}_s \qquad \mathcal{D}_s = \begin{pmatrix} \zeta & 0 & 0 \\ 0 & \zeta & 0 \\ 0 & 0 & 1 \end{pmatrix} \qquad \zeta = \frac{\kappa_H^s}{\kappa_z^s} \\
&\mathcal{D}_f^* = \kappa_z^f \mathcal{D}_f \qquad \mathcal{D}_f = \begin{pmatrix} \eta & 0 & 0 \\ 0 & \eta & 0 \\ 0 & 0 & 1 \end{pmatrix} \qquad \eta = \frac{\kappa_H^f}{\kappa_z^f} \,.
\end{aligned} \tag{4.2}$$

being the principal axis (x, y, z) of $\mathcal{K}^*$ coinciding with the conductivity tensors' ones. Since the medium porosity is high, a Darcy-Brinkman model is employed. Accounting for the Oberbeck - Boussinesq approximation, starting from [27, 17],

the model is

$$\begin{cases} \mathbf{v} = \mu^{-1}\mathcal{K}^* \cdot \left[-\nabla p + \rho_f g \alpha T_f \mathbf{k} - \dfrac{2\Omega\rho_f}{\varepsilon}\mathbf{k}\times\mathbf{v} + \tilde{\mu}\Delta\mathbf{v} \right] \\ \nabla\cdot\mathbf{v} = 0 \\ \varepsilon(\rho c)_f T^f_{,t} + (\rho c)_f \mathbf{v}\cdot\nabla T_f = \varepsilon\nabla\cdot(\mathcal{D}^*_f\cdot\nabla T_f) + h(T_s - T_f) \\ (1-\varepsilon)(\rho c)_s T^s_{,t} = (1-\varepsilon)\nabla\cdot(\mathcal{D}^*_s\cdot\nabla T_s) - h(T_s - T_f) \end{cases} \tag{4.3}$$

where $\mathbf{v}$, p, T_f and T_s are (seepage) velocity, reduced pressure, fluid phase temperature and solid phase temperature, respectively; $\tilde{\mu}$, μ, ρ_f, ρ_s, c, g, α, Ω, ε, h are effective and dynamic viscosity, fluid density, solid density, specific heat, gravity acceleration, thermal expansion coefficient, angular velocity, porosity and interaction coefficient, respectively. The following boundary conditions are coupled to (4.3)

$$\begin{aligned} &T_s = T_f = T_L \quad \text{on } z = 0, \qquad T_s = T_f = T_U \quad \text{on } z = d, \\ &\mathbf{v}\cdot\mathbf{n} = 0 \quad \text{on } z = 0, d \end{aligned} \tag{4.4}$$

being $\mathbf{n}$ the unit outward normal to planes $z = 0, d$.

System (4.3) admits the following conduction solution m_0:

$$m_0 = \left\{ \mathbf{v}_b = \mathbf{0}\,, \quad \bar{T}_s = \bar{T}_f = -\beta z + T_L\,, \quad p_b = -\rho_f g\alpha\beta\frac{z^2}{2} + \rho_f g\alpha T_L z + cost \right\} \tag{4.5}$$

where $\beta = \dfrac{T_L - T_U}{d} (> 0)$ is the adverse temperature gradient.

We are interested in studying the stability of the steady solution (4.5). Let us introduce the following perturbation fields $\{\mathbf{u}, \theta, \varphi, \pi\}$ so as to obtain a new solution for (4.3)

$$\mathbf{v} = \mathbf{u} + \mathbf{v}_b \qquad T_f = \theta + \bar{T}_f \qquad T_s = \varphi + \bar{T}_s \qquad p = \pi + p_b. \tag{4.6}$$

Once the dimensionless quantities are introduced

$$x_i = x_i^* d, \quad t = t^*\frac{\varepsilon d}{U}, \quad \pi = \pi^* P, \quad u_i = u_i^* U, \quad \theta = \theta^* T', \quad \varphi = \varphi^* T' \tag{4.7}$$

where

$$P = \frac{U\mu d}{K_z}\,, \qquad U = \frac{\varepsilon\kappa_z^f}{(\rho c)_f d}\,, \qquad T' = \beta d\sqrt{\frac{\kappa_z^f \varepsilon\mu}{\beta g\alpha K_z \rho_f^2 c_f d^2}}, \tag{4.8}$$

the dimensionless system for the perturbation fields, omitting all the asterisks, is

$$\begin{cases} \mathcal{K}^{-1}\cdot\mathbf{u} = -\nabla\pi + R\theta\mathbf{k} - \mathcal{T}\mathbf{k}\times\mathbf{u} + \mathrm{Da}\Delta\mathbf{u} \\ \nabla\cdot\mathbf{u} = 0 \\ \theta_{,t} + \mathbf{u}\cdot\nabla\theta = Rw + \eta\Delta_1\theta + \theta_{,zz} + H(\varphi - \theta) \\ A\varphi_{,t} - \zeta\Delta_1\varphi - \varphi_{,zz} + H\gamma(\varphi - \theta) = 0 \end{cases} \tag{4.9}$$

where

$$\gamma = \frac{\varepsilon\kappa_z^f}{(1-\varepsilon)\kappa_z^s}\,, \qquad A = \frac{(\rho c)_s\kappa_z^f}{(\rho c)_f\kappa_z^s}\,, \qquad H = \frac{hd^2}{\varepsilon\kappa_z^f}$$

$$R^2 = \frac{K_z\rho_f^2 c_f d^2\beta g\alpha}{\mu\varepsilon\kappa_z^f} \quad \text{Rayleigh number}$$

$$\mathrm{Da} = \frac{K_z\tilde{\mu}}{\mu d^2} \quad \text{Darcy number}\,, \qquad \mathcal{T} = \frac{2\Omega\rho_f K_z}{\varepsilon\mu} \quad \text{Taylor number.}$$

To system (4.9) we append the following initial conditions

$$\mathbf{u}(\mathbf{x},0)=\mathbf{u}_0(\mathbf{x})\,, \quad \theta(\mathbf{x},0)=\theta_0(\mathbf{x})\,, \quad \varphi(\mathbf{x},0)=\varphi_0(\mathbf{x})\,, \quad \pi(\mathbf{x},0)=\pi_0(\mathbf{x}) \tag{4.10}$$

where $\nabla\cdot\mathbf{u}_0 = 0$, and the following stress-free boundary conditions

$$u_{,z} = v_{,z} = w = \theta = \varphi = 0 \qquad \text{on } z = 0{,}1. \tag{4.11}$$

In order to study the stability of the null solution of (4.9), let us assume that perturbations are periodic in x and y directions with periods $\frac{2\pi}{a_x}$ and $\frac{2\pi}{a_y}$, respectively. Let

$$V = \left[0, \frac{2\pi}{a_x}\right] \times \left[0, \frac{2\pi}{a_y}\right] \times [0,1] \tag{4.12}$$

be the periodicity cell, we assume that perturbations belong to $W^{2,2}(V)$, $\forall t \in \mathbb{R}^+$ and they can be expanded as a Fourier series uniformly convergent in V.

4.3 Onset of steady convection

In order to perform a linear instability analysis, we rewrite $(4.9)_1$ in a more convenient form in which only relevant unknown fields appear. Hence, let us apply the double curl and the curl to $(4.9)_1$ and let us retain only the third component. The resulting equations are multiplied by ξ so as to obtain

$$\begin{cases} \xi\Delta_1 w + w_{,zz} = \xi R\Delta_1\theta + \xi\mathcal{T}\,(u_{,yz} - v_{,xz}) + \xi\mathrm{Da}\Delta\Delta w \\ (1-\xi\mathrm{Da}\Delta)\,(u_{,yz} - v_{,xz}) = -\xi\mathcal{T} w_{,zz} \end{cases} \tag{4.13}$$

where $(4.13)_2$ is consequence of a further derivation with respect to z. A single equation is obtained once the operator $(1-\xi\mathrm{Da}\Delta)$ is applied to $(4.13)_1$ and $(4.13)_2$ is substituted in the resulting equation. This procedure allows us to write the linear version of (4.9) as follows

$$\begin{cases} \xi\Delta_1 w + w_{,zz} - \xi^2\mathrm{Da}\Delta\Delta_1 w - \xi\mathrm{Da}\Delta w_{,zz} = \xi R\Delta_1\theta + \\ \qquad\qquad -\xi^2 R\mathrm{Da}\Delta\Delta_1\theta - \xi^2\mathcal{T}^2 w_{,zz} + \xi\mathrm{Da}\Delta\Delta w - \xi^2\mathrm{Da}^2\Delta\Delta\Delta w \\ \theta_{,t} = Rw + \eta\Delta_1\theta + \theta_{,zz} + H(\varphi-\theta) \\ A\varphi_{,t} - \zeta\Delta_1\varphi - \varphi_{,zz} + H\gamma(\varphi-\theta) = 0 \end{cases} \tag{4.14}$$

Since (4.14) is autonomous, we look for solutions whose time dependence is separated from the temporal one, i.e.

$$\hat{\varphi}(t,\mathbf{x}) = \varphi(\mathbf{x})\; e^{\sigma t} \quad \forall \hat{\varphi} \in (w,\theta,\varphi) \qquad \sigma \in \mathbb{C} \tag{4.15}$$

By virtue of (4.15), (4.14) becomes

$$\begin{cases} \xi\Delta_1 w + w_{,zz} - \xi^2 \mathrm{Da}\Delta\Delta_1 w - \xi\mathrm{Da}\Delta w_{,zz} + \xi^2 R\mathrm{Da}\Delta\Delta_1\theta + \\ \qquad -\xi R\Delta_1\theta + \xi^2\mathcal{T}^2 w_{,zz} - \xi\mathrm{Da}\Delta\Delta w + \xi^2\mathrm{Da}^2\Delta\Delta\Delta w = 0 \\ \sigma\theta - Rw - \eta\Delta_1\theta - \theta_{,zz} - H\varphi + H\theta = 0 \\ A\sigma\varphi - \zeta\Delta_1\varphi - \varphi_{,zz} + H\gamma\varphi - H\gamma\theta = 0 \end{cases} \tag{4.16}$$

Then we denote by $(\cdot,\cdot)$ and $\|\cdot\|$ the scalar product on the Hilbert space $L^2(V)$, and the related norm, respectively. Let us multiply $(4.16)_1$ by $\frac{w^*}{\xi}$, $(4.16)_2$ by $(1-\xi\mathrm{Da}\Delta)\,\Delta_1\theta^*$ and $(4.16)_3$ by $(1-\xi\mathrm{Da}\Delta)\,\Delta_1\frac{\varphi^*}{\gamma}$, where the asterisks denote the complex conjugate. By virtue of boundary conditions (4.11), integrating over the periodicity cell V yields

$$\begin{cases} -\|\nabla_1 w\|^2 - \xi^{-1}\|w_{,z}\|^2 - \xi\ \mathrm{Da}\|\nabla\nabla_1 w\|^2 - \mathrm{Da}\|\nabla w_{,z}\|^2 \\ -R\,(\Delta_1\theta, w^*) + \xi R\mathrm{Da}\,(\Delta\Delta_1\theta, w^*) - \xi\ \mathcal{T}^2\|w_{,z}\|^2 \\ -\mathrm{Da}\|\nabla\nabla w\|^2 - \xi\ \mathrm{Da}^2\|\nabla\nabla\nabla w\|^2 = 0 \\ \\ -\sigma\|\nabla_1\theta\|^2 - \sigma\ \xi\ \mathrm{Da}\|\nabla\nabla_1\theta\|^2 - R\,(w, \Delta_1\theta^*) + \xi R\mathrm{Da}\,(w, \Delta\Delta_1\theta^*) \\ -\eta\|\Delta_1\theta\|^2 - \xi\ \eta\ \mathrm{Da}\|\nabla\Delta_1\theta\|^2 - \|\nabla_1\theta_{,z}\|^2 - \xi\ \mathrm{Da}\|\nabla\nabla_1\theta_{,z}\|^2 \\ -H\,(\varphi, \Delta_1\theta^*) + H\xi\mathrm{Da}\,(\varphi, \Delta\Delta_1\theta^*) - H\|\nabla_1\theta\|^2 - \xi H\mathrm{Da}\|\nabla\nabla_1\theta\|^2 = 0 \\ \\ -\frac{A\ \sigma}{\gamma}\|\nabla_1\ \varphi\|^2 - \frac{A\ \sigma}{\gamma}\ \xi\ \mathrm{Da}\|\nabla\nabla_1\varphi\|^2 - \frac{\zeta}{\gamma}\|\Delta_1\varphi\|^2 \\ -\frac{\xi\ \mathrm{Da}\ \zeta}{\gamma}\|\nabla\Delta_1\varphi\|^2 - \frac{\xi\ \mathrm{Da}}{\gamma}\|\nabla\nabla_1\varphi_{,z}\|^2 - \frac{1}{\gamma}\|\nabla_1\varphi_{,z}\|^2 - H\|\nabla_1\varphi\|^2 \\ -H\ \xi\ \mathrm{Da}\|\nabla\nabla_1\varphi\|^2 - H\,(\theta, \Delta_1\varphi^*) + H\ \xi\ \mathrm{Da}\,(\theta, \Delta\Delta_1\varphi^*) = 0 \end{cases} \tag{4.17}$$

Since $(\varphi, \Delta_1\theta^*) = (\Delta_1\varphi, \theta^*)$ and $(\varphi, \Delta\Delta_1\theta^*) = (\Delta\Delta_1\varphi, \theta^*)$, (4.17) yields

$$\begin{aligned} &\sigma\left[\|\nabla_1\theta\|^2 + \ \xi\ \mathrm{Da}\|\nabla\nabla_1\theta\|^2 + \tfrac{A}{\gamma}\|\nabla_1\ \varphi\|^2 + \tfrac{A}{\gamma}\ \xi\ \mathrm{Da}\|\nabla\nabla_1\varphi\|^2\right] = \\ &= -\|\nabla_1 w\|^2 - \xi^{-1}\|w_{,z}\|^2 - \xi\ \mathrm{Da}\|\nabla\nabla_1 w\|^2 - \mathrm{Da}\|\nabla w_{,z}\|^2 \\ &- R\,[(\Delta_1\theta, w^*) + (w, \Delta_1\theta^*)] + \xi\ R\ \mathrm{Da}\,[(\Delta\Delta_1\theta, w^*) + (w, \Delta\Delta_1\theta^*)] \\ &- \xi\ \mathcal{T}^2\|w_{,z}\|^2 - \mathrm{Da}\|\nabla\nabla w\|^2 - \xi\ \mathrm{Da}^2\|\nabla\nabla\nabla w\|^2 - \eta\|\Delta_1\theta\|^2 \\ &- \xi\ \eta\ \mathrm{Da}\|\nabla\Delta_1\theta\|^2 - \|\nabla_1\theta_{,z}\|^2 - \xi\ \mathrm{Da}\|\nabla\nabla_1\theta_{,z}\|^2 \\ &- H\,[(\Delta_1\varphi, \theta^*) + (\theta, \Delta_1\varphi^*)] + H\ \xi\ \mathrm{Da}\,[(\Delta\Delta_1\varphi, \theta^*) + (\theta, \Delta\Delta_1\varphi^*)] \\ &- H\|\nabla_1\theta\|^2 - \xi\ H\ \mathrm{Da}\|\nabla\nabla_1\theta\|^2 - \tfrac{\zeta}{\gamma}\|\Delta_1\varphi\|^2 - \tfrac{\xi\ \mathrm{Da}\ \zeta}{\gamma}\|\nabla\Delta_1\varphi\|^2 \\ &- \tfrac{1}{\gamma}\|\nabla_1\varphi_{,z}\|^2 - \tfrac{\xi\ \mathrm{Da}}{\gamma}\|\nabla\nabla_1\varphi_{,z}\|^2 - H\|\nabla_1\varphi\|^2 - H\ \xi\ \mathrm{Da}\|\nabla\nabla_1\varphi\|^2 \end{aligned} \tag{4.18}$$

Every term in (4.18) is real, then necessarily σ is real as well. Thus, we have shown the validity of the strong form of the principle of exchange of stabilities. Therefore, convection can occur only through a steady motion.

Since our aim is to determine the critical Rayleigh number beyond which instability occurs, we focus on the marginal state in (4.16). By virtue of principle of exchange of stabilities, we set $\sigma = 0$ in (4.16) so as to obtain

$$\begin{cases} \xi\Delta_1 w + w_{,zz} - \xi^2 \mathrm{Da}\Delta\Delta_1 w - \xi\mathrm{Da}\Delta w_{,zz} - \xi R\Delta_1\theta + \xi^2 R\mathrm{Da}\Delta\Delta_1\theta + \\ \qquad \xi^2\mathcal{T}^2 w_{,zz} - \xi\mathrm{Da}\Delta\Delta w + \xi^2\mathrm{Da}^2\Delta\Delta\Delta w = 0 \\ -Rw - \eta\Delta_1\theta - \theta_{,zz} - H\varphi + H\theta = 0 \\ -\zeta\Delta_1\varphi - \varphi_{,zz} + H\gamma\varphi - H\gamma\theta = 0 \end{cases} \tag{4.19}$$

Because of periodicity of perturbation fields, accounting for boundary conditions (4.11) and since the sequence $\{\sin n\pi z\}_{n\in\mathbb{N}}$ is a complete orthogonal system for $L^2([0,1])$, we look for solution of (4.19) such that

$$f(x,y,z) = \sum_{n=1}^{+\infty} \bar{f}_n(x,y,z) \qquad \forall f \in \{w,\theta,\varphi\} \tag{4.20}$$

where $\bar{f}_n = \tilde{f}_n(x,y)\sin(n\pi z)$ and

$$\Delta_1\bar{f}_n = -a^2\bar{f}_n \qquad \frac{\partial^2\bar{f}_n}{\partial z^2} = -n^2\pi^2\bar{f}_n \qquad (a^2 = a_x^2 + a_y^2) \tag{4.21}$$

where a is the wavenumber arising from spatial periodicity.

Let us define the following operators

$$\begin{aligned} \mathcal{L}_1 &\equiv \xi\Delta_1 + \partial_{,zz} - \xi^2\mathrm{Da}\Delta\Delta_1 - \xi\mathrm{Da}\Delta\partial_{,zz} + \xi^2\mathcal{T}^2\partial_{,zz} - \xi\mathrm{Da}\Delta\Delta + \\ &\quad + \xi^2\mathrm{Da}^2\Delta\Delta\Delta \\ \mathcal{L}_2 &\equiv -\eta\Delta_1 - \partial_{,zz} + H \\ \mathcal{L}_3 &\equiv -\zeta\Delta_1 - \partial_{,zz} + H\gamma \end{aligned} \tag{4.22}$$

so that the system (4.19) becomes

$$\begin{cases} \mathcal{L}_1 w = (1 - \xi\mathrm{Da}\Delta)\, R\xi\Delta_1\theta \\ \mathcal{L}_2\theta = Rw + H\varphi \\ \mathcal{L}_3\varphi = H\gamma\theta\,. \end{cases} \tag{4.23}$$

Now let us apply $\mathcal{L}_1$ and $\mathcal{L}_3$ to $(4.23)_2$ so that

$$\mathcal{L}_1\mathcal{L}_2\mathcal{L}_3\theta = R\mathcal{L}_3\mathcal{L}_1 w + H\mathcal{L}_1\mathcal{L}_3\varphi\,. \tag{4.24}$$

By substituting $(4.23)_1 - (4.23)_3$ in (4.24), we get

$$\mathcal{L}_1\mathcal{L}_2\mathcal{L}_3\theta = R^2\mathcal{L}_3\,(1 - \xi\mathrm{Da}\Delta)\,\xi\Delta_1\theta + H^2\gamma\mathcal{L}_1\theta\,. \tag{4.25}$$

By splitting $\mathcal{L}_3$ in the first term, we obtain

$$\begin{aligned}\mathcal{L}_1\mathcal{L}_2\left(-\zeta\Delta_1-\partial_{,zz}\right)\theta+\mathcal{L}_1 H\gamma\left(-\eta\Delta_1-\partial_{,zz}\right)\theta=\\ =R^2\left(-\zeta\Delta_1-\partial_{,zz}+H\gamma\right)\left(1-\xi\mathrm{Da}\Delta\right)\xi\Delta_1\theta\,.\end{aligned}\tag{4.26}$$

By splitting $\mathcal{L}_2$ in the first term in (4.3)

$$\begin{aligned}\mathcal{L}_1 H\left(-\zeta\Delta_1-\partial_{,zz}\right)\theta+\mathcal{L}_1\left(-\eta\Delta_1-\partial_{,zz}\right)\left(-\zeta\Delta_1-\partial_{,zz}+H\gamma\right)\theta=\\ =R^2\left(-\zeta\Delta_1-\partial_{,zz}+H\gamma\right)\left(1-\xi\mathrm{Da}\Delta\right)\xi\Delta_1\theta\,.\end{aligned}\tag{4.27}$$

Let us substitute (4.20) in (4.3) and retain only the n-th component. Then, from (4.3)

$$\begin{aligned}&\left[-\xi a^2-n^2\pi^2-\xi^2 a^2\mathrm{Da}\delta_n-\xi n^2\pi^2\mathrm{Da}\delta_n-\xi^2\mathcal{T}^2n^2\pi^2-\xi\mathrm{Da}\delta_n^2-\xi^2\mathrm{Da}^2\delta_n^3\right]\\ &\left[H\left(\zeta a^2+n^2\pi^2\right)+\left(\eta a^2+n^2\pi^2\right)\left(\zeta a^2+n^2\pi^2+H\gamma\right)\right]=\\ &=-R^2\left(\zeta a^2+n^2\pi^2+H\gamma\right)\left(1+\xi\mathrm{Da}\ \delta_n\right)\xi a^2\end{aligned}\tag{4.28}$$

being $\delta_n=(a^2+n^2\pi^2)$.

From (4.28) it follows that the critical Rayleigh number for the onset of steady convection is

$$R_S=\min_{(n^2,a^2)\in\mathbb{N}\times\mathbb{R}^+}f(n^2,a^2)\tag{4.29}$$

being

$$\begin{aligned}&f(n^2,a^2)=\\ &\frac{\xi a^2+n^2\pi^2+\xi^2\mathrm{Da}\ a^2\delta_n+\xi\mathrm{Da}\ n^2\pi^2\delta_n+\xi^2\mathcal{T}^2n^2\pi^2+\xi\mathrm{Da}\ \delta_n^2+\xi^2\mathrm{Da}^2\delta_n^3}{\left(1+\xi\mathrm{Da}\ \delta_n\right)\xi a^2}\\ &\left[\eta a^2+n^2\pi^2+H\frac{\zeta a^2+n^2\pi^2}{\zeta a^2+n^2\pi^2+H\gamma}\right]\end{aligned}\tag{4.30}$$

We can easily remark that the minimum with respect to n^2 is attained in $n^2=1$, since $f(\cdot,a^2)$ is a strictly increasing function. Hence

$$\begin{aligned}R_S=\min_{a^2\in\mathbb{R}^+}&\left[\frac{\xi a^2+\pi^2+\xi\mathrm{Da}\ \delta^2}{\xi a^2}+\frac{\xi^2\mathcal{T}^2\pi^2}{\left(1+\xi\mathrm{Da}\ \delta\right)\xi a^2}\right]\cdot\\ &\left[\eta a^2+\pi^2+H\frac{\zeta a^2+\pi^2}{\zeta a^2+\pi^2+H\gamma}\right]\end{aligned}\tag{4.31}$$

where $\delta=(a^2+\pi^2)$.

Let us remark that $f(1,a^2)$ is a strictly increasing function of $\mathcal{T}$ and η, therefore the stabilizing effect of rotation and fluid thermal conductivity has been proved.

In particular, the effect of rotation on the onset of instability is expected since the Coriolis force acts in the horizontal direction, discouraging the motion in the vertical one.

Moreover, it is easy to note that if $\mathrm{Da} = 0$, (4.31) coincides with the result found in [17] and [27]. While, for a low porous medium in absence of rotation, i.e. $\mathcal{T} = 0$ and $\mathrm{Da} = 0$, results coincide with the ones found in [14]. In addition, by assuming that the layer is isotropic, i.e. $\xi = \eta = \zeta = 1$, the critical Rayleigh number (4.31) is the same as that one found in [12].

4.4 Nonlinear stability analysis

In this section we want to perform a nonlinear stability analysis of conduction solution m_0. The application of the energy method yields a loss of the rotation term. Therefore, we employ a differential constraint approach ([17, 13]) in order to capture the influence of rotation. Then, let us multiply $(4.9)_3$ by θ and $(4.9)_4$ by φ and integrate over the periodicity cell V. By defining the Lyapunov functional $E(t)$

$$E(t) = \frac{1}{2}\|\theta\|^2 + \frac{A}{2\gamma}\|\varphi\|^2, \tag{4.32}$$

the production term $I(t)$

$$I(t) = (\theta, w) \tag{4.33}$$

and the dissipation function $D(t)$

$$D(t) = \eta\|\nabla_1\theta\|^2 + \|\theta_{,z}\|^2 + \frac{\zeta}{\gamma}\|\nabla_1\varphi\|^2 + \frac{1}{\gamma}\|\varphi_{,z}\|^2 + H\|\varphi - \theta\|^2 \tag{4.34}$$

we find out that

$$\frac{dE}{dt} = -D\left(1 - R\frac{I}{D}\right) \leq -D\left(1 - \frac{R}{R_E}\right) \tag{4.35}$$

where

$$\frac{1}{R_E} = \max_{\mathcal{H}^*}\frac{I}{D} \tag{4.36}$$

with

$$\begin{aligned}\mathcal{H}^* = \{(w,\theta,\varphi) \ : \ & w = \theta = \varphi = 0 \text{ on } z = 0{,}1; \text{ periodic in } x \text{ and } y \\ & \text{directions, with period } \frac{2\pi}{a_x}, \frac{2\pi}{a_y} \text{ respectively; } D < \infty; \text{ verifying } (4.16)_1\}\end{aligned} \tag{4.37}$$

the space of the kinematically admissible perturbations. Eq. (4.35) tells us that $R < R_E$ is a sufficient condition for the nonlinear stability of m_0.

Let us define

$$\begin{aligned} g(\mathbf{x}) &= \xi\Delta_1 w + w_{,zz} - \xi^2 \mathrm{Da}\Delta\Delta_1 w - \xi\mathrm{Da}\Delta w_{,zz} - \xi R\Delta_1\theta + \\ &\quad \xi^2 R\mathrm{Da}\Delta\Delta_1\theta + \xi^2\mathcal{T}^2 w_{,zz} - \xi\mathrm{Da}\Delta\Delta w + \xi^2\mathrm{Da}^2\Delta\Delta\Delta w \\ \mathcal{H} &= \{(w,\theta,\varphi) \ : \ w=\theta=\varphi=0 \text{ on } z=0{,}1; \text{ periodic in } x \text{ and } y \\ &\quad \text{directions, with period } \frac{2\pi}{a_x}, \frac{2\pi}{a_y} \text{ respectively; } D<\infty\}. \end{aligned} \tag{4.38}$$

The variational problem (4.36) is equivalent to

$$\frac{1}{R_E} = \max_{\mathcal{H}} \frac{I + \int_V \lambda \ g \ dV}{D} \tag{4.39}$$

where $\lambda(\mathbf{x})$ is a Lagrange multiplier.

By employing the Poincaré inequality in (4.34), we get

$$D(t) \geq a\pi^2\|\theta\|^2 + b\frac{\pi^2}{\gamma}\|\varphi\|^2 \tag{4.40}$$

being $a = \min\{1,\eta\}$ and $b = \min\{1,\zeta\}$. Hence, if $R < R_E$, from (4.35) it turns out that

$$\frac{dE}{dt} \leq -\left(a\pi^2\|\theta\|^2 + b\frac{\pi^2}{\gamma}\|\varphi\|^2\right)\left(1 - \frac{R}{R_E}\right) \leq -\pi^2\left(\frac{R_E - R}{R_E}\right)cE(t) \tag{4.41}$$

where $c = \min\left\{2a, \frac{2b}{A}\right\}$. Eq. (4.41) yields the exponential decay of temperature perturbation fields.

Now let us remark that, by multiplying $(4.9)_1$ by $\mathbf{u}$ and by virtue of Cauchy-Schwartz, we obtain the exponential decay of $\mathbf{u}$, i.e.

$$\|\mathbf{u}\|^2 \leq \xi_* R^2\|\theta\|^2 \tag{4.42}$$

where $\xi_* = \max\{\xi,1\}$.

Thus, we have shown that the condition $R < R_E$ implies the global nonlinear and exponential stability of conduction solution m_0.

Now let us solve the variational problem (4.39) to determine the critical Rayleigh number R_E. The Euler-Lagrange equations, together with the constraint equation, are

$$\begin{cases} \xi\Delta_1 w + w_{,zz} - \xi^2\mathrm{Da}\Delta\Delta_1 w - \xi\mathrm{Da}\Delta w_{,zz} - \xi R_E\Delta_1\theta + \xi^2\mathcal{T}^2 w_{,zz} + \\ \qquad \xi^2 R_E\mathrm{Da}\Delta\Delta_1\theta - \xi\mathrm{Da}\Delta\Delta w + \xi^2\mathrm{Da}^2\Delta\Delta\Delta w = 0 \\ \theta + \xi\Delta_1\lambda + \lambda_{,zz} - \xi^2\mathrm{Da}\Delta\Delta_1\lambda - \xi\mathrm{Da}\Delta\lambda_{,zz} + \xi^2\mathcal{T}^2\lambda_{,zz} - \xi\mathrm{Da}\Delta\Delta\lambda + \\ \qquad + \xi^2\mathrm{Da}^2\Delta\Delta\Delta\lambda = 0 \\ R_E w + \xi^2 R_E^2\mathrm{Da}\Delta\Delta_1\lambda - \xi R_E^2\Delta_1\lambda + 2\eta\Delta_1\theta + 2\theta_{,zz} + 2H(\varphi - \theta) = 0 \\ \zeta\Delta_1\varphi + \varphi_{,zz} - H\gamma(\varphi - \theta) = 0 \end{cases} \tag{4.43}$$

Recalling the definitions in (4.22), (4.43) becomes

$$\begin{cases} \mathcal{L}_1 w = (1 - \xi \mathrm{Da}\Delta)\, R_E \xi \Delta_1 \theta \\ \mathcal{L}_1 \lambda = -\theta \\ 2\mathcal{L}_2 \theta = R_E w + 2H\varphi - (1 - \xi \mathrm{Da}\Delta)\, R_E^2 \xi \Delta_1 \lambda \\ \mathcal{L}_3 \varphi = H\gamma\theta \end{cases} \tag{4.44}$$

By applying $\mathcal{L}_1$ to $(4.44)_3$ and substituting $(4.44)_2$ and $(4.44)_1$, we obtain

$$-\mathcal{L}_1\mathcal{L}_2\theta + H\mathcal{L}_1\varphi + R_E\mathcal{L}_1 w = 0. \tag{4.45}$$

The application of $\mathcal{L}_3$ to (4.45) leads to the following equation

$$-\mathcal{L}_1\mathcal{L}_2\mathcal{L}_3\theta + H\mathcal{L}_1\mathcal{L}_3\varphi + R_E\mathcal{L}_3\mathcal{L}_1 w = 0 \tag{4.46}$$

which coincides with (4.24). As consequence, we have obtained the coincidence between the global nonlinear stability threshold R_E and the linear instability threshold R_S, implying the absence of subcritical instability region. This result allows us to claim that the condition $R < R_E = R_S$ is a necessary and sufficient condition for the stability of m_0, therefore in this respect the result is optimal.

4.5 Results and Discussion

In this section we would like to point out how parameters affect the onset of convection. Given the complex expression obtained in (4.31) for the critical Rayleigh number R_S, it is not always easy to show analytically how parameters modify the occurrence of instability. That is why the expression for the critical Rayleigh number (4.31) is analysed numerically for different values of parameters with the aim of highlighting how they affect the onset of convection. In particular, we will show the dependence of R_S with respect to the Taylor number, permeability, thermal conductivities and the Da number.

We would like to point out that results are reported as function of the interphase heat transfer coefficient H. This parameter is not easily measurable, as claimed in [27]. That is why we have decided to fix the range $(10^{-2}, 10^6)$ in which H can vary and to show the influence of parameters on R_S for any H.

Figure 4.1 shows the behaviour of the critical Rayleigh number R_S for increasing values of $\mathcal{T}$. The stabilizing effect of rotation on the onset of convection is clear, for any value of H, even though it is less remarkable when $H \to 0$. This result is not surprising since we have previously pointed out that the derivative of R_S in (4.31) with respect to $\mathcal{T}$ is strictly positive. Moreover, the stabilizing effect is expected from a physical point of view since rotation acts on the fluid in the horizontal direction, making the motion along the vertical axis more difficult.

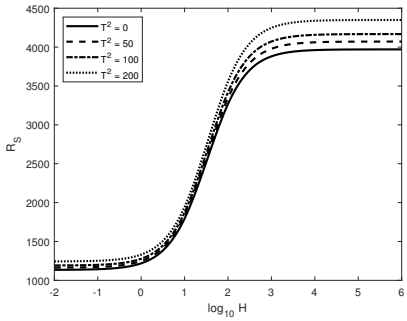

Figure 4.1: Critical Rayleigh number as function of the inter-phase heat transfer coefficient H for different values of the Taylor number $\mathcal{T}$ with $\xi = \zeta = \eta = 0.5$, $\gamma = 0.4$ and $\mathrm{Da} = 2$.

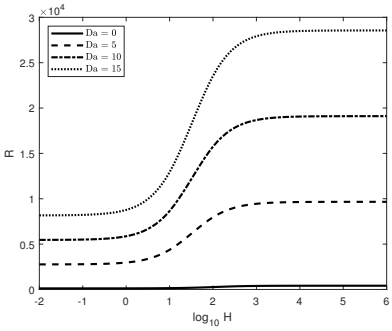

Figure 4.2: Critical Rayleigh number as function of the inter-phase heat transfer coefficient H for different values of the Da number Da with $\xi = \zeta = \eta = 0.5$, $\gamma = 0.4$ and $\mathcal{T}^2 = 20$.

We would like to underline that both for small and large values of H, the curves tend to become parallel to the x axis. The region where a plateau is reached represents the local thermal equilibrium situation and it will characterize the following figures, as well. Physically, if $H \to 0$, the solid phase is separated from the fluid one and it ceases to affect the fluid thermal field. While, if $H \to \infty$, solid and fluid temperature end up with being identical.

In Figure 4.2, the stabilizing effect of the Da number Da on conduction is highlighted. Note that if $\mathrm{Da} = 0$, results are valid for the classical Da model, as pointed out previously. It is well known that when porosity ε tends to 1, the classical Da model needs to be replaced by the Da-Brinkman model, for which $\mathrm{Da} \neq 0$. Since the Da-Brinkman model is closer to a model describing the fluid motion in absence of porous medium (clear fluid), for which it is common knowledge that the critical Rayleigh number is greater than that one in a porous medium, result in Figure 4.2 is consistent.

In Figure 4.3a, the behaviour of R_S with respect to permeability parameter ξ

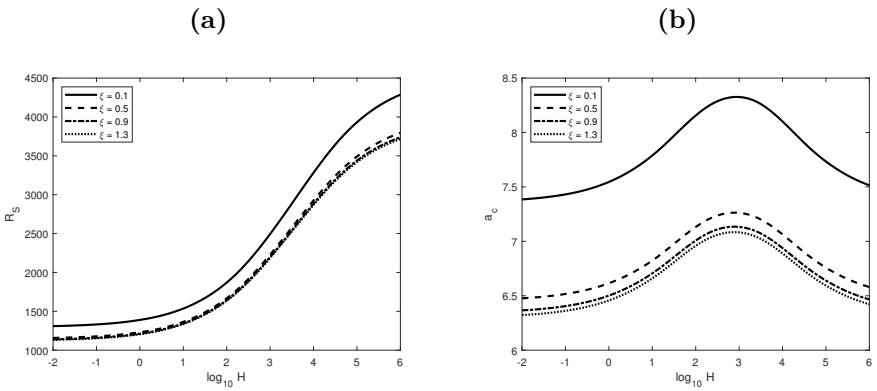

Figure 4.3: (a) Critical Rayleigh number (b) critical wavenumber as function of the inter-phase heat transfer coefficient H for different values of ξ with $\zeta = \eta = 0.5$, $\gamma = 0.4$, $\mathcal{T}^2 = 20$ and $\mathrm{Da} = 2$.

is shown. The destabilizing effect of permeability is evident, for any values of H, in agreement with findings of [27] and [14]. Recalling the definition of the Rayleigh number, this kind of behaviour is expected, since R is directly proportional to K_z. Physically, increasing K_H eases the fluid motion in the horizontal direction, implying an easier occurrence of instability. Figure 4.3b shows how cell dimension changes for different values of permeability. In particular, when permeability in the horizontal direction K_H grows, periodicity cells get wider.

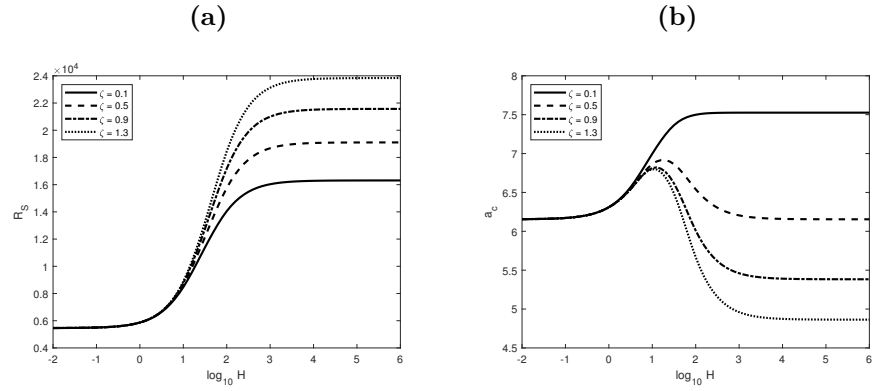

Figure 4.4: (a) Critical Rayleigh number (b) critical wavenumber as function of the inter-phase heat transfer coefficient H for different values of ζ with $\xi = \eta = 0.5$, $\gamma = 0.4$, $\mathcal{T}^2 = 20$ and $\mathrm{Da} = 10$.

Now let us analyse how R_S varies with respect to thermal conductivities. Figure 4.4a shows the stabilizing effect of solid thermal conductivity on conduction. The growth of R_S with ζ means that solid thermal conductivity delays the onset of convection. Physically, the greater the solid thermal conductivity is the more easily the solid matrix absorbs heat from the fluid. The delaying effect is evident for large

values of the inter-phase heat transfer coefficient H, while it is less remarkable for smaller values of H. This is not surprising since, as already pointed out, when $H \to 0$ solid phase does not affect the fluid thermal field. This behaviour is evident also in Figure 4.4b, where it is highlighted how cell dimension varies with respect to ζ. In particular, for small values of H, the influence is negligible, while if H is great, ζ promotes wider periodicity cells.

Analogous result is obtained when looking at the effect of the fluid thermal conductivity parameter η on the periodicity cell dimension. Figure 4.5b shows that η promotes wider periodicity cells, as well.

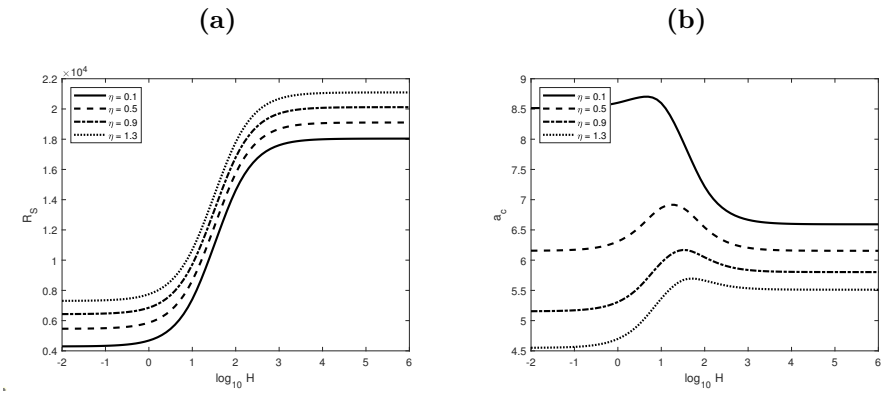

Figure 4.5: (a) Critical Rayleigh number (b) critical wavenumber as function of the inter-phase heat transfer coefficient H for different values of η with $\xi = \zeta = 0.5$, $\gamma = 0.4$, $\mathcal{T}^2 = 20$ and $\mathrm{Da} = 10$.

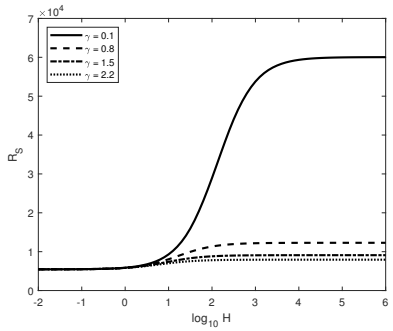

Figure 4.6: Critical Rayleigh number as function of the inter-phase heat transfer coefficient H for different values of γ with $\xi = \zeta = \eta = 0.5$, $\mathcal{T}^2 = 20$ and $\mathrm{Da} = 10$.

The stabilizing effect of η is highlighted in Figure 4.5a, where for any H, R_S grows for increasing η. This behaviour is consistent with the analytical result for which the derivative of R_S in (4.31) with respect to η is strictly positive. From a physical point of view, increasing κ_z^f implies that heat flows easier in the vertical direction within the fluid, fostering the onset of instability.

The effect of κ_z^f on the critical Rayleigh number is evident also by looking at Figure 4.6, where the behaviour of R_S with respect to the thermal conductivities' ratio γ is shown. Since $\gamma = \dfrac{\varepsilon\kappa_z^f}{(1-\varepsilon)\kappa_z^s}$ by definition, increasing κ_z^f implies growing γ, which yields a decrease for R_S, i.e. a destabilizing effect, as shown in Figure 4.6.

4.6 Conclusions

The onset of convection in an anisotropic rotating porous medium with high porosity in local thermal non-equilibrium has been studied. Only steady convection is allowed, since we proved that the strong form of the principle of exchanges of stability holds. A detailed proof of that has been provided. The critical Rayleigh number for the onset of steady convection is determined via the linear instability analysis. Moreover, the global nonlinear stability has been studied and the energy method has been adopted. Coincidence between the linear instability and the global nonlinear stability thresholds has been proved. This means that a necessary and sufficient condition for the onset of convection has been obtained.

Numerical simulations have been required in order to highlight the influence of parameters on the onset of convection. It has been pointed out that horizontally isotropic permeability has a destabilising effect on conduction. This is because increasing permeability eases the fluid motion, implying an easier occurrence of instability. Whereas, anisotropic thermal conductivities stabilise conduction, delaying the onset of convection. Moreover, it has been shown that, as expected, rotation and the Darcy number have a stabilising effect on conduction, as well as the thermal conductivities' ratio γ.

Chapter 5

Effect of Vadasz term on the onset of convection in a Darcy-Brinkman anisotropic rotating porous medium in LTNE

5.1 Introduction

This chapter is devoted to study the effect of the Vadasz inertia term on the onset of convective motions for a Darcy-Brinkman model. The topic studied is the content of a future publication in collaboration with Prof. F. Capone. Linear instability analysis is performed to determine the critical Rayleigh number for the onset of convection. The model analysed allows oscillatory convective motions to occur. Indeed, at the criticality, both real and pure imaginary eigenvalues are possible. As consequence, the critical Rayleigh numbers for the onset of both steady and oscillatory convection are determined. Moreover, conditions for the non-existence of oscillatory convection are provided.

The outline of the chapter is the following: section 5.2 is devoted to the mathematical model describing the fluid motion in presence of a rotating anisotropic porous medium in LTNE. We determine the basic steady solution, whose stability we are interested in and consequently we obtain the dimensionless system of perturbations. In section 5.3, linear instability analysis is performed in order to determine the critical Rayleigh numbers for both steady and oscillatory convection. Finally, section 5.4 involves the study of the effect of anisotropic permeability, anisotropic thermal conductivities, rotation, the Darcy number and, most importantly, the Vadasz number on the onset of convection.

5.2 Mathematical model

Let $\mathscr{F}$ be an incompressible fluid, initially at rest, saturating a horizontal porous layer, whose depth is d, confined between two planes, $z = 0$ and $z = d$. We assume the layer to be heated from below and we denote by T_L the temperature of the lower plane $z = 0$ and by T_U the temperature of the upper plane $z = d$. In addition, the layer rotates about the upward vertical axis z with constant angular velocity Ω. Therefore, the Coriolis force affects the fluid motion within the porous medium, together with gravitational and drag forces. Moreover, we assume that fluid and solid phases are not in thermal equilibrium, namely heat exchanges between the phases are allowed. Then, we refer to the fluid temperature with T_f and to the solid temperature with T_s, by saying that the porous medium is in local thermal non-equilibrium (LTNE). Then

$$T_s = T_f = T_L \qquad \text{on } z = 0, \qquad T_s = T_f = T_U \qquad \text{on } z = d \tag{5.1}$$

with $T_L > T_U$.

In addition, the porous medium is horizontally isotropic, i.e. its features, such as thermal conductivity and permeability, are homogeneous in the horizontal direction. Let $\mathcal{K}_*$ be the permeability tensor, $\mathcal{D}_s^*$ and $\mathcal{D}_f^*$ be the thermal conductivity tensors of solid phase and fluid phase, respectively. By assuming that the principal axis (x, y, z) of $\mathcal{K}_*$ coincide with the conductivity tensors' ones, it turns out (see [27, 17])

$$\begin{aligned}
&\mathcal{K} = K_z \mathcal{K}_* \qquad \mathcal{K}_* = \begin{pmatrix} \xi & 0 & 0 \\ 0 & \xi & 0 \\ 0 & 0 & 1 \end{pmatrix} \qquad \xi = \frac{K_H}{K_z} \\
&\mathcal{D}_s = \kappa_z^s \mathcal{D}_s^* \qquad \mathcal{D}_s^* = \begin{pmatrix} \zeta & 0 & 0 \\ 0 & \zeta & 0 \\ 0 & 0 & 1 \end{pmatrix} \qquad \zeta = \frac{\kappa_H^s}{\kappa_z^s} \\
&\mathcal{D}_f = \kappa_z^f \mathcal{D}_f^* \qquad \mathcal{D}_f^* = \begin{pmatrix} \eta & 0 & 0 \\ 0 & \eta & 0 \\ 0 & 0 & 1 \end{pmatrix} \qquad \eta = \frac{\kappa_H^f}{\kappa_z^f}
\end{aligned} \tag{5.2}$$

Since the problem at stake involves a porous medium with high porosity, a more suitable Darcy-Brinkman model needs to be adopted (see [1]). Under these hypotheses, starting from models proposed in [90, 15], the mathematical model is

$$\begin{cases}
\rho_f c_a \mathbf{v}_{,t} = -\nabla p - \dfrac{2\Omega\rho_f}{\varepsilon}\mathbf{k} \times \mathbf{v} - \mu\mathcal{K}^{-1} \cdot \mathbf{v} + \rho_f g \alpha T_f \mathbf{k} + \tilde{\mu}\Delta\mathbf{v} \\
\nabla \cdot \mathbf{v} = 0 \\
\varepsilon(\rho c)_f T_{,t}^f + (\rho c)_f \mathbf{v} \cdot \nabla T_f = \varepsilon \nabla \cdot (\mathcal{D}_f \cdot \nabla T_f) + h(T_s - T_f) \\
(1-\varepsilon)(\rho c)_s T_{,t}^s = (1-\varepsilon)\nabla \cdot (\mathcal{D}_s \cdot \nabla T_s) - h(T_s - T_f)
\end{cases} \tag{5.3}$$

where the Oberbeck-Boussinesq approximation is adopted and where $\mathbf{v}$, p, T_f and T_s are (seepage) velocity, reduced pressure, fluid phase temperature and solid phase temperature, respectively; while μ, $\tilde{\mu}$, ρ_f, ρ_s, c, g, α, c_a, ε, Ω, h are dynamic and effective viscosity, fluid density, solid density, specific heat, gravity acceleration, thermal expansion coefficient, acceleration coefficient, porosity, angular velocity and interaction coefficient, respectively.

The boundary conditions (5.4) are coupled to (5.3)

$$\begin{aligned} &T_s = T_f = T_L \quad \text{on } z = 0, \qquad T_s = T_f = T_U \quad \text{on } z = d, \\ &\mathbf{v} \cdot \mathbf{n} = 0 \quad \text{on } z = 0, d \end{aligned} \tag{5.4}$$

where $\mathbf{n}$ is the unit outward normal to planes $z = 0, d$.

Model (5.3) admits the following steady solution m_0, which describes a situation with fluid at rest and heat spreading by conduction,

$$m_0 = \left\{ \mathbf{v}_b = \mathbf{0}\,, \quad \bar{T}_s = \bar{T}_f = -\beta z + T_L\,, \quad p_b = -\rho_f g \alpha \beta \frac{z^2}{2} + \rho_f g \alpha T_L z + cost \right\} \tag{5.5}$$

where $\beta = \dfrac{T_L - T_U}{d} (> 0)$ is the adverse temperature gradient.

This paper is intended to investigate the stability of the m_0 solution with respect to perturbations to initial data. Therefore, we introduce the following perturbation fields $\{\mathbf{u}, \theta, \varphi, \pi\}$ on seepage velocity, fluid and solid temperature and pressure, respectively. The new solution of (5.3) will be

$$\mathbf{v} = \mathbf{u} + \mathbf{v}_b \qquad T_f = \theta + \bar{T}_f \qquad T_s = \varphi + \bar{T}_s \qquad p = \pi + p_b. \tag{5.6}$$

Let us introduce the dimensionless quantities

$$x_i = x_i^* d, \quad t = t^* \tau, \quad \pi = \pi^* P, \quad u_i = u_i^* U, \quad \theta = \theta^* T', \quad \varphi = \varphi^* T' \tag{5.7}$$

where

$$\tau = \frac{\rho d^2 c_\alpha}{\mu}\,, \quad P = \frac{U \mu d}{K_z}\,, \qquad U = \frac{\varepsilon \kappa_z^f}{(\rho c)_f d}\,, \qquad T' = \beta d \sqrt{\frac{\kappa_z^f \varepsilon \mu}{\beta g \alpha K_z \rho_f^2 c_f d^2}}, \tag{5.8}$$

then, the dimensionless system for perturbation fields, omitting all the asterisks, is

$$\begin{cases} \mathcal{K}^{-1} \cdot \mathbf{u} + Va^{-1} \mathbf{u}_{,t} = -\nabla \pi + R\theta \mathbf{k} - \mathcal{T} \mathbf{k} \times \mathbf{u} + Da \Delta \mathbf{u} \\ \nabla \cdot \mathbf{u} = 0 \\ \theta_{,t} + \mathbf{u} \cdot \nabla \theta = Rw + \eta \Delta_1 \theta + \theta_{,zz} + H(\varphi - \theta) \\ A \varphi_{,t} - \zeta \Delta_1 \varphi - \varphi_{,zz} + H\gamma(\varphi - \theta) = 0 \end{cases} \tag{5.9}$$

where

$$\gamma = \frac{\varepsilon \kappa_z^f}{(1-\varepsilon)\kappa_z^s}\,, \qquad A = \frac{(\rho c)_s \kappa_z^f}{(\rho c)_f \kappa_z^s}\,, \qquad H = \frac{h d^2}{\varepsilon \kappa_z^f}$$

$$R^2 = \frac{K_z \rho_f^2 c_f d^2 \beta g \alpha}{\mu \varepsilon \kappa_z^f} \quad \text{Rayleigh number,} \qquad \mathrm{Da} = \frac{K_z \tilde{\mu}}{\mu d^2} \quad \text{Darcy number,}$$
$$\mathcal{T} = \frac{2\Omega \rho_f K_z}{\varepsilon \mu} \quad \text{Taylor number,} \qquad Va = \frac{c_f d^2 \mu}{K_z \kappa_z^f c_a} \quad \text{Vadasz number.}$$

System (5.9) is coupled to the following initial conditions

$$\mathbf{u}(\mathbf{x},0) = \mathbf{u}_0(\mathbf{x}), \quad \theta(\mathbf{x},0) = \theta_0(\mathbf{x}), \quad \varphi(\mathbf{x},0) = \varphi_0(\mathbf{x}), \quad \pi(\mathbf{x},0) = \pi_0(\mathbf{x}) \tag{5.10}$$

where $\nabla \cdot \mathbf{u}_0 = 0$, and the following stress-free boundary conditions

$$u_{,z} = v_{,z} = w = \theta = \varphi = 0 \qquad \text{on } z = 0,1. \tag{5.11}$$

Let us assume that perturbations are periodic in x and y directions with periods $\frac{2\pi}{a_x}$ and $\frac{2\pi}{a_y}$, respectively. Let

$$V = \left[0, \frac{2\pi}{a_x}\right] \times \left[0, \frac{2\pi}{a_y}\right] \times [0,1] \tag{5.12}$$

be the periodicity cell, it is assumed that perturbations belong to $W^{2,2}(V)$, $\forall t \in \mathbb{R}^+$ and they can be expanded as a Fourier series uniformly convergent in V.

5.3 Linear theory

In order to proceed to the linear instability analysis of the null solution of (5.9), we take the curl and the double curl of $(5.9)_1$. By retaining only the third component of the resulting equations and by virtue of $(5.9)_2$, defining $\omega = \boldsymbol{\omega} \cdot \mathbf{k}$ with $\boldsymbol{\omega} = \nabla \times \mathbf{u}$ vorticity, we get

$$\begin{cases} \xi^{-1}\omega + Va^{-1}\omega_{,t} = \mathcal{T} w_{,z} + \mathrm{Da}\Delta\omega \\ \left(\xi\Delta_1 + \xi Va^{-1}\partial_{,t}\Delta_1 + \partial_{,zz} + \xi Va^{-1}\partial_{,t}\partial_{,zz} - \xi \mathrm{Da}\Delta\Delta\right) w = \\ \qquad\qquad = \xi R \Delta_1 \theta - \xi \mathcal{T} \omega_{,z} \end{cases} \tag{5.13}$$

where $(5.13)_2$ has been multiplied by ξ. By applying a further derivation with respect to z and by multiplying by ξ, Eq. $(5.13)_1$ becomes

$$\left(1 + \xi Va^{-1}\partial_{,t} - \xi \mathrm{Da}\Delta\right) \omega_{,z} = \xi \mathcal{T} w_{,zz} \tag{5.14}$$

As a consequence, we can apply the operator $(1 + \xi Va^{-1}\partial_{,t} - \xi \mathrm{Da}\Delta)$ to $(5.13)_2$ and plug (5.14) into the resulting equation so as to obtain

$$\begin{aligned} \left(\xi\Delta_1 + \partial_{,zz} + \xi Va^{-1}\partial_{,t}\Delta - \xi \mathrm{Da}\Delta\Delta\right)\left(1 + \xi Va^{-1}\partial_{,t} - \xi \mathrm{Da}\Delta\right) w = \\ = \xi R \Delta_1 \left(1 + \xi Va^{-1}\partial_{,t} - \xi \mathrm{Da}\Delta\right)\theta - \xi^2 \mathcal{T}^2 w_{,zz} \end{aligned} \tag{5.15}$$

Hence, the linear version of model (5.9) becomes

$$\begin{cases} \left(\xi\Delta_1 + \partial_{,zz} + \xi Va^{-1}\partial_{,t}\Delta - \xi \mathrm{Da}\Delta\Delta\right)\left(1 + \xi Va^{-1}\partial_{,t} - \xi\mathrm{Da}\Delta\right) w = \\ \qquad\qquad = \xi R\Delta_1\left(1 + \xi Va^{-1}\partial_{,t} - \xi\mathrm{Da}\Delta\right)\theta - \xi^2\mathcal{T}^2 w_{,zz} \\ \theta_{,t} = Rw + \eta\Delta_1\theta + \theta_{,zz} + H(\varphi - \theta) \\ A\varphi_{,t} - \zeta\Delta_1\varphi - \varphi_{,zz} + H\gamma(\varphi - \theta) = 0 \end{cases} \tag{5.16}$$

System (5.16) is autonomous, then solutions are such that the time dependence is separated from the spatial one, i.e.

$$\hat{\varphi}(t, \mathbf{x}) = \varphi(\mathbf{x})\ e^{\sigma t} \quad \forall \hat{\varphi} \in \{w, \theta, \varphi\} \qquad \sigma \in \mathbb{C} \tag{5.17}$$

In addition, because of periodicity of perturbation fields, accounting for boundary conditions (5.11) and since the sequence $\{\sin n\pi z\}_{n\in\mathbb{N}}$ is a complete orthogonal system for $L^2([0,1])$, we can look for solution of (5.16) such that

$$\varphi(x, y, z) = \sum_{n=1}^{+\infty} \bar{\varphi_n}(x, y, z) \qquad \forall \varphi \in \{w, \theta, \varphi\} \tag{5.18}$$

where $\bar{\varphi_n} = \tilde{\varphi_n}(x, y)\sin(n\pi z)$ and

$$\Delta_1\bar{\varphi_n} = -a^2\bar{\varphi_n} \qquad \partial_{,zz}\bar{\varphi_n} = -n^2\pi^2\bar{\varphi_n} \qquad (a^2 = a_x^2 + a_y^2) \tag{5.19}$$

where a is the wavenumber arising from spatial periodicity.
Now, let us define the following operators

$$\begin{aligned} &\mathcal{L} \equiv \left(\xi\Delta_1 + \partial_{,zz} + \xi Va^{-1}\partial_{,t}\Delta - \xi\mathrm{Da}\Delta\Delta\right)\left(1 + \xi Va^{-1}\partial_{,t} - \xi\mathrm{Da}\Delta\right) + \xi^2\mathcal{T}^2\partial_{,zz} \\ &\mathcal{L}_1 \equiv \partial_{,t} - \eta\Delta_1 - \partial_{,zz} + H \\ &\mathcal{L}_2 \equiv A\partial_{,t} - \zeta\Delta_1 - \partial_{,zz} + H\gamma \end{aligned} \tag{5.20}$$

so that we can write (5.16) in the following way

$$\begin{cases} \mathcal{L}w = \xi R\Delta_1\left(1 + \xi Va^{-1}\partial_{,t} - \xi\mathrm{Da}\Delta\right)\theta \\ \mathcal{L}_1\theta = Rw + H\varphi \\ \mathcal{L}_2\varphi = H\gamma\theta \end{cases} \tag{5.21}$$

In order to get a single equation in the unknown θ, let us apply the operator $\mathcal{L}_1$ and $\mathcal{L}_2$ to $(5.21)_1$. Thus, one obtains

$$\mathcal{L}\mathcal{L}_1\mathcal{L}_2\theta = R\mathcal{L}_2\mathcal{L}w + H\mathcal{L}\mathcal{L}_2\varphi \tag{5.22}$$

which becomes

$$\mathcal{L}\mathcal{L}_1\mathcal{L}_2\theta = \xi R^2\Delta_1\left(1 + \xi Va^{-1}\partial_{,t} - \xi\mathrm{Da}\Delta\right)\mathcal{L}_2\theta + H^2\gamma\mathcal{L}\theta \tag{5.23}$$

by virtue of $(5.21)_2$-$(5.21)_3$. Then, we split $\mathcal{L}_2$ in the first term of (5.23)

$$\begin{aligned}\mathcal{L}\mathcal{L}_1\left(A\partial_{,t}-\zeta\Delta_1-\partial_{,zz}\right)\theta+H\gamma\mathcal{L}\left(\partial_{,t}-\eta\Delta_1-\partial_{,zz}\right)\theta=\\ =\xi R^2\Delta_1\left(1+\xi Va^{-1}\partial_{,t}-\xi\mathrm{Da}\Delta\right)\mathcal{L}_2\theta\end{aligned}\tag{5.24}$$

and we split $\mathcal{L}_1$ in the first term of (5.24)

$$\begin{aligned}\mathcal{L}\left(\partial_{,t}-\eta\Delta_1-\partial_{,zz}\right)\mathcal{L}_2\theta+H\mathcal{L}\left(A\partial_{,t}-\zeta\Delta_1-\partial_{,zz}\right)\theta=\\ \xi R^2\Delta_1\left(1+\xi Va^{-1}\partial_{,t}-\xi\mathrm{Da}\Delta\right)\mathcal{L}_2\theta\end{aligned}\tag{5.25}$$

From (5.25), we can determine the critical value for the Rayleigh number beyond which either steady or oscillatory convection occurs. To this aim, we substitute (5.17)-(5.18) in (5.25) and retain only the n-th component. As a consequence, we obtain

$$\begin{aligned}&[-\xi a^2-n^2\pi^2-\xi\mathrm{Da}\delta_n^2-\xi^2\mathrm{Da}\delta_n a^2-\xi\mathrm{Da}n^2\pi^2\delta_n-\xi^2\mathrm{Da}^2\delta_n^3-\xi^2\mathcal{T}^2n^2\pi^2+\\&+\sigma\xi Va^{-1}\left(-\delta_n-\xi a^2-n^2\pi^2-2\xi\mathrm{Da}\delta_n^2\right)-\sigma^2\xi^2Va^{-2}\delta_n]\cdot\\&\left[\left(\sigma+\eta a^2+n^2\pi^2\right)\left(A\sigma+\zeta a^2+n^2\pi^2+H\gamma\right)+H\left(A\sigma+\zeta a^2+n^2\pi^2\right)\right]=\\&=-\xi R^2a^2\left(A\sigma+\zeta a^2+n^2\pi^2+H\gamma\right)\left(1+\sigma\xi Va^{-1}+\xi\mathrm{Da}\delta_n\right)\end{aligned}\tag{5.26}$$

being $\delta_n=a^2+n^2\pi^2$.

Accounting for (5.26), one can simply deduce that the eigenvalue σ can assume pure imaginary values, meaning that the principle of exchange of stabilities does not hold. The illuminating paper by Vadasz [54] suggests that this is due to the presence of the Vadasz inertia term in the momentum Eq. $(5.9)_1$. For this reason, we can claim that the Vadasz number (coupled to the action of rotation) allows convection to arise either via oscillatory or steady motions .

It is well known that instability occurs once the eigenvalue crosses either the axis of pure imaginary numbers or the zero value. Therefore, we set once $\sigma=0$ and once $\sigma=i\omega$ $(\omega\in\mathbb{R}-\{0\})$ in (5.26).

5.3.1 Steady convection

In order to determine the critical Rayleigh number for steady convection, we set $\sigma=0$ in (5.26) so as to obtain

$$\begin{aligned}&R^2=F(n^2,a^2)=\\&=\frac{\left(1+\xi\mathrm{Da}\delta_n\right)\left(\xi a^2+n^2\pi^2+\xi\mathrm{Da}\delta_n^2\right)+\xi^2\mathcal{T}^2n^2\pi^2}{\xi a^2\left(1+\xi\mathrm{Da}\delta_n\right)}\\&\left[\eta a^2+n^2\pi^2+H\frac{\zeta a^2+n^2\pi^2}{\zeta a^2+n^2\pi^2+H\gamma}\right]\end{aligned}\tag{5.27}$$

Starting from (5.27), the critical threshold R_S is determined by solving the minimum problem

$$R_S = \min_{(n^2,a^2)\in\mathbb{N}\times\mathbb{R}^+} F(n^2, a^2) \tag{5.28}$$

Since $F(n^2, a^2)$ is a strictly increasing function with respect to n^2, the critical threshold is

$$R_S = \min_{a^2\in\mathbb{R}^+} F(1, a^2) \tag{5.29}$$

Let us remark that

- R_S does not depend on the Vadasz number Va. This means that steady convection is not affected by inertia effects. Indeed, the critical threshold R_S coincides with the steady threshold found by [90];

- if the porous medium is isotropic, i.e. $\xi = \eta = \zeta = 1$, the critical threshold R_S is the same as that one found by [15];

- if the medium porosity is low, namely the Brinkmann model is no longer suitable to describe the fluid motion (i.e. $\mathrm{Da} = 0$), R_S coincides with the steady threshold determined by [91], where the authors studied the Darcy model. In addition, if the medium is isotropic, R_S reduces to the threshold found by [92];

- it is straightforward to notice that R_S is a strictly increasing function with respect to $\mathcal{T}$ and η, which implies that rotation and fluid thermal conductivity have a delaying effect on the onset of convection. Physical meaning of this behaviour is pointed out in Section 5.4;

- since the derivative of $F(1, a^2)$ with respect to ξ is

$$\partial_\xi F(1, a^2) = \xi^2 \left(\mathcal{T}^2 - \mathrm{Da}^2\delta^2\right) - 2\xi\mathrm{Da}\delta - 1 \tag{5.30}$$

  being $\delta = a^2 + \pi^2$, the behaviour of R_S with respect to ξ depends on $\mathcal{T}$. In particular, if $\mathcal{T} = 0$, the derivative is negative. Such a result proves analytically the stabilising effect of permeability on the onset of convection in absence of rotation.

5.3.2 Oscillatory convection

In order to determine the critical Rayleigh number for oscillatory convection, we set $\sigma = i\omega$ ($\omega \in \mathbb{R} - \{0\}$) in (5.26)

$$\begin{aligned} R^2 &= G(n^2, a^2) = \\ &= \frac{\left(1 + i\omega\xi Va^{-1} + \xi \mathrm{Da}\delta_n\right)\left(\xi a^2 + n^2\pi^2 + \xi \mathrm{Da}\delta_n^2 + i\omega\xi Va^{-1}\delta_n\right) + \xi^2\mathcal{T}^2 n^2\pi^2}{\xi a^2\left(1 + i\omega\xi Va^{-1} + \xi \mathrm{Da}\delta_n\right)} \\ &\left[i\omega + \eta a^2 + n^2\pi^2 + H\frac{Ai\omega + \zeta a^2 + n^2\pi^2}{Ai\omega + \zeta a^2 + n^2\pi^2 + H\gamma}\right] \end{aligned} \tag{5.31}$$

The Rayleigh number is a real number, that is why the imaginary part in (5.31) has to be set equal to zero. By doing so, set $\omega_* = \omega^2$, the following equation arises

$$\frac{J_1\omega_*^2 + J_2\omega_* + J_3}{a^2\left[\left(\delta_\zeta + \gamma H\right)^2 + A^2\omega_*\right] Va\xi\left[\omega_*\xi^2 + \left(Va + \mathrm{Da}\delta_n Va\xi\right)^2\right]} = 0 \tag{5.32}$$

which provides a condition for the existence of oscillatory convection, where

$$\begin{aligned} J_1 =& A^2\xi^2\left[H\xi\delta_n + Va\left(\xi a^2 + n^2\pi^2 + \delta_n^2\xi\mathrm{Da}\right) + \xi\delta_n\left(\eta a^2 + n^2\pi^2\right)\right] \\ J_2 =& A^2Va^2\{\xi(\mathrm{Da}\delta_n\xi + 1)^2\left[a^2Va + \delta_n(\mathrm{Da}\delta_n Va + \delta_\eta + H)\right] + \\ & \pi^2n^2\left[Va(\mathrm{Da}\delta_n\xi + 1)\left(\mathrm{Da}\delta_n\xi + T^2\xi^2 + 1\right) - T^2\xi^3(\delta_\eta + H)\right]\} + \\ & A\gamma H^2Va\xi^2\left[\xi\left(a^2 + \mathrm{Da}\delta_n^2\right) + \pi^2n^2\right] + \xi^2(\delta_\zeta + \gamma H) \\ & \{\xi\left[Va\left(a^2 + \mathrm{Da}\delta_n^2\right)(\delta_\zeta + \gamma H) + \delta_n\delta_\eta(\delta_\zeta + \gamma H) + \delta_n\delta_\zeta H\right] + \\ & \pi^2n^2Va\left(\delta_\zeta + \gamma H\right)\} \\ J_3 =& Va^2\gamma H^2\{AVa(\mathrm{Da}\delta_n\xi + 1)[\xi\left(a^2 + \mathrm{Da}\delta_n^2\right)(\mathrm{Da}\delta_n\xi + 1) + \\ & \pi^2n^2\left(\mathrm{Da}\delta_n\xi + T^2\xi^2 + 1\right)] + \\ & \gamma[\xi(\mathrm{Da}\delta_n\xi + 1)^2\left(a^2Va + \delta_n(\mathrm{Da}\delta_n Va + \delta_\eta)\right) + \\ & \pi^2n^2\left(Va(\mathrm{Da}\delta_n\xi + 1)\left(\mathrm{Da}\delta_n\xi + T^2\xi^2 + 1\right) - \delta_\eta T^2\xi^3\right)]\} + \\ & Va^2\delta_\zeta^2\{\xi(\mathrm{Da}\delta_n\xi + 1)^2\left[a^2Va + \delta_n(\mathrm{Da}\delta_n Va + \delta_\eta + H)\right] + \\ & \pi^2n^2\left[Va(\mathrm{Da}\delta_n\xi + 1)\left(\mathrm{Da}\delta_n\xi + T^2\xi^2 + 1\right) - T^2\xi^3(\delta_\eta + H)\right]\} + \\ & Va^2\delta_\zeta\gamma H\{\xi(\mathrm{Da}\delta_n\xi + 1)^2\left[2a^2Va + \delta_n(2\mathrm{Da}\delta_n Va + 2\delta_\eta + H)\right] + \\ & \pi^2n^2\left[2Va(\mathrm{Da}\delta_n\xi + 1)\left(\mathrm{Da}\delta_n\xi + T^2\xi^2 + 1\right) - T^2\xi^3(2\delta_\eta + H)\right]\} \end{aligned} \tag{5.33}$$

and

$$\begin{aligned} \delta_\eta &= \eta a^2 + n^2\pi^2 \\ \delta_\zeta &= \zeta a^2 + n^2\pi^2 \end{aligned} \tag{5.34}$$

Let us notice that, since J_1 is always positive, oscillatory convection cannot occur when either

$$J_2^2 - 4J_1J_3 < 0 \tag{5.35}$$

or

$$\begin{cases} J_2 > 0 \\ J_3 > 0 \end{cases} \tag{5.36}$$

Once the positive root of (5.32) has been determined, it is substituted in (5.31) and the critical Rayleigh number for the onset of oscillatory convection is determined by solving the following minimum problem:

$$R_O = \min_{(n^2,a^2)\in\mathbb{N}\times\mathbb{R}^+} G_1(n^2,a^2,\omega^2(n^2,a^2))|_{\omega^2=\omega_c^2} \tag{5.37}$$

ω_c^2 being such that $Im(G(n^2,a^2,\omega_c^2(n^2,a^2))) = 0$, and

$$\begin{aligned}
&G_1\left(n^2,a^2,\omega^2(n^2,a^2)\right) = Re\left(G\left(n^2,a^2,\omega^2(n^2,a^2)\right)\right) = \\
&\left[\delta_\zeta H + \delta_\eta(\delta_\zeta+\gamma H) - A\omega^2\right]\left[-A\omega^2\xi + (\delta_\zeta+\gamma H)Va(1+\mathrm{Da}\delta_n\xi)\right] \\
&\left[-\delta_n\omega^2\xi^2 + n^2\pi^2\mathcal{T}^2Va^2\xi^2 + Va^2(1+\mathrm{Da}\delta_n\xi)\left(n^2\pi^2+\xi a^2+\mathrm{Da}\delta_n^2\xi\right)\right] + \\
&\Bigg[\left[\delta_\zeta H + \delta_\eta(\delta_\zeta+\gamma H) - A\omega^2\right]Va\xi\left(\delta_n + n^2\pi^2 + a^2\xi + 2\mathrm{Da}\delta_n^2\xi\right) \\
&[AVa + (\delta_\zeta+\gamma H + A\mathrm{Da}\delta_n Va)\xi] + [\delta_\zeta+\gamma H + A(\delta_\eta+H)]\,Va\xi \\
&\left(\delta_n + n^2\pi^2 + a^2\xi + 2\mathrm{Da}\delta_n^2\xi\right)\left[A\omega^2\xi - (\delta_\zeta+\gamma H)Va(1+\mathrm{Da}\delta_n\xi)\right] + \\
&[\delta_\zeta+\gamma H + A(\delta_\eta+H)]\,[AVa + \xi(\delta_\zeta+\gamma H + A\mathrm{Da}\delta_n Va)] \\
&\left[-\delta_n\omega^2\xi^2 + n^2\pi^2\mathcal{T}^2Va^2\xi^2 + Va^2(1+\mathrm{Da}\delta_n\xi)(n^2\pi^2+\xi a^2+\mathrm{Da}\delta_n^2\xi)\right]\Bigg] \\
&\frac{\omega^2}{a^2\left[(\delta_\zeta+\gamma H)^2 + A^2\omega^2\right]Va\xi\left[\omega^2\xi^2 + (Va+\mathrm{Da}\delta_n Va\xi)^2\right]}
\end{aligned} \tag{5.38}$$

We would like to remark that if (5.32) admits two positive roots, then both of them are plugged into (5.31) and the lowest threshold arising from the two is the critical value we were looking for.

Accounting for the physical meaning of R_O, we have to prove that $G_1\left(n^2,a^2,\omega^2(n^2,a^2)\right)$ is positive. First, we write G_1 as follows so that it is easier to understand where this functions lives:

$$G_1\left(n^2,a^2,\omega^2(n^2,a^2)\right) = \frac{\Lambda_1\omega_*^3 + \Lambda_2\omega_*^2 + \Lambda_3\omega_* + \Lambda_4}{\Lambda_5\omega_*^2 + \Lambda_6\omega_* + \Lambda_7} \tag{5.39}$$

where

$$
\begin{aligned}
\Lambda_1 =& - A^2\delta\xi^3\\
\Lambda_2 =& a^2A^2\delta_\eta Va\xi^3 + a^2A^2HVa\xi^3 - A^2\mathrm{Da}^2\delta^3Va^2\xi^3 + A^2\mathrm{Da}\delta^2\delta_\eta Va\xi^3 +\\
& A^2\mathrm{Da}\delta^2HVa\xi^3 - 2A^2\mathrm{Da}\delta^2Va^2\xi^2 - A^2\delta Va^2\xi + \pi^2A^2\delta_\eta n^2Va\xi^2 +\\
& \pi^2A^2Hn^2Va\xi^2 + \pi^2A^2n^2\mathcal{T}^2Va^2\xi^3 - A\delta\gamma H^2\xi^3 - \delta\delta_\zeta^2\xi^3 -\\
& 2\delta\delta_\zeta\gamma H\xi^3 - \delta\gamma^2H^2\xi^3\\
\Lambda_3 =& Va\Bigg\{A^2Va^2(\delta_\eta + H)(\mathrm{Da}\delta\xi + 1)\{\xi(a^2 + \mathrm{Da}\delta^2)(\mathrm{Da}\delta\xi + 1) +\\
& \pi^2n^2\left(\mathrm{Da}\delta\xi + \mathcal{T}^2\xi^2 + 1\right)\} +\\
& \xi(\delta_\zeta + \gamma H)\Bigg[\xi^2\Bigg((a^2 + \mathrm{Da}\delta^2)[\delta_\eta(\delta_\zeta + \gamma H) + \delta_\zeta H] -\\
& Va(\delta_\zeta + \gamma H)(\mathrm{Da}^2\delta^3 - \pi^2n^2\mathcal{T}^2)\Bigg) - \delta Va(\delta_\zeta + \gamma H) +\\
& \xi\Bigg(\pi^2n^2[\delta_\eta(\delta_\zeta + \gamma H) + \delta_\zeta H] - 2\mathrm{Da}\delta^2Va(\delta_\zeta + \gamma H)\Bigg)\Bigg] -\\
& A\gamma H^2Va\xi\left[\xi^2\left(\mathrm{Da}^2\delta^3 - \pi^2n^2\mathcal{T}^2\right) + 2\mathrm{Da}\delta^2\xi + \delta\right]\Bigg\}\\
\Lambda_4 =& Va^3(\mathrm{Da}\delta\xi + 1)(\delta_\zeta + \gamma H)\left[\delta_\eta(\delta_\zeta + \gamma H) + \delta_\zeta\right]\\
& \left[(\xi a^2 + \mathrm{Da}\delta^2\xi)(\mathrm{Da}\delta\xi + 1) + \pi^2n^2\left(\mathrm{Da}\delta\xi + \mathcal{T}^2\xi^2 + 1\right)\right]\\
\Lambda_5 =& a^2A^2Va\xi^3\\
\Lambda_6 =& a^2Va\xi\left[A^2(\mathrm{Da}\delta Va\xi + Va)^2 + \xi^2(\delta_\zeta + \gamma H)^2\right]\\
\Lambda_7 =& a^2Va^3\xi(\mathrm{Da}\delta\xi + 1)^2(\delta_\zeta + \gamma H)^2
\end{aligned}
\tag{5.40}
$$

It is straightforward to notice that the denominator is always positive, as well as Λ_4, while $\Lambda_1 < 0$. Despite we know nothing about the sign of Λ_2 and Λ_3, we can say that G_1 lives in the first quarter for any $\omega^2 \in [0, \bar{\omega}^2]$, where $\bar{\omega}^2$ such that $G_1(n^2, a^2, \bar{\omega}^2) = 0$. Numerically, it is easy to notice that the following system

$$
\begin{cases}
Im(G(n^2, a^2, \omega^2(n^2, a^2))) = 0\\
G_1(n^2, a^2, \omega^2(n^2, a^2)) = 0
\end{cases}
\tag{5.41}
$$

does not admit any solution $\omega^2(n^2, a^2)$. Furthermore, and most importantly, numerical simulations show that $\omega_c^2(n^2, a^2) < \bar{\omega}^2(n^2, a^2)$, $\forall(n^2, a^2)$. Hence, $G_1(n^2, a^2, \omega_c^2(n^2, a^2)) > 0$, $\forall(n^2, a^2)$.

Remark 5. *If $\mathcal{T} = 0$, from (5.33) it turns out that $J_2, J_3 > 0$. Hence, by virtue of (5.36), conditions for the existence of oscillatory convection are not satisfied and only steady convection can occur.*

Remark 6. *If $Va \to \infty$, by performing the limit in (5.32), it turns out that (5.32) admits only negative solution. As a consequence, only steady convection can occur and the analysis is the same as the one presented in [90].*

5.4 Numerical results

Given the complex expression of the critical thresholds, both for oscillatory and steady convection, a numerical analysis is required in order to draw the attention on how parameters affect the onset of instability. In particular, in this section, we will point out the effect of rotation, the Darcy number and anisotropic permeability and thermal conductivities on the motionless steady state. A particular attention will be paid to the effect of Vadasz inertia term, which can cause the onset of convection via oscillatory motion, as already pointed out.

Before proceeding to the analysis, let us underline that, due to its complexity, it is not possible to solve analytically the minimum problem (5.37)-(5.38). Numerical simulations show that the minimum for $G_1(n^2, a^2, \omega_c^2(n^2, a^2))$ with respect to n^2 is attained in $n^2 = 1$, for a completely arbitrary choice of parameters. That is why we can reduce our analysis to the following minimum problem

$$R_O = \min_{a^2 \in \mathbb{R}^+} G_1(1, a^2, \omega_c^2(1, a^2)) \tag{5.42}$$

Once R_O has been determined, we can define the critical Rayleigh number Ra as

$$Ra = \min\{R_S, R_O\} \tag{5.43}$$

If $Ra = R_S$ ($Ra = R_O$), convection can occur through steady (oscillatory) motions.

In order to show the influence of parameters on the critical Rayleigh number Ra, we adopt the same procedure as done in [86, 27], namely we report the critical threshold as function of the inter-phase heat transfer coefficient H. This parameter, which is defined by $H = \dfrac{hd^2}{\varepsilon \kappa_z^f}$, is not always easily measured. That is why we need to introduce a range of values between which H can vary. Starting from its definition, $(10^{-2}, 10^6)$ is a reasonable interval.

Figures 5.1a-5.1b show the influence of rotation on R_S and R_O, respectively. The delaying effect of rotation on the onset of convection comes out. We have previously shown analytically that the critical threshold R_S for steady convection increases with $\mathcal{T}$, so the result in Figure 5.1a is expected. In addition, what Figures 5.1a-5.1b show is physically reasonable because in the momentum Eq. $(5.9)_1$ the term due to rotation has only horizontal component, namely rotation acts horizontally on the fluid motion, discouraging the motion in the vertical direction. We managed to prove that, when $\mathcal{T} = 0$, conditions for the existence of oscillatory convection are not satisfied. As a consequence, in Figure 5.1b, if $\mathcal{T} = 0$, the plot of R_O does

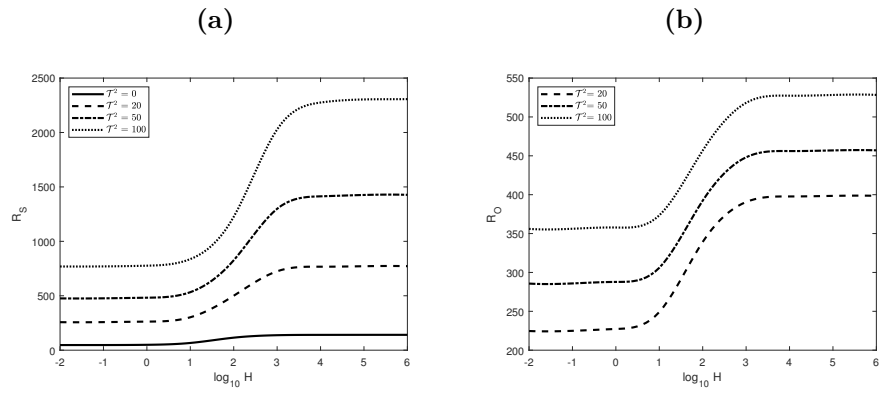

Figure 5.1: Critical Rayleigh number as function of the inter-phase heat transfer coefficient H for different values of the Taylor number $\mathcal{T}$ with $\xi = \zeta = \eta = 1$, $\gamma = 0.5$, $A = 0.01$, $Va = 10$ and $\mathrm{Da} = 0.01$.

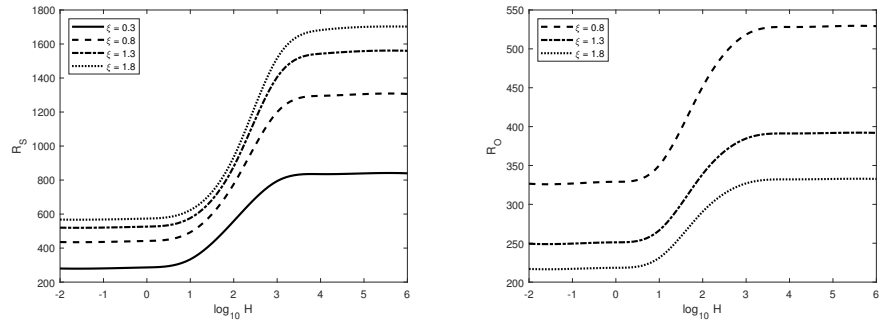

Figure 5.2: Critical Rayleigh number as function of the inter-phase heat transfer coefficient H for different values of permeability ξ with $\zeta = \eta = 1$, $\gamma = 0.5$, $A = 0.01$, $Va = 10$, $\mathcal{T}^2 = 50$ and $\mathrm{Da} = 0.01$.

not appear. This result is in agreement with results in [16] and, in addition, it is expected since the inertia term leads to the occurrence of oscillatory convection only when coupled to the rotation term, as already pointed out [54].

In Figures 5.2a-5.2b the behaviour of R_S and R_O with respect to permeability ξ is shown. It is evident the different influence of ξ on the onset of oscillatory and steady convection. Increasing the horizontal permeability makes the onset of oscillatory motions easier, discouraging the onset of steady ones. Actually, since we managed to determine the derivative $\partial_\xi F(1, a^2)$, we proved analytically that the behaviour of R_S with respect to ξ depends on $\mathcal{T}$. The destabilizing effect of ξ on the onset of steady convection has been proved analytically if $\mathcal{T} = 0$. While if $\mathcal{T} \neq 0$, ξ keeps on encouraging the onset of instability, but, unlike the previous case, oscillatory motions are preferred instead of steady ones, as shown in Figure 5.3. In Table 5.1, the behaviour of the critical Rayleigh number Ra with respect to

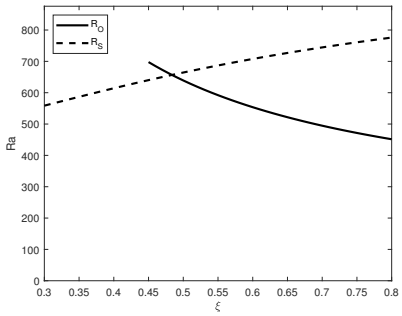

Figure 5.3: Critical Rayleigh number as function of the permeability parameter ξ with $\zeta = \eta = 1$, $\gamma = 0.5$, $H = 100$, $A = 0.01$, $Va = 10$, $\mathcal{T}^2 = 50$ and Da $= 0.01$.

(a) $\mathcal{T}^2 = 50$

ξ	R_O	R_S
0.30	∄	**558.6386**
0.42	∄	**624.7509**
0.43	725.4627	**629.9432**
0.48	660.8735	**654.8910**
0.49	**649.7135**	659.6715
0.70	**494.7303**	744.5317

(b) $\mathcal{T}^2 = 0$

ξ	$R_S \equiv Ra$
0.30	207.4724
0.35	190.6250
0.40	177.5048
0.50	158.2614
0.60	144.7119
0.70	134.5796

Table 5.1: Critical Rayleigh number Ra for different values of ξ with $\zeta = \eta = 1$, $A = 0.01$, $\gamma = 0.5$, $H = 100$, Da $= 0.01$, $Va = 10$, (a) $\mathcal{T}^2 = 50$ (b) $\mathcal{T} = 0$.

ξ is shown, both with and without rotation. In particular, in Table 5.1a, the values of Ra are bold. While in Table 5.1b, given the absence of oscillatory convection, Ra coincides with R_S.

Figures 5.4a-5.4b show the effect of solid thermal conductivity on the onset of convection. In both Figures, increasing values of ζ yields growing critical thresholds. This result is physically reasonable since the greater solid thermal conductivity is, the more easily solid matrix absorbs heat from fluid, implying a delay in the onset of convection. Moreover, when $H \to 0$, the effect of solid thermal conductivity is less remarkable. Assuming that H goes to zero means that heat exchange between fluid and solid is forbidden, that is why changing the solid thermal conductivity parameter ζ does not affect the critical threshold for the onset of convection. Analogous results were obtained in [90].

In Figure 5.5, the stabilizing effect of ζ on the onset of instability is evident, as well as the existence of a transition point ζ_T before which thermal convection occurs through steady motions and beyond which it arises through oscillatory motions.

Figures 5.6a-5.6b show the behaviour of R_S and R_O with respect to variations

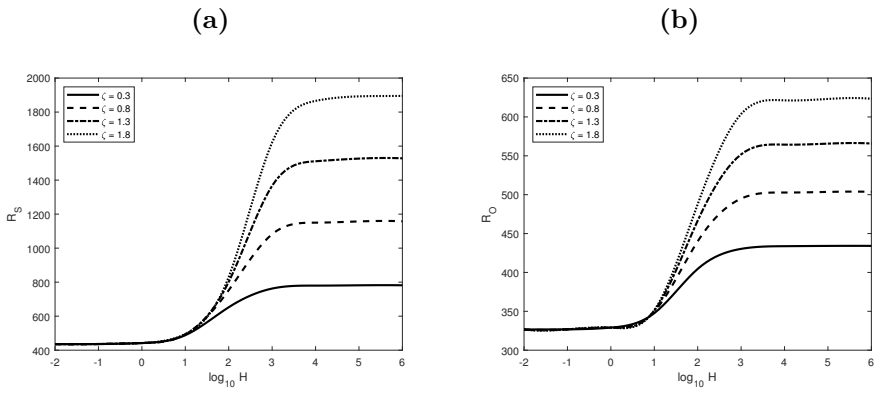

Figure 5.4: Critical Rayleigh number as function of the inter-phase heat transfer coefficient H for different values of the solid thermal conductivity parameter ζ with $\xi = \eta = 1$, $\gamma = 0.5$, $A = 0.01$, $Va = 10$, $\mathcal{T}^2 = 50$ and $\mathrm{Da} = 0.01$.

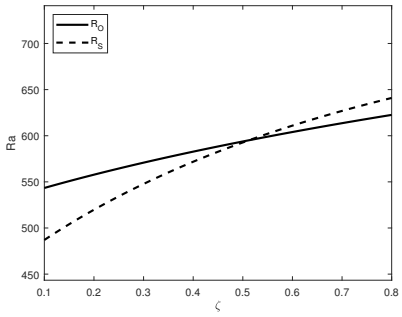

Figure 5.5: Critical Rayleigh number as function of the solid thermal conductivity parameter ζ with $\xi = 0.5$, $\eta = 1$, $\gamma = 0.5$, $H = 100$, $A = 0.01$, $Va = 10$, $\mathcal{T}^2 = 50$ and $\mathrm{Da} = 0.01$.

of the fluid thermal conductivity parameter η. This parameter has a stabilizing effect on conduction, delaying the onset of convection. Result in Figure 5.6a is in agreement with the analytical result pointed out in Section 5.3. From a physical point of view, increasing κ_z^f, which implies by definition a decreasing η, allows heat to spread in the vertical direction within the fluid more easily, encouraging the onset of convection. We would like to point out that in Figure 5.6b, conditions (5.35)-(5.36) for the non-existence of oscillatory convection are verified for some values of H and η, for the set of parameters chosen. As a consequence it is not possible to plot R_O for any H and η in Figure 5.6b.

In Figure 5.7, it is highlighted the existence of a threshold value for η. Once η overcomes this critical value, convection occurs through oscillatory motion (i.e. $Ra \equiv R_O$). Before this value, only steady convection can arise ($Ra \equiv R_S$).

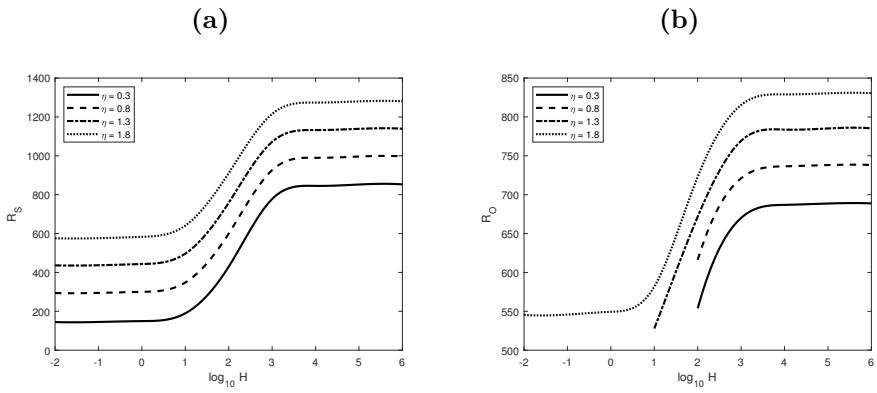

Figure 5.6: Critical Rayleigh number as function of the inter-phase heat transfer coefficient H for different values of the fluid thermal conductivity parameter η with $\xi = 0.5$, $\zeta = 1$, $\gamma = 0.5$, $A = 0.01$, $Va = 10$, $\mathcal{T}^2 = 50$ and $\mathrm{Da} = 0.01$.

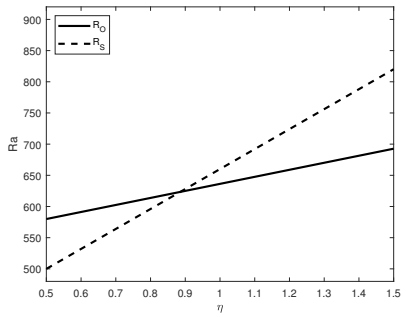

Figure 5.7: Critical Rayleigh number as function of the solid thermal conductivity parameter η with $\xi = 0.5$, $\zeta = 1$, $\gamma = 0.5$, $H = 100$, $A = 0.01$, $Va = 10$, $\mathcal{T}^2 = 50$ and $\mathrm{Da} = 0.01$.

The effect of κ_z^f on the critical Rayleigh number is highlighted in Figures 5.8a-5.8b, as well. From these Figures, the destabilising effect of γ on the critical thresholds comes up and, as consequence, since by definition γ is proportional to κ_z^f, increasing κ_z^f encourages the onset of instability.

In order to capture the influence of Da on Ra as best as we can, we decided not to plot R_S and R_O as functions of H. Instead, we report the behaviour of the critical threshold for a fixed H. In Figure 5.9, a parabolic behaviour of R_S and the existence of a value of Da beyond which R_O does not exist are evident. Nevertheless, the critical threshold Ra for the onset of instability exhibits an increasing trend with respect to Da, as shown in Table 5.2 where Ra is bold. When considering the Darcy-Brinkman model, which is closer to a model for clear fluids (in absence of porous medium), we would expect the critical Rayleigh number to get closer to the critical value for clear fluids. It is well known that the critical value for clear fluids is greater than the one for fluids in presence of porous medium (i.e. the presence

Da	R_O	R_S
0.001	**296.9241**	957.2011
0.04	**697.7111**	782.9615
0.05	796.2326	**783.4380**
0.06	895.7849	**786.0607**
0.07	996.6127	**790.1571**
0.08	∄	**795.3360**
0.10	∄	**808.0355**
0.20	∄	**896.0463**
0.30	∄	**1004.8**

Table 5.2: Critical Rayleigh number Ra for different values of Da with $\xi = \zeta = \eta = 1$, $A = 0.01$, $\gamma = 0.5$, $H = 100$, $Va = 10$, $\mathcal{T}^2 = 50$.

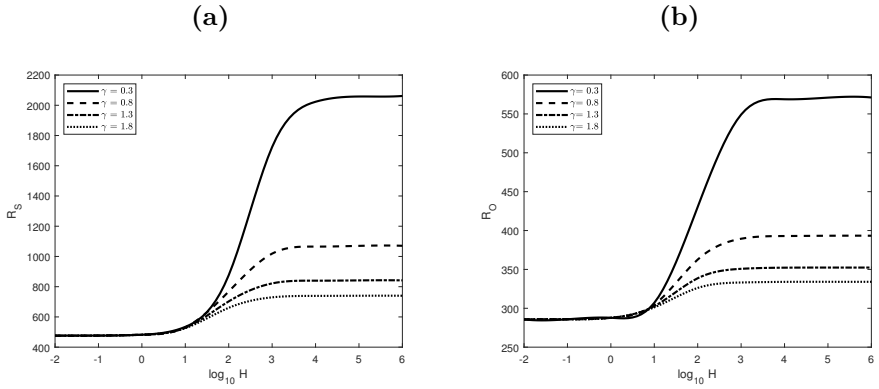

Figure 5.8: Critical Rayleigh number as function of the inter-phase heat transfer coefficient H for different values of the diffusivity ratio γ with $\xi = \zeta = \eta = 1$, $A = 0.01$, $\mathcal{T}^2 = 50$, $Va = 10$ and $\mathrm{Da} = 0.01$.

of a porous medium eases the onset of instability). Hence, result in Figure 5.9 is reasonable.

The influence of the Vadasz number Va on the onset of convection is highlighted in Figure 5.10. In this case, we report only the behaviour of R_O since, as shown in (5.29), R_S does not depend on Va. In Figure 5.10, the stabilising effect of Va is clear. For some values of Va and H it is not possible to plot R_O since conditions for the existence of oscillatory convection are not satisfied.

A focus on the behaviour of Ra with respect to Va, for a fixed H, is given in Figure 5.11, where it is shown that increasing Vadasz number makes the critical threshold increase at least up to a certain value, beyond which the critical Rayleigh number is constant and convection arises through steady motion. If $Va \to \infty$, as we have pointed out in Remark 6, oscillatory convection cannot occur. In fact, looking at model (5.9), when $Va \to \infty$, the inertia term disappears and model (5.9) reduces

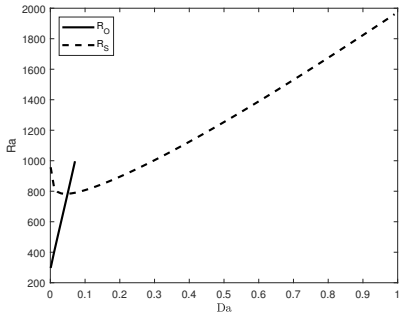

Figure 5.9: Critical Rayleigh number as function of the Darcy number Da with $\xi = \eta = \zeta = 1$, $\gamma = 0.5$, $H = 100$, $A = 0.01$, $Va = 10$ and $\mathcal{T}^2 = 50$.

to that one studied in [90] for which the principle of exchange of stabilities holds and convection occurs only through steady motion. On the other hand, if $Va \to 0$, the inertia term strongly affects the model and instability occurs earlier, through oscillatory motion. As a result, the inertia term encourages the onset of convection and such a result is not surprising. Indeed, we can write by definition $Va = \dfrac{\mathrm{Pr}}{\mathrm{Da}\ c_a}$, where $\mathrm{Pr} = \dfrac{\tilde{\mu} c_f}{\kappa_z^f}$ is the Prandtl number and c_a is inversely proportional to ε [1]. Then, it immediately follows that if porosity $\varepsilon \to 0$, i.e. the medium becomes less porous, then $Va \to 0$ and the critical Rayleigh number decreases, which is expected as the presence of a porous medium has a destabilising effect on conduction, as already pointed out.

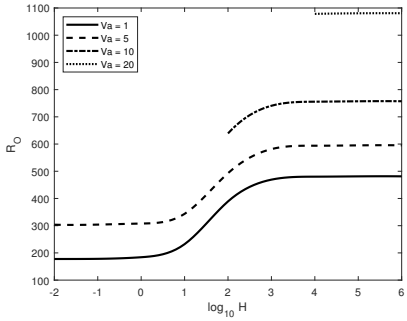

Figure 5.10: Critical Rayleigh number as function of the inter-phase heat transfer coefficient H for different values of the Vadasz number Va with $\xi = 0.5$, $\eta = \zeta = 1$, $\gamma = 0.5$, $A = 0.01$, $\mathcal{T}^2 = 50$ and $\mathrm{Da} = 0.01$.

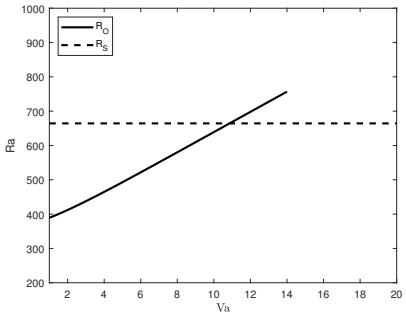

Figure 5.11: Critical Rayleigh number as function of the Vadasz number Va with $\xi = 0.5$, $\eta = \zeta = 1$, $\gamma = 0.5$, $H = 100$, $A = 0.01$, $Va = 10$, $\mathcal{T}^2 = 50$ and $\mathrm{Da} = 0.01$.

5.5 Conclusions

The study undertaken in this chapter was devoted to investigate the effect of the inertia term in the momentum equation of a Darcy-Brinkman model on the onset of convective motions. In this chapter, we performed a linear instability analysis to show that the presence of the Vadasz term leads to different physical phenomena. Specifically, the presence of inertia term makes the onset of convection possible via either oscillatory or steady motions. Moreover, we proved analytically that the Vadasz term does not affect steady convection, namely we recovered same results as in [90]. Conditions for the non-existence of oscillatory convective motions were determined numerically because of the high complexity of the critical Rayleigh number expression.

In addition, we studied the effect of parameters on the onset of both steady and oscillatory convective motions. We proved analytically that the influence of anisotropic permeability ξ on steady convection depends on the Taylor number $\mathcal{T}$, while numerically we showed the stabilising effect of rotation, thermal conductivities (both fluid and solid one) and of the Darcy number Da on the onset of instability.

Chapter 6

Onset of convection in LTNE Darcy-Brinkman anisotropic porous layer: Cattaneo effect in the solid

6.1 Introduction

In the present chapter, results from [44] are shown. The influence of second sound phenomenon on the onset of convection in a highly porous medium in LTNE regime, exhibiting horizontal isotropy in permeability and thermal conductivity, is investigated. In particular, we assume the second sound effect is greater in solids: hence, we use Cattaneo's law to describe the heat flux only in the solid phase, while Fourier's law is retained and used to model the flux in the fluid phase ([37, 39, 40, 41]). Linear and nonlinear analyses for the stability of conduction solution for the problem at stake are performed. It is proved that the employment of Cattaneo's law as governing equation for heat flux in solid can lead to the occurrence of oscillatory convection.

In section 6.2, the mathematical model is introduced. Then, the dimensionless system governing the evolution of perturbation fields related to conduction solution is obtained. In section 6.3, the instability analysis is performed and the critical threshold beyond which thermal convection occurs is determined. We prove that the onset of steady convection is not affected by the thermal relaxation time and we determine conditions for the non-existence of oscillatory convection. Section 6.4 is devoted to the global nonlinear stability analysis of the conduction solution by employing the energy method with the L^2-norm. Finally, in section 6.5, numerical simulations (related to two cases of practical interest) are carried out in order to focus the attention on the influence of second sound, inter-phase heat transfer,

permeability and thermal conductivity on the onset of instability. It is proved that, if the thermal relaxation time τ appearing in the dimensionless number $\hat{\tau}$ is great, oscillatory convection is the dominant mechanism. While, when τ goes to zero, only steady convection can arise. Analogous considerations are valid when taking into account the effect of Sg, given the proportionality between $\hat{\tau}$ and Sg. Moreover, since R_S and R_O are increasing functions of Da, the Darcy number has a stabilizing effect on the onset of convection. It turns out that permeability ξ has a destabilising effect on the onset of convection, while both fluid (η) and solid (ζ) thermal conductivities have a stabilising effect. Periodicity cell gets wider for increasing values of ξ and η, while a mixed behaviour is highlighted with respect to ζ. Moreover, the influence of inter-phase heat transfer coefficient H is analysed. The existence of a transition value H_T and a mixed influence, depending on ζ, on periodicity cell dimension is highlighted.

6.2 Statement of the problem

Let $\mathscr{F}$ be an incompressible fluid at rest saturating the horizontal porous layer $\mathbb{R}^2 \times [0, d]$, uniformly heated from below. Let T_L be the temperature of the lower plane and let T_U be the temperature of the upper plane, with $T_L > T_U$. Under the assumption of LTNE, defining by T_f the temperature of fluid phase and by T_s the temperature of solid phase, we suppose

$$\begin{aligned} &T_f = T_s = T_L \text{ on } z = 0, \\ &T_f = T_s = T_U \text{ on } z = d. \end{aligned} \tag{6.1}$$

We assume that the temperature T_s in solid phase satisfies Cattaneo's law, while the temperature T_f in fluid phase satisfies Fourier's law.

Furthermore, horizontal isotropy in permeability, fluid and solid thermal conductivity, as well, is considered [35]. Hence, by setting $\mathcal{K}$ the permeability tensor and $\mathcal{D}_f$ and $\mathcal{D}_s$ the thermal conductivity tensors of fluid and solid phase, respectively, by assuming that they share the same principal axis (x, y, z), they can be written in diagonal form, i.e.

$$\begin{aligned} &\mathcal{K} = K_z \tilde{\mathcal{K}} \quad \tilde{\mathcal{K}} = \begin{pmatrix} \xi & 0 & 0 \\ 0 & \xi & 0 \\ 0 & 0 & 1 \end{pmatrix} \quad \xi = \frac{K_x}{K_z} = \frac{K_y}{K_z} \\ &\mathcal{D}_s = \kappa_z^s \tilde{\mathcal{D}}_s \quad \tilde{\mathcal{D}}_s = \begin{pmatrix} \zeta & 0 & 0 \\ 0 & \zeta & 0 \\ 0 & 0 & 1 \end{pmatrix} \quad \zeta = \frac{\kappa_x^s}{\kappa_z^s} = \frac{\kappa_y^s}{\kappa_z^s} \\ &\mathcal{D}_f = \kappa_z^f \tilde{\mathcal{D}}_f \quad \tilde{\mathcal{D}}_f = \begin{pmatrix} \eta & 0 & 0 \\ 0 & \eta & 0 \\ 0 & 0 & 1 \end{pmatrix} \quad \eta = \frac{\kappa_x^f}{\kappa_z^f} = \frac{\kappa_y^f}{\kappa_z^f} \, . \end{aligned} \tag{6.2}$$

For the problem at stake, accounting for highly porous materials, the Darcy-Brinkman model, by employing the Oberbeck-Boussinesq approximation, is the following [1, 46]

$$\begin{cases} \dfrac{\mu}{\mathcal{K}}\mathbf{v} = -\nabla p + \rho_f \alpha T_f g\mathbf{k} + \tilde{\mu}\Delta\mathbf{v} \\ \nabla\cdot\mathbf{v} = 0 \\ \varepsilon(\rho c)_f \dfrac{\partial T_f}{\partial t} + (\rho c)_f \mathbf{v}\cdot\nabla T_f = \varepsilon\nabla\cdot(\mathcal{D}_f\nabla T_f) + h(T_s - T_f) \\ (1-\varepsilon)(\rho c)_s \dfrac{\partial T_s}{\partial t} = -(1-\varepsilon)\nabla\cdot\mathbf{Q} - h(T_s - T_f) \\ \tau\dfrac{\partial \mathbf{Q}}{\partial t} = -\mathbf{Q} - \mathcal{D}_s\nabla T_s \end{cases} \tag{6.3}$$

where $\mathbf{v}$, p, T_s, T_f and $\mathbf{Q}$ are (seepage) velocity, pressure, solid phase temperature, fluid phase temperature and heat flux in the solid phase, respectively; μ, $\tilde{\mu}$, ρ_f, ρ_s, g, α, ε, c, h, τ are dynamic viscosity, effective viscosity, fluid density, solid density, gravity acceleration, thermal expansion coefficient, porosity, specific heat, interaction coefficient and solid thermal relaxation time, respectively.

To system (6.3) we append the following boundary conditions

$$\begin{aligned} &T_s = T_f = T_L \text{ on } z = 0, \quad T_s = T_f = T_U \text{ on } z = d, \\ &\mathbf{v}\cdot\mathbf{n} = 0 \quad \text{on } z = 0, d \end{aligned} \tag{6.4}$$

being $\mathbf{n}$ the unit outward normal to planes $z = 0, d$.

The steady conduction solution of (6.3) is

$$m_0 = \{\mathbf{v}_b = \mathbf{0}, \quad T_b^f = T_b^s = -\beta z + T_L, p_b(z), \quad \mathbf{Q}_b = \kappa_z^s \beta\mathbf{k}\} \tag{6.5}$$

where $\beta = \dfrac{T_L - T_U}{d} (> 0)$ is the adverse temperature gradient and $p_b(z)$ is solution of

$$\frac{dp}{dz} = -\rho_f\alpha\beta g z + \rho_f \alpha g T_L\,. \tag{6.6}$$

To study the stability of m_0, let $(\mathbf{u}, \theta, \varphi, \pi, \mathbf{q})$ be the perturbation fields to seepage velocity, fluid temperature, solid temperature, pressure and heat flux, respectively. The evolution equations of $(\mathbf{u}, \theta, \varphi, \pi, \mathbf{q})$ are:

$$\begin{cases} \dfrac{\mu}{\mathcal{K}}\mathbf{u} = -\nabla\pi + \rho_f\alpha\theta g\mathbf{k} + \tilde{\mu}\Delta\mathbf{u} \\ \nabla\cdot\mathbf{u} = 0 \\ \varepsilon(\rho c)_f \dfrac{\partial\theta}{\partial t} + (\rho c)_f \mathbf{u}\cdot\nabla\theta = (\rho c)_f \beta w + \varepsilon\nabla\cdot(\mathcal{D}_f\nabla\theta) + h(\varphi - \theta) \\ (1-\varepsilon)(\rho c)_s \dfrac{\partial\varphi}{\partial t} = -(1-\varepsilon)\nabla\cdot\mathbf{q} - h(\varphi - \theta) \\ \tau\dfrac{\partial\mathbf{q}}{\partial t} = -\mathbf{q} - \mathcal{D}_s\nabla\varphi. \end{cases} \tag{6.7}$$

Let us introduce the dimensionless quantities

$$x_i = \tilde{x}_i d, \quad t = \tilde{t}\frac{\varepsilon d}{U}, \quad \pi = \tilde{\pi} P, \quad u_i = \tilde{u}_i U,$$

$$\theta = \tilde{\theta} T', \quad \varphi = \tilde{\varphi} T', \quad q_i = \tilde{q}_i Q^* \tag{6.8}$$

where

$$P = \frac{\mu U d}{K_z}, \quad U = \frac{\varepsilon \kappa_z^f}{d(\rho c)_f}, T' = \sqrt{\frac{\varepsilon \kappa_z^f \mu \beta}{\rho_f^2 c_f g \alpha K_z}}, \quad Q^* = \frac{\kappa_z^s T'}{d}. \tag{6.9}$$

Omitting the tilde, the dimensionless system for perturbation fields is

$$\begin{cases} \dfrac{\mathbf{u}}{\mathcal{K}} = -\nabla \pi + R\theta \mathbf{k} + \mathrm{Da}\Delta \mathbf{u} \\ \nabla \cdot \mathbf{u} = 0 \\ \dfrac{\partial \theta}{\partial t} + \mathbf{u} \cdot \nabla \theta = Rw + \nabla \cdot (\mathcal{D}_f \nabla \theta) + H(\varphi - \theta) \\ A\dfrac{\partial \varphi}{\partial t} = -\nabla \cdot \mathbf{q} - H\gamma(\varphi - \theta) \\ \hat{\tau}\dfrac{\partial \mathbf{q}}{\partial t} = -\mathbf{q} - \mathcal{D}_s \nabla \varphi \end{cases} \tag{6.10}$$

with

$$\begin{aligned} &\hat{\tau} = \mathrm{Sg}\frac{\kappa_z^f}{4\mu c_f}, \qquad H = \frac{hd^2}{\varepsilon \kappa_z^f}, \qquad \gamma = \frac{\varepsilon \kappa_z^f}{(1-\varepsilon)\kappa_z^s}, \qquad A = \frac{(\rho c)_s \kappa_z^f}{(\rho c)_f \kappa_z^s}, \\ &R^2 = \frac{K_z \rho_f^2 c_f d^2 \beta g \alpha}{\mu \varepsilon \kappa_z^f}, \qquad \mathrm{Da} = \frac{\tilde{\mu} K_z}{\mu d^2}, \qquad \mathrm{Sg} = \frac{4\tau \mu}{\rho_f d^2} \end{aligned} \tag{6.11}$$

where R^2, Da and Sg are, respectively, the Rayleigh number, the Darcy number and the Straughan number [93].

By defining $q = \nabla \cdot \mathbf{q}$ and applying the divergence operator to Eq. $(6.10)_5$, from (6.10) one obtains

$$\begin{cases} \dfrac{\mathbf{u}}{\mathcal{K}} = -\nabla \pi + R\theta \mathbf{k} + \mathrm{Da}\Delta \mathbf{u} \\ \nabla \cdot \mathbf{u} = 0 \\ \dfrac{\partial \theta}{\partial t} + \mathbf{u} \cdot \nabla \theta = Rw + \nabla \cdot (\mathcal{D}_f \nabla \theta) + H(\varphi - \theta) \\ A\dfrac{\partial \varphi}{\partial t} = -q - H\gamma(\varphi - \theta) \\ \hat{\tau}\dfrac{\partial q}{\partial t} = -q - \nabla \cdot (\mathcal{D}_s \nabla \varphi)\,. \end{cases} \tag{6.12}$$

Moreover, by applying the operator $\tau\dfrac{\partial}{\partial t}+1$ to $(6.12)_4$ and substituting $(6.12)_5$ in the resulting equation, we get

$$\begin{cases} \dfrac{\mathbf{u}}{\mathcal{K}} = -\nabla\pi + R\theta\mathbf{k} + \mathrm{Da}\Delta\mathbf{u} \\ \nabla\cdot\mathbf{u} = 0 \\ \dfrac{\partial\theta}{\partial t} + \mathbf{u}\cdot\nabla\theta = Rw + \nabla\cdot(\mathcal{D}_f\nabla\theta) + H(\varphi-\theta) \\ A\left(\hat{\tau}\dfrac{\partial}{\partial t}+1\right)\dfrac{\partial\varphi}{\partial t} = \nabla\cdot(\mathcal{D}_s\nabla\varphi) - H\gamma\left(\hat{\tau}\dfrac{\partial}{\partial t}+1\right)(\varphi-\theta). \end{cases} \tag{6.13}$$

To system (6.13) we append the following initial conditions

$$\mathbf{u}(\mathbf{x},0) = \mathbf{u}_0(\mathbf{x})\,, \qquad \pi(\mathbf{x},0) = \pi_0(\mathbf{x})\,, \qquad \theta(\mathbf{x},0) = \theta_0(\mathbf{x})\,, \qquad \varphi(\mathbf{x},0) = \varphi_0(\mathbf{x}) \tag{6.14}$$

where $\nabla\cdot\mathbf{u}_0 = 0$, and the following boundary conditions (stress-free)

$$\frac{\partial u}{\partial z} = \frac{\partial v}{\partial z} = w = \theta = \varphi = 0 \qquad \text{on } z = 0,1. \tag{6.15}$$

On denoting by

$$V = \left[0, \frac{2\pi}{a_x}\right] \times \left[0, \frac{2\pi}{a_y}\right] \times [0,1] \tag{6.16}$$

the periodicity cell, and assuming that perturbations are periodic in x and y directions, with periods $\dfrac{2\pi}{a_x}$ and $\dfrac{2\pi}{a_y}$, respectively, we will assume that, $\forall f \in \{\mathbf{u},\theta,\varphi,\nabla\pi\}$,

$$f : (\mathbf{x},t) \in V\times\mathbb{R}^+ \to f(\mathbf{x},t) \in \mathbb{R},\ \ f \in W^{2,2}(V)\ \forall t\in\mathbb{R}^+$$

and that it can be expanded in a Fourier series uniformly convergent in V.

6.3 Instability analysis

Let us consider the linear version of the system (6.13), i.e.

$$\begin{cases} \dfrac{\mathbf{u}}{\mathcal{K}} = -\nabla\pi + R\theta\mathbf{k} + \mathrm{Da}\Delta\mathbf{u} \\ \nabla\cdot\mathbf{u} = 0 \\ \dfrac{\partial\theta}{\partial t} = Rw + \nabla\cdot(\mathcal{D}_f\nabla\theta) + H(\varphi-\theta) \\ A\left(\hat{\tau}\dfrac{\partial}{\partial t}+1\right)\dfrac{\partial\varphi}{\partial t} = \nabla\cdot(\mathcal{D}_s\nabla\varphi) - H\gamma\left(\hat{\tau}\dfrac{\partial}{\partial t}+1\right)(\varphi-\theta). \end{cases} \tag{6.17}$$

By taking the third component of the double curl of $(6.17)_1$, one obtains:

$$\begin{cases} \xi\Delta_1 w + \dfrac{\partial^2 w}{\partial z^2} = \xi R\Delta_1\theta + \xi \mathrm{Da}\Delta\Delta w \\ \dfrac{\partial\theta}{\partial t} = Rw + \eta\Delta_1\theta + \dfrac{\partial^2\theta}{\partial z^2} + H(\varphi-\theta) \\ A\left(\hat{\tau}\dfrac{\partial}{\partial t}+1\right)\dfrac{\partial\varphi}{\partial t} = \zeta\Delta_1\varphi + \dfrac{\partial^2\varphi}{\partial z^2} - H\gamma\left(\hat{\tau}\dfrac{\partial}{\partial t}+1\right)(\varphi-\theta) \end{cases} \tag{6.18}$$

where $\Delta_1 = \dfrac{\partial^2}{\partial x^2} + \dfrac{\partial^2}{\partial y^2}$.

Since system (6.18) is autonomous, we can seek solutions for which

$$f'(x,y,z,t) = f(x,y,z)\, e^{\sigma t} \quad \forall f' \in \{w,\theta,\varphi\}. \tag{6.19}$$

Substituting (6.19), (6.18) becomes

$$\begin{cases} \xi\Delta_1 w + \dfrac{\partial^2 w}{\partial z^2} = \xi R\Delta_1\theta + \xi \mathrm{Da}\Delta\Delta w \\ \sigma\theta = Rw + \eta\Delta_1\theta + \dfrac{\partial^2\theta}{\partial z^2} + H(\varphi-\theta) \\ (\hat{\tau}\sigma+1)(A\sigma+H\gamma)\varphi = \zeta\Delta_1\varphi + \dfrac{\partial^2\varphi}{\partial z^2} + H\gamma(\hat{\tau}\sigma+1)\theta. \end{cases} \tag{6.20}$$

Accounting for boundary conditions (6.15) and the periodicity of the perturbation fields in the horizontal direction, since the sequence $\{\sin n\pi z\}_{n\in\mathbb{N}}$ is a complete orthogonal system for $L^2([0,1])$, the solution of (6.20) can be expanded as

$$f(x,y,z) = \sum_{n=1}^{+\infty} \bar{f}_n(x,y,z) \qquad \forall f \in \{w,\theta,\varphi\} \tag{6.21}$$

where $\bar{f}_n = \tilde{f}_n(x,y)\sin(n\pi z)$ and

$$\Delta_1\bar{f}_n = -a^2\bar{f}_n \qquad \frac{\partial^2\bar{f}_n}{\partial z^2} = -n^2\pi^2\bar{f}_n \tag{6.22}$$

with $a^2 = a_x^2 + a_y^2$.

Let us define the following operators

$$\begin{aligned} \mathcal{L}_1 &\equiv \xi\Delta_1 + \frac{\partial^2}{\partial z^2} - \xi\mathrm{Da}\Delta\Delta \\ \mathcal{L}_2 &\equiv \sigma - \eta\Delta_1 - \frac{\partial^2}{\partial z^2} + H \\ \mathcal{L}_3 &\equiv A\sigma + H\gamma \\ \mathcal{L}_4 &\equiv \hat{\tau}\sigma + 1. \end{aligned} \tag{6.23}$$

Then, (6.20) becomes

$$\begin{cases} \mathcal{L}_1 w = \xi R \Delta_1 \theta \\ \mathcal{L}_2 \theta = R w + H \varphi \\ \mathcal{L}_5 \varphi = H \gamma \mathcal{L}_4 \theta \end{cases} \tag{6.24}$$

where $\mathcal{L}_5 \equiv \mathcal{L}_4 \mathcal{L}_3 - \zeta \Delta_1 - \dfrac{\partial^2}{\partial z^2}$.

By applying $\mathcal{L}_5$ and $\mathcal{L}_1$ to $(6.24)_2$ and substituting $(6.24)_1$-$(6.24)_3$ in the resulting equation, one obtains

$$\mathcal{L}_5 \mathcal{L}_1 \mathcal{L}_2 \theta = \xi R^2 \mathcal{L}_5 \Delta_1 \theta + H^2 \gamma \mathcal{L}_1 \mathcal{L}_4 \theta \ . \tag{6.25}$$

Splitting $\mathcal{L}_2$ in (6.25), it follows that

$$\mathcal{L}_1 \mathcal{L}_5 \left(\sigma - \eta \Delta_1 - \frac{\partial^2}{\partial z^2} \right) \theta + H \mathcal{L}_1 \mathcal{L}_5 \theta = \xi R^2 \mathcal{L}_5 \Delta_1 \theta + H^2 \gamma \mathcal{L}_1 \mathcal{L}_4 \theta \tag{6.26}$$

from which, splitting $\mathcal{L}_5$ only in the second term, one recovers

$$\begin{aligned} &\mathcal{L}_1 \mathcal{L}_5 \left(\sigma - \eta \Delta_1 - \frac{\partial^2}{\partial z^2} \right) \theta + H \mathcal{L}_1 \left(\mathcal{L}_4 A \sigma - \zeta \Delta_1 - \frac{\partial^2}{\partial z^2} \right) \theta + H^2 \gamma \mathcal{L}_1 \mathcal{L}_4 \theta = \\ &= \xi R^2 \mathcal{L}_5 \Delta_1 \theta + H^2 \gamma \mathcal{L}_1 \mathcal{L}_4 \theta \ . \end{aligned} \tag{6.27}$$

Substituting (6.21) in (6.27) and retaining only the n-th component, we get

$$\begin{aligned} R^2 = \frac{\xi a^2 + n^2 \pi^2 + \xi \mathrm{Da} \left(a^2 + n^2 \pi^2 \right)^2}{\xi a^2} \Bigg[\sigma + \eta a^2 + \\ n^2 \pi^2 + H \frac{(\sigma \hat{\tau} + 1) A \sigma + \zeta a^2 + n^2 \pi^2}{(\sigma \hat{\tau} + 1)(A \sigma + H \gamma) + \zeta a^2 + n^2 \pi^2} \Bigg] . \end{aligned} \tag{6.28}$$

6.3.1 Steady convection

In order to determine the critical Rayleigh number for the onset of steady convection, let us set $\sigma = 0$ in (6.28) and hence

$$R_S = \min_{(n^2, a^2) \in \mathbb{N} \times \mathbb{R}^+} f(n^2, a^2) \tag{6.29}$$

where

$$\begin{aligned} f(n^2, a^2) = \frac{\xi a^2 + n^2 \pi^2 + \xi \mathrm{Da} \left(a^2 + n^2 \pi^2 \right)^2}{\xi a^2} \\ \left[\eta a^2 + n^2 \pi^2 + H \frac{\zeta a^2 + n^2 \pi^2}{H \gamma + \zeta a^2 + n^2 \pi^2} \right] . \end{aligned} \tag{6.30}$$

Since $f(n^2, a^2)$ is an increasing function of n^2, it attains its minimum at $n^2 = 1$, hence

$$R_S = \min_{a^2 \in \mathbb{R}^+} f(1, a^2). \tag{6.31}$$

The absence of $\hat{\tau}$ in (6.31) implies that R_S does not depend on the solid thermal relaxation time. As consequence, second sound, allowed in heat propagation in solid, does not affect the occurrence of steady convection.

Let us remark that, if the porous medium is isotropic, i.e. $\xi = \eta = \zeta = 1$, (6.31) becomes

$$R_S = \min_{a^2 \in \mathbb{R}^+} \frac{\left(a^2 + \pi^2\right)^2 \left(1 + \mathrm{Da}(a^2 + \pi^2)\right)}{a^2} \left[\frac{H(1+\gamma) + a^2 + \pi^2}{H\gamma + a^2 + \pi^2}\right]. \tag{6.32}$$

which coincides with the result found in [94].

Moreover, let us observe that, when $\mathrm{Da} \to 0$, namely in absence of effective viscosity $\tilde{\mu}$, (6.31) coincides with the result found in [14].

6.3.2 Oscillatory convection

It is well known that oscillatory convection arises once the eigenvalue σ is pure imaginary.

Setting $\sigma = i\omega$ with $\omega \in \mathbb{R} - \{0\}$ in (6.28), we obtain

$$\begin{aligned} R^2 = \tilde{g}(n^2, a^2) = \frac{\xi a^2 + n^2\pi^2 + \xi \mathrm{Da}\left(a^2 + n^2\pi^2\right)^2}{\xi a^2} \Bigg[& i\omega + \eta a^2 + \\ & n^2\pi^2 + H \frac{(i\omega\hat{\tau} + 1)Ai\omega + \zeta a^2 + n^2\pi^2}{(i\omega\hat{\tau} + 1)(Ai\omega + H\gamma) + \zeta a^2 + n^2\pi^2}\Bigg]. \end{aligned} \tag{6.33}$$

Since R^2 is a real number, defining $\omega_* = \omega^2$, the condition for the existence of oscillatory convection is the following

$$J_1\, \omega_*^2 + J_2\, \omega_* + J_3 = 0 \tag{6.34}$$

where

$$\begin{aligned} J_1 &= A^2\, \hat{\tau}^2 \\ J_2 &= A^2 + H^2\gamma^2\hat{\tau}^2 - 2A\hat{\tau}a^2\zeta - 2An^2\hat{\tau}\pi^2 + AH^2\gamma\hat{\tau}^2 \\ J_3 &= H^2\gamma^2 - \hat{\tau}\pi^2 H^2 n^2\gamma - \hat{\tau}H^2\gamma a^2\zeta + AH^2\gamma + \\ &\quad 2\pi^2 H n^2\gamma + 2H\gamma a^2\zeta + \pi^4 n^4 + 2\pi^2 n^2 a^2\zeta + a^4\zeta^2. \end{aligned} \tag{6.35}$$

Let us remark that, since J_1 is positive, oscillatory convection cannot occur when either

$$J_2^2 - 4J_1J_3 < 0 \tag{6.36}$$

or

$$\begin{cases} J_2 > 0 \\ J_3 > 0. \end{cases} \tag{6.37}$$

Once (6.34) is solved with respect to ω^2, the critical Rayleigh number for the onset of oscillatory convection is obtained by substituting the positive solution of (6.34) in (6.33), i.e.

$$R_O = \min_{(n^2,a^2)\in\mathbb{N}\times\mathbb{R}^+} g(n^2, a^2, \omega^2(n^2, a^2)) \tag{6.38}$$

being

$$g(n^2, a^2, \omega^2(n^2, a^2)) = \frac{\xi a^2 + n^2\pi^2 + \mathrm{Da}\xi\left(a^2 + n^2\pi^2\right)^2}{\xi a^2 A_1} \left[A_1\left(\eta a^2 + n^2\pi^2\right) + B_1 A_2 + AH\omega^2\left(A + H\gamma\hat{\tau}\right)\right] \tag{6.39}$$

where

$$\begin{aligned} A_1 &= {A_2}^2 + \omega^2\left(A + H\,\gamma\,\hat{\tau}\right)^2 \\ A_2 &= H\,\gamma + a^2\,\zeta + n^2\,\pi^2 - A\,\omega^2\,\hat{\tau} \\ B_1 &= H\left(a^2\,\zeta + n^2\,\pi^2\right) - A\,H\,\omega^2\,\hat{\tau}. \end{aligned} \tag{6.40}$$

Let us remark that when $\hat{\tau} = 0$, from (6.35) it turns out that $J_1 = 0$ and $J_2, J_3 > 0$, and hence, by virtue of (6.37), oscillatory convection cannot arise. Hence, we can claim that the second sound phenomenon in solid phase can imply the existence of instability by means of oscillatory motion.

For the Eq. (6.38) to make sense, we need to assure $g(n^2, a^2, \omega^2(n^2, a^2)) > 0$. However, this condition is simply verified since the term $B_1\,A_2 + A\,H^2\,\omega^2\,\gamma\,\hat{\tau}$ is strictly positive.

Remark 7. *We remark that, by comparing $f(n^2, a^2)$ with $g(n^2, a^2)$, the following necessary condition for the onset of steady convection holds:*

$$H < \frac{A^2\left(1 + \omega^2\hat{\tau}^2\right)}{\gamma\hat{\tau}^2 n^2\pi^2}. \tag{6.41}$$

Remark 8. *Let us underline that on accounting for (6.30)-(6.31) and (6.38)-(6.39) it arises that R_S and R_O are increasing functions of* Da *and hence that the Darcy number has a stabilizing effect on the onset of convection.*

6.4 Global nonlinear stability

In order to study the nonlinear stability of m_0, we use the energy method following the non-standard procedure adopted in [46].

To this end, let us multiply $(6.10)_1$ by $\mathbf{u}$, $(6.10)_3$ by θ, $(6.10)_4$ by φ and $(6.10)_5$ by $\mathbf{q}$ and then integrate over the periodicity cell V. By virtue of boundary conditions (6.15), the resulting equations are

$$\begin{cases} R(\theta,w)-\dfrac{\|u\|^2}{\xi}-\dfrac{\|v\|^2}{\xi}-\|w\|^2-\mathrm{Da}\|\nabla\mathbf{u}\|^2=0 \\ \dfrac{1}{2}\dfrac{d}{dt}\|\theta\|^2=R(w,\theta)-\eta\left\|\dfrac{\partial\theta}{\partial x}\right\|^2-\eta\left\|\dfrac{\partial\theta}{\partial y}\right\|^2-\left\|\dfrac{\partial\theta}{\partial z}\right\|^2+H(\theta,\varphi)-H\|\theta\|^2 \\ \dfrac{A}{2}\dfrac{d}{dt}\|\varphi\|^2=H\gamma(\theta,\varphi)-(\nabla\cdot q,\varphi)-H\gamma\|\varphi\|^2 \\ \dfrac{\hat\tau}{2}\dfrac{d}{dt}\left(\dfrac{1}{\zeta}\left(\|q_x\|^2+\|q_y\|^2\right)+\|q_z\|^2\right)=-\dfrac{1}{\zeta}\left(\|q_x\|^2+\|q_y\|^2\right)-\|q_z\|^2-(\nabla\varphi,q) \end{cases} \tag{6.42}$$

where $\mathbf{q}=(q_x,q_y,q_z)$, while $(\cdot,\cdot)$ and $\|\cdot\|$ are the scalar product and the norm on $L^2(V)$, respectively.

By adding $(6.42)_3$ to $(6.42)_4$ and multiplying by ζ, we obtain

$$\begin{aligned} &\frac{d}{dt}\left(\frac{A\zeta}{2}\|\varphi\|^2+\frac{\hat\tau}{2}\left(\|q_x\|^2+\|q_y\|^2\right)+\frac{\hat\tau\zeta}{2}\|q_z\|^2\right)= \\ &H\gamma\zeta(\theta,\varphi)-\|q_x\|^2-\|q_y\|^2-\zeta\|q_z\|^2-H\gamma\zeta\|\varphi\|^2. \end{aligned} \tag{6.43}$$

Now, we perform $(6.42)_2+\lambda_1(6.42)_1+\lambda_2(6.43)$ in order to derive

$$\frac{dE(t)}{dt}=RI-D-\lambda_2\left(\|q_x\|^2+\|q_y\|^2\right)-\lambda_2\zeta\|q_z\|^2 \tag{6.44}$$

where the energy functional is

$$E(t)=\frac{\hat\tau\lambda_2}{2}\left(\|q_x\|^2+\|q_y\|^2+\zeta\|q_z\|^2\right)+\frac{A\zeta\lambda_2}{2}\|\varphi\|^2+\frac{\|\theta\|^2}{2} \tag{6.45}$$

while the dissipation function and the production term are, respectively

$$\begin{aligned} D(t)&=H\gamma\zeta\lambda_2\|\varphi\|^2+\eta\left\|\frac{\partial\theta}{\partial x}\right\|^2+\eta\left\|\frac{\partial\theta}{\partial y}\right\|^2+\left\|\frac{\partial\theta}{\partial z}\right\|^2 \\ &+\frac{\lambda_1\|u\|^2}{\xi}+\frac{\lambda_1\|v\|^2}{\xi}+\lambda_1\|w\|^2+\lambda_1\mathrm{Da}\|\nabla\mathbf{u}\|^2 \end{aligned} \tag{6.46}$$

$$I(t)=(1+\lambda_1)(\theta,w)+\frac{H}{R}(1+\lambda_2\gamma\zeta)(\theta,\varphi). \tag{6.47}$$

Now let us define

$$\frac{1}{R_N}=\max_{\mathcal{H}}\frac{I}{D} \tag{6.48}$$

with

$$\mathcal{H} = \{(\mathbf{u},\theta,\varphi) \in W^{2,2}(V) : w = \theta = \varphi = 0 \text{ on } z = 0,1; \text{periodic in } x \text{ and } y \text{ directions,with period } \frac{2\pi}{a_x}, \frac{2\pi}{a_y} \text{ respectively; } D < \infty\} \tag{6.49}$$

the space of the kinematically admissible perturbations. Hence, (6.44) yields

$$\frac{dE}{dt} \leq -D\left(1 - \frac{R}{R_N}\right) - \left(\|q_x\|^2 + \|q_y\|^2\right) - \zeta\|q_z\|^2. \tag{6.50}$$

As consequence, $R < R_N$ is a sufficient condition for the stability of m_0. In this respect, let us define

$$\alpha = 1 - \frac{R}{R_N} > 0 \tag{6.51}$$

and applying the Poincarè inequality, we obtain

$$D(t) \geq \lambda_2 H\gamma\zeta\|\varphi\|^2 + \left(\eta^*\pi^2 + H\right)\|\theta\|^2 \tag{6.52}$$

being $\eta^* = \min\{\eta, 1\}$. Hence,

$$\begin{aligned} &\frac{dE}{dt} \leq -\alpha\lambda_2 H\gamma\zeta\|\varphi\|^2 - \alpha\left(\eta^*\pi^2 + H\right)\|\theta\|^2 \\ &- \left(\|q_x\|^2 + \|q_y\|^2\right) - \zeta\|q_z\|^2 \leq -cE(t) \end{aligned} \tag{6.53}$$

where $c = \min\left\{\frac{2\alpha H\gamma}{A}, 2\alpha\left(\eta^*\pi^2 + H\right), \frac{2}{\hat{\tau}}\right\}$. Eq. (6.53) yields the exponential decay of the energy functional $E(t)$, implying the global stability of m_0 with respect to $E(t)$.

Remark 9. *Let us remark that, from* $(6.42)_1$*, by applying the Poincarè inequality and Cauchy Schwarz inequality, one obtains*

$$\|\boldsymbol{u}\|^2 \leq \frac{\xi_*^2 R^2}{1 + 2\xi_* \mathrm{Da}\pi^2}\|\theta\|^2 \tag{6.54}$$

being $\xi_* = \max\{\xi, 1\}$ *and hence the decay of* $\|\theta\|^2$ *implies the decay of* $\|\boldsymbol{u}\|^2$*, too.*

Now, in order to find the global nonlinear stability threshold R_N, let us solve the variational problem (6.48). The Euler-Lagrange equations related to (6.48) are

$$\begin{cases} (1+\lambda_1) R\theta\mathbf{k} + 2\mathrm{Da}\lambda_1\Delta\mathbf{u} - \dfrac{2\lambda_1}{\xi}u\mathbf{i} - \dfrac{2\lambda_1}{\xi}v\mathbf{j} - 2\lambda_1 w\mathbf{k} = \nabla l \\ (1+\lambda_1) Rw + H(1+\lambda_2\gamma\zeta)\varphi + 2\eta\dfrac{\partial^2\theta}{\partial x^2} + 2\eta\dfrac{\partial^2\theta}{\partial y^2} + 2\dfrac{\partial^2\theta}{\partial z^2} - 2H\theta = 0 \\ (1+\lambda_2\gamma\zeta)\theta - 2\lambda_2\gamma\zeta\varphi = 0 \end{cases} \tag{6.55}$$

where $l(\mathbf{x})$ is a Lagrange multiplier. By retaining the third component of the double curl of $(6.55)_1$ and by recalling that $\nabla \cdot \mathbf{u} = 0$, we obtain

$$\begin{cases} -(1+\lambda_1) R\Delta_1\theta\mathbf{k} - 2\mathrm{Da}\lambda_1\Delta\Delta\mathbf{u} + \dfrac{2\lambda_1}{\xi}\dfrac{\partial^2 w}{\partial z^2} + 2\lambda_1\Delta_1 w = 0 \\ (1+\lambda_1) Rw + H(1+\lambda_2\gamma\zeta)\varphi + 2\eta\dfrac{\partial^2\theta}{\partial x^2} + 2\eta\dfrac{\partial^2\theta}{\partial y^2} + 2\dfrac{\partial^2\theta}{\partial z^2} - 2H\theta = 0 \\ (1+\lambda_2\gamma\zeta)\theta - 2\lambda_2\gamma\zeta\varphi = 0 \end{cases} \tag{6.56}$$

The nonlinear stability threshold is then given by

$$R_N = \max_{(\lambda_1,\lambda_2)\in\mathbb{R}^2} \min_{(n^2,a^2)\in\mathbb{N}\times\mathbb{R}^+} h(\lambda_1,\lambda_2,n^2,a^2) \tag{6.57}$$

where, accounting for (6.56),

$$\begin{aligned} h(\lambda_1,\lambda_2,n^2,a^2) = {} & \frac{4\left[\xi\mathrm{Da}\lambda_1\left(a^2+n^2\pi^2\right)^2 + \lambda_1\left(\xi a^2+n^2\pi^2\right)\right]}{\xi a^2\left(1+\lambda_1\right)^2} \\ & \left[\eta a^2 + n^2\pi^2 + H\left(1 - \frac{\left(1+\lambda_2\gamma\zeta\right)^2}{4\lambda_2\gamma\zeta}\right)\right]. \end{aligned} \tag{6.58}$$

Hence, we find

$$R_N = \min_{(n^2,a^2)\in\mathbb{N}\times\mathbb{R}^+} h\left(1,\frac{1}{\gamma\zeta},n^2,a^2\right) = \min_{(n^2,a^2)\in\mathbb{N}\times\mathbb{R}^+} h_1(n^2,a^2) \tag{6.59}$$

where

$$h_1(n^2,a^2) = \frac{\xi\mathrm{Da}\left(a^2+n^2\pi^2\right)^2 + \left(\xi a^2+n^2\pi^2\right)}{\xi a^2}\left(\eta a^2+n^2\pi^2\right). \tag{6.60}$$

From (6.30), (6.39) and (6.60) it follows that

$$\begin{aligned} h_1(n^2,a^2) < f(n^2,a^2) \quad \forall (n^2,a^2)\in\mathbb{N}\times\mathbb{R}^+ \\ h_1(n^2,a^2) < g(n^2,a^2) \quad \forall (n^2,a^2)\in\mathbb{N}\times\mathbb{R}^+ \end{aligned} \tag{6.61}$$

and hence

$$R_N < \min\{R_S, R_O\} \tag{6.62}$$

Moreover, accounting for (6.59) and (6.60), it arises that R_N is an increasing function of Da and η, while it decreases with ξ. In addition, when $H \to 0$, conditions for the existence of R_O are not satisfied and the difference

$$f(n^2,a^2) - h_1(n^2,a^2) = \frac{H(\zeta a^2+n^2\pi^2)}{H\gamma+\zeta a^2+n^2\pi^2} \tag{6.63}$$

tends to zero. This is an expected result since assuming that fluid and solid do not exchange heat between each other makes the system $(6.18)_1$-$(6.18)_2$ self-adjoint.

6.5 Results and Discussion

In this section, we furnish numerical simulations in order to analyse the influence of second sound, interaction coefficient and anisotropy of the medium on the onset of convection.

First of all, let us underline that, due to the complexity of R_O given by (6.38)-(6.40), we have not been able to prove that the critical oscillatory threshold is achieved for $n = 1$, while all the numerical simulations we have performed have verified this. For this reason, in the following, we will assume:

$$R_O = \min_{a^2 \in \mathbb{R}^+} g(1, a^2, \omega^2(1, a^2)). \tag{6.64}$$

As done in [48], and previously in [46], all the computations are confined to two cases of great interest, namely oxide of aluminium (Al_2O_3) and copper (CuO) materials, because of their real-life employment in heat exchangers. Specifically, figures will be delivered for the case of copper oxide, while tables will show results for both materials. In Table 6.1 the diffusivity ratio and the weighted conductivity ratio are collected for both materials.

Al_2O_3	CuO
$A_{Al_2O_3} = 1.4210^{-2}$	$A_{CuO} = 8.664 \times 10^{-4}$
$\gamma_{Al_2O_3} = 7.33710^{-3}$	$\gamma_{CuO} = 6.403 \times 10^{-4}$

Table 6.1: Diffusivity ratio A and weighted conductivity ratio γ for oxide of aluminium (Al_2O_3) and copper (CuO).

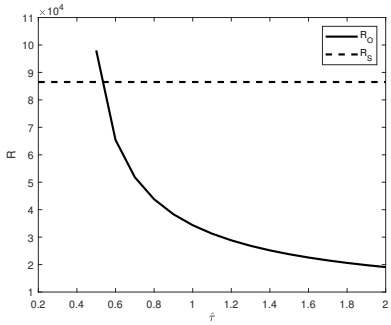

Figure 6.1: R_O and R_S as functions of $\hat{\tau}$ with $A = A_{CuO}$, $\gamma = \gamma_{CuO}$, $\xi = 1$, $\eta = 1$, $\zeta = 1$, Da $= 10$ and $H = 200$.

In Figure 6.1, the critical Rayleigh number behaviour with respect to the dimensionless parameter $\hat{\tau}$, defined in $(6.11)_1$, which depends on the thermal relaxation time τ, the depth of the layer d and the fluid thermal diffusivity, is shown. Let

us underline that, due to proportionality between $\hat{\tau}$ and Sg, analogous results are obtained on studying the effect of Sg on the critical Rayleigh number. The steady threshold R_S, defined in (6.31), is not affected by $\hat{\tau}$. That is why its value is constant in Figure 6.1. On the other hand, R_O exhibits a decreasing behaviour with respect to $\hat{\tau}$, which allows us to claim that, when $\hat{\tau} \neq 0$, oscillatory convection can occur.

Of course, when $\hat{\tau}$ goes to zero, we would expect to obtain the same results found by assuming the validity of Fourier's law in solid phase, too. In fact, by assuming $\hat{\tau} = 0$ and comparing results with those ones found in [95], it arises an excellent agreement, as shown in Table 6.2.

(a) [95]

H	R_S	a_c
0.01	39.4992	3.1423
0.1	39.6779	3.1494
100	72.3411	3.2706
1000	78.1924	3.1568

(b) Present study

H	R_S	a_c
0.01	39.4992	3.1423
0.1	39.6779	3.1494
100	72.3411	3.2706
1000	78.1924	3.1568

Table 6.2: Comparison of critical Rayleigh number R_S and square root of critical wave number a_c for different value of H with $\xi = \eta = \zeta = 1$, $\mathrm{Da} = 10^{-6}$ and $\gamma = 1$.

(a)

$\hat{\tau}$	R_O	R_S
0.2	∄	86511
0.4	∄	86511
0.5	98029	86511
0.6	65415	86511
1	34342	86511
2	19084	86511

(b)

$\hat{\tau}$	R_O	R_S
0.2	∄	34484
0.3	∄	34484
0.4	30693	34484
0.5	22124	34484
1	12974	34484
2	9609	34484

Table 6.3: (a) Values of R_O and R_S for different values of $\hat{\tau}$ with $A = A_{CuO}$, $\gamma = \gamma_{CuO}$, $\xi = 1$, $\eta = 1$, $\zeta = 1$, $\mathrm{Da} = 10$ and $H = 200$. (b) Values of R_O and R_S for fixed values of $\hat{\tau}$ with $A = A_{Al_2O_3}$, $\gamma = \gamma_{Al_2O_3}$, $\xi = 1$, $\eta = 1$, $\zeta = 1$, $\mathrm{Da} = 10$ and $H = 70$.

Moreover, by reading Tables 6.3a-6.3b, performed computations did not find oscillatory convection for $\hat{\tau}$ lower than a certain value $\hat{\tau}_c$.

The behaviour of R_S and R_O with respect to the inter-phase heat transfer coefficient has been analysed numerically. From Figure 6.2a and by reading Table 6.4a, it arises that R_S is an increasing function of H while R_O is a decreasing function of H.

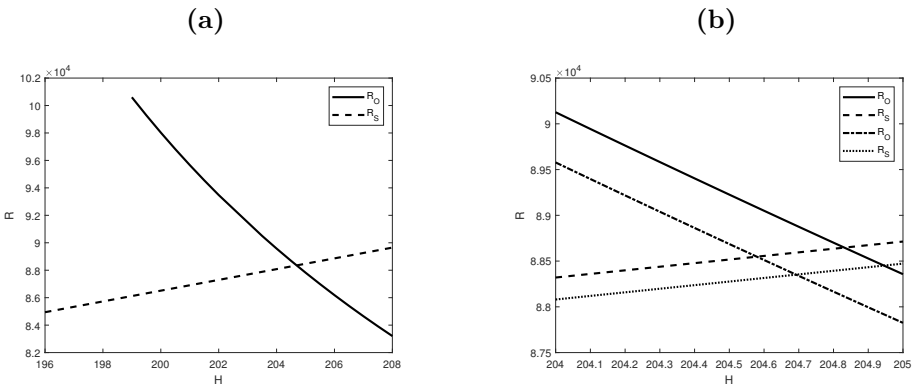

Figure 6.2: (a) R_O and R_S as functions of H with $A = A_{CuO}$, $\gamma = \gamma_{CuO}$, $\xi = 1$, $\eta = 1$, $\zeta = 1$, Da $= 10$ and $\hat{\tau} = 0.5$.
(b) R_O and R_S as functions of H for $\xi = 0.5$ (continuous and dashed lines), $\xi = 1$ (dashdotted and dotted lines) with $A = A_{CuO}$, $\gamma = \gamma_{CuO}$, $\eta = 1$, $\zeta = 1$, Da $= 10$ and $\hat{\tau} = 0.5$.

(a)

H	R_O	a^2_{cO}	R_S	a^2_{cS}
198	∄	∄	85727	9.0661
198.7	∄	∄	86001	9.0681
198.8	101140	2.3693	86041	9.0684
204.6	88512	2.8169	88315	9.0851
204.7	88338	2.8239	88355	9.0854
205	87825	2.8444	88472	9.0862

(b)

H	R_O	a^2_{cO}	R_S	a^2_{cS}
60	∄	∄	30676	7.9212
60.5	∄	∄	30867	7.9288
60.7	∄	∄	30944	7.9318
60.8	30013	2.9743	30982	7.9333
61	29654	3.0315	31058	7.9363
62	28103	3.2958	31440	7.9510

Table 6.4: (a) Values of R_O and R_S and respective critical wave numbers for different values of H with $A = A_{CuO}$, $\gamma = \gamma_{CuO}$, $\xi = 1$, $\eta = 1$, $\zeta = 1$, Da $= 10$ and $\hat{\tau} = 0.5$. (b) Values of R_O and R_S and respective critical wave numbers for different values of H with $A = A_{Al_2O_3}$, $\gamma = \gamma_{Al_2O_3}$, $\xi = 1$, $\eta = 1$, $\zeta = 1$, Da $= 10$ and $\hat{\tau} = 0.5$.

Moreover, Figure 6.2a finds out the existence of a critical value H_T for which

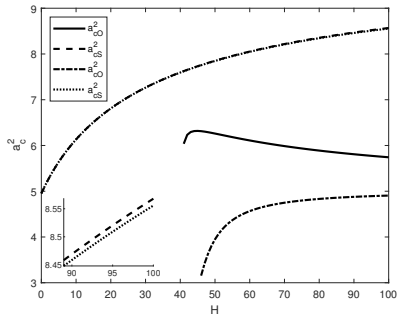

Figure 6.3: a_{cO}^2 and a_{cS}^2 as functions of H for $\zeta = 0.1$ (continuous and dashed lines), $\zeta = 1$ (dashdotted and dotted lines) with $A = A_{CuO}$, $\gamma = \gamma_{CuO}$, $\xi = 1$, $\eta = 1$, Da $= 10$ and $\hat{\tau} = 10$.

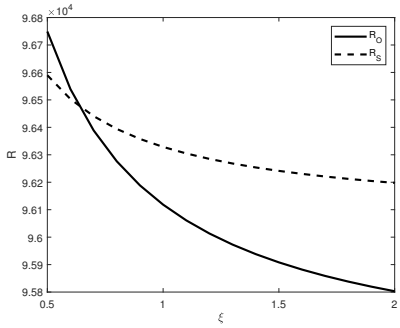

Figure 6.4: R_O and R_S as functions of ξ with $A = A_{CuO}$, $\gamma = \gamma_{CuO}$, $\eta = 1$, $\zeta = 2$, Da $= 10$, $H = 224.5$ and $\hat{\tau} = 0.5$.

convection moves from a steady motion to an oscillatory one. H_T depends on the fixed parameters. In fact, for example, Figure 6.2b shows that H_T gets lower for increasing values of ξ.

In Figure 6.3, we find out that the oscillatory wave number a_{cO} exhibits a different behaviour with respect to H depending on ζ, while the steady wave number a_{cS} does not change. In particular, a_{cS} exhibits an increasing behaviour with respect to H.

In Figure 6.4 the behaviour of the critical Rayleigh number with respect to permeability ξ is highlighted. Although setting a precise value for the inter-phase heat transfer coefficient H is not significant since this quantity is usually not easily measured ([27]), assuming fixed H is useful to determine the influence of ξ on the onset of convection. Both the steady and oscillatory critical thresholds exhibit a decreasing behaviour with respect to ξ. Hence, increasing ξ implies a reduction of the critical Rayleigh number, namely convection is promoted in place of conduction. Physically, due to definition of ξ, increasing the horizontal permeability eases the fluid motion in the horizontal direction, implying that instability is reached more

(a)

ξ	R_O	a^2_{cO}	R_S	a^2_{cS}
0.5	96749	2.3474	96590	9.1869
0.6	96539	2.3460	96503	9.1721
0.7	96389	2.3451	96441	9.1616
0.8	96276	2.3443	96394	9.1536
1	96118	2.3433	96329	9.1425
2	95803	2.3413	96198	9.1202

(b)

ξ	R_O	a^2_{cO}	R_S	a^2_{cS}
0.5	13081	5.0769	92026	8.6496
0.6	13062	5.0695	91938	8.6350
0.7	13048	5.0642	91875	8.6246
0.8	13038	5.0602	91828	8.6168
1	13023	5.0546	91762	8.6058
2	12995	5.0434	91630	8.5838

Table 6.5: (a) Values of R_O and R_S and respective critical wave numbers for different values of ξ with $A = A_{CuO}$, $\gamma = \gamma_{CuO}$, $\eta = 1$, $\zeta = 2$, Da $= 10$, $H = 224.5$ and $\hat{\tau} = 0.5$. (b) Values of R_O and R_S and respective critical wave numbers for different values of ξ with $A = A_{Al_2O_3}$, $\gamma = \gamma_{Al_2O_3}$, $\eta = 1$, $\zeta = 2$, Da $= 10$, $H = 224.5$ and $\hat{\tau} = 0.5$.

(a) **(b)**

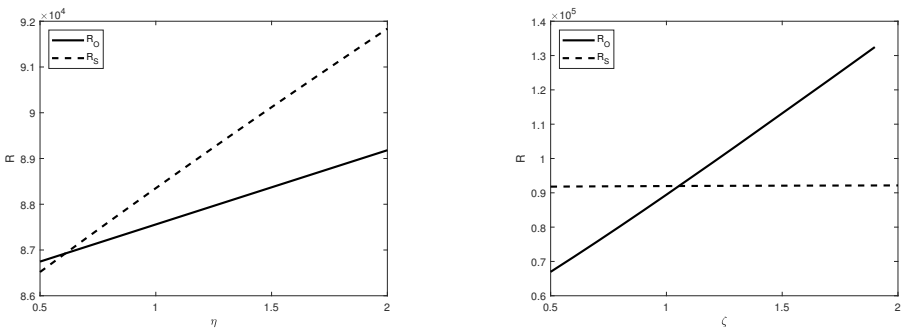

Figure 6.5: (a) R_O and R_S as functions of η with $A = A_{CuO}$, $\gamma = \gamma_{CuO}$, $\xi = 2$, $\zeta = 1$, Da $= 10$, $H = 205$ and $\hat{\tau} = 0.5$.
(b) R_O and R_S as functions of ζ with $A = A_{CuO}$, $\gamma = \gamma_{CuO}$, $\xi = 1$, $\eta = 2$, Da $= 10$, $H = 205$ and $\hat{\tau} = 0.5$.

easily. Furthermore, in Tables 6.5a-6.5b it is evident that periodicity cell gets wider for increasing values of ξ, since the critical wave number shows a decreasing

(a)

η	R_O	a^2_{cO}	R_S	a^2_{cS}
0.5	86746	2.8491	86519	9.4177
0.6	86909	2.8478	86891	9.3427
0.7	87072	2.8464	87260	9.2699
0.8	87234	2.8449	87626	9.1993
1	87559	2.8422	88351	9.0641
2	89181	2.8282	91837	8.4856

(b)

η	R_O	a^2_{cO}	R_S	a^2_{cS}
0.5	11033	6.1772	81112	8.8716
0.6	11289	6.0143	81464	8.8027
0.7	11540	5.8653	81812	8.7358
0.8	11786	5.7281	82159	8.6707
1	12267	5.4836	82844	8.5461
2	14494	4.6317	86147	8.0104

Table 6.6: (a) Values of R_O and R_S and respective critical wave numbers for different values of η with $A = A_{CuO}$, $\gamma = \gamma_{CuO}$, $\xi = 2$, $\zeta = 1$, Da $= 10$, $H = 205$ and $\hat{\tau} = 0.5$. (b) Values of R_O and R_S and respective critical wave numbers for different values of η with $A = A_{Al_2O_3}$, $\gamma = \gamma_{Al_2O_3}$, $\xi = 2$, $\zeta = 1$, Da $= 10$, $H = 205$ and $\hat{\tau} = 0.5$.

behaviour.

From Figures 6.5a-6.5b it arises that R_S and R_O are increasing functions of η and ζ, even though the influence of ζ on the steady threshold is rather unremarkable. The influence of these parameters is physically admissible since increasing thermal conductivity encourages heat transfer. In particular, large values of solid conductivity imply that the solid matrix absorbs heat from the fluid more easily. While, looking at the definition of η, when κ_z^f grows, η decreases and convection is promoted because the upward heat transfer within the fluid is encouraged. On the other hand, the influence of η on periodicity cell size is similar to the influence of ξ. As shown in Tables 6.6a-6.6b, the critical wave number exhibits a decreasing behaviour. While ζ has a mixed effect on periodicity cell size, as pointed out in Tables 6.7a-6.7b. Firstly, when convection occurs via oscillatory motion, ζ makes the critical wave number decrease. While, after the transition point, the critical wave number inverts its behaviour.

(a)

ζ	R_O	a^2_{cO}	R_S	a^2_{cS}
0.5	66973	4.4291	91798	8.5104
0.7	75752	3.6524	91878	8.5071
1	89452	2.8305	91971	8.5058
1.1	∄	∄	9.1996	8.5059
1.4	∄	∄	9.2061	8.5069
1.6	∄	∄	9.2096	8.5081
2	∄	∄	9.2153	8.5108

(b)

ζ	R_O	a^2_{cO}	R_S	a^2_{cS}
0.5	26058	4.2986	33516	6.9534
0.9	31700	2.9538	33648	6.9449
1	33260	2.7088	33674	6.9446
1.1	∄	∄	33699	6.9446
1.2	∄	∄	33721	6.9450
1.6	∄	∄	33796	6.9485
2	∄	∄	33854	6.9537

Table 6.7: (a) Values of R_O and R_S and respective critical wave numbers for different values of ζ with $A = A_{CuO}$, $\gamma = \gamma_{CuO}$, $\xi = 1$, $\eta = 2$, Da $= 10$, $H = 205$ and $\hat{\tau} = 0.5$. (b) Values of R_O and R_S and respective critical wave numbers for different values of ζ with $A = A_{Al_2O_3}$, $\gamma = \gamma_{Al_2O_3}$, $\xi = 1$, $\eta = 2$, Da $= 10$, $H = 60$ and $\hat{\tau} = 0.5$.

6.6 Conclusions

Linear and nonlinear stability analyses of the conduction solution in an anisotropic highly porous layer in local thermal non-equilibrium has been performed. We proved the Cattaneo's law as governing equation for heat flux in solid can lead to the occurrence of oscillatory convection. Indeed, it has been proved that, if the dimensionless parameter $\hat{\tau}$ is great, oscillatory convection is the dominant mechanism. On the other hand, when $\hat{\tau}$ goes to zero, only steady convection can arise. In addition, we pointed out that the critical Rayleigh number for steady convection does not depend on $\hat{\tau}$, meaning that Cattaneo's law does not affect the onset of steady convection. Moreover, we proved the stabilising effect the Darcy number on the onset of convection as R_S and R_O are increasing functions of Da.

Both steady and oscillatory critical thresholds are determined in a closed form and numerical analysis has been performed in order to highlight the influence of second sound effect, inter-phase heat transfer and anisotropy of the medium on the onset of instability. We showed the destabilising effect of horizontal isotropic

permeability ξ on the onset of convection, while the opposite effect of both fluid (η) and solid (ζ) thermal conductivities is pointed out.

Chapter 7

Natural convection in a fluid saturating an anisotropic porous medium in LTNE: effect of depth-dependent viscosity

7.1 Introduction

In the present chapter, results obtained in the paper [96] are shown. Linear and nonlinear stability analyses of the conduction solution of the Vadasz-Darcy model describing the motion of a depth-dependent viscosity fluid in anisotropic porous medium in LTNE are performed. Linear instability analysis leads to a generalised eigenvalue problem which can be solved by means of the Chebyshev-tau method coupled with the QZ algorithm. Nonlinear stability analysis is carried out by employing the energy method. The optimal result of coincidence between the linear instability threshold and the global nonlinear stability threshold is obtained. Moreover, it is proved that fluid viscosity decreasing with depth leads to lower values of the Rayleigh number, i.e. is has a destabilising effect on the onset of convection. Physically, viscosity drag reduces with depth, namely the fluid meets fewer obstacles to its motion. Comparing results with those ones found under LTE assumption in [60], we are able to remark that the presence of LTNE makes the influence of variable viscosity more intense.

Section 7.2 is devoted to the formulation of the mathematical model describing the motion of a depth-dependent viscosity fluid in presence of an anisotropic porous medium, in LTNE regime. In this Section, the basic steady solution and the dimensionless model governing the evolution of perturbation fields are determined. In section 7.3, the instability analysis is performed in order to determine the generalised eigenvalue problem which is solved by means of the Chebyshev-tau method

coupled to the QZ algorithm. In section 7.4, the global nonlinear stability analysis of the conduction solution is carried out by employing the energy method. Finally, in section 7.5, numerical results are reported, with particular attention devoted to the influence of variable viscosity, mechanical and thermal anisotropy, weighted conductivity ratio and interaction coefficient on the onset of instability.

7.2 Physical set-up

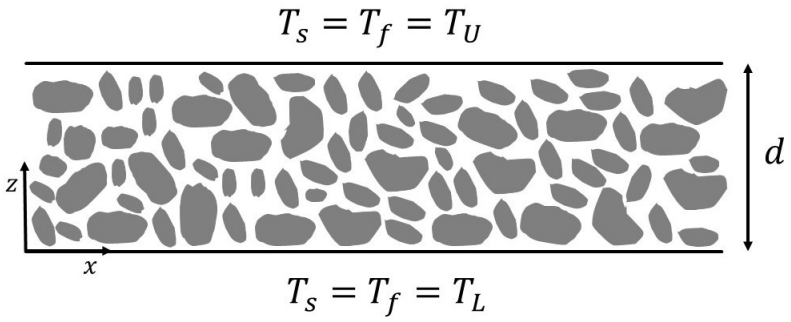

Figure 7.1: Horizontal porous layer

Let us take into account a horizontal porous layer, whose depth is d, saturated by an incompressible fluid $\mathscr{F}$ initially at rest. We choose a cartesian frame of reference (x, y, z), being the z-axis vertically upward. A uniform temperature gradient is imposed and maintained across the medium. Let T_L be the temperature on the lower plane $z = 0$ delimiting the layer and let T_U be the temperature on the upper plane $z = d$. We assume the layer to be heated from below, i.e. $T_L > T_U$. Moreover, the hypothesis of local thermal non-equilibrium holds for the porous medium at stake, i.e. the heat exchange between solid matrix and fluid is allowed. Based on this assumption, we need to define two different temperatures, one for the fluid phase, another for the solid one. Let us denote by T_f the temperature of the fluid phase and by T_s the temperature of the solid phase. Then, by virtue of previous considerations,

$$T_s = T_f = T_L \qquad \text{on } z = 0; \qquad T_s = T_f = T_U \qquad \text{on } z = d \tag{7.1}$$

with $T_L > T_U$.

The porous medium exhibits some anisotropic properties. Specifically, permeability and solid thermal conductivity are horizontally isotropic. Let $\mathcal{K}$ be the permeability tensor and let $\mathcal{D}_s$ be the solid thermal conductivity one. By assuming

that both tensors share the same principal axis (x, y, z), they can be written in diagonal form, i.e.

$$\begin{aligned} \mathcal{K} &= K_z \mathcal{K}_* \qquad \mathcal{K}_* = \begin{pmatrix} \xi & 0 & 0 \\ 0 & \xi & 0 \\ 0 & 0 & 1 \end{pmatrix} \qquad \xi = \frac{K_H}{K_z} \\ \mathcal{D}_s &= \kappa_z^s \mathcal{D}_s^* \qquad \mathcal{D}_s^* = \begin{pmatrix} \zeta & 0 & 0 \\ 0 & \zeta & 0 \\ 0 & 0 & 1 \end{pmatrix} \qquad \zeta = \frac{\kappa_H^s}{\kappa_z^s} \end{aligned} \tag{7.2}$$

In addition, we allow viscosity to be strongly dependent on temperature, at least at the steady state where temperature linearly increases with depth [65]. As consequence, we assume the following behaviour of viscosity with respect to z [60, 58]:

$$\mu(z) = \mu_0 f(z), \qquad f(z) = e^{c'(z-\frac{d}{2})} \tag{7.3}$$

being μ_0 and c' positive constants.

Under previous assumptions, by employing the Oberbeck-Boussinesq approximation, the Vadasz-Darcy model is [9]

$$\begin{cases} \rho_f c_a \mathbf{v}_{,t} = -\nabla p' + \rho_f \alpha g T_f \mathbf{k} - \mu(z) \mathcal{K}^{-1} \mathbf{v} \\ \nabla \cdot \mathbf{v} = 0 \\ \varepsilon \rho_f c_f T_{f,t} + \rho_f c_f \mathbf{v} \cdot \nabla T_f = \varepsilon \kappa_f \Delta T_f + h(T_s - T_f) \\ (1-\varepsilon) \rho_s c_s T_{s,t} = (1-\varepsilon) \nabla \cdot (\mathcal{D}_s \nabla T_s) - h(T_s - T_f) \end{cases} \tag{7.4}$$

where $\mathbf{v}$, p, T_f and T_s are (seepage) velocity, pressure, fluid phase temperature and solid phase temperature, respectively; while $\mu(z)$ is the fluid viscosity according to (7.3); κ_f, ρ_f, ρ_s, c_f, c_s, g, α, c_a, ε, h are fluid thermal conductivity, fluid and solid density, specific heat of fluid and solid phase, gravity acceleration, thermal expansion coefficient, acceleration coefficient, porosity, angular velocity and interaction coefficient, respectively.

The following boundary conditions are coupled to (7.4)

$$\begin{aligned} &T_s = T_f = T_L \quad \text{on } z = 0, \qquad T_s = T_f = T_U \quad \text{on } z = d, \\ &\mathbf{v} \cdot \mathbf{n} = 0 \quad \text{on } z = 0, d \end{aligned} \tag{7.5}$$

where $T_L > T_U$ and $\mathbf{n}$ is the unit outward normal to planes $z = 0, d$

The basic steady solution of (7.4) is:

$$m_0 = \left\{ \mathbf{v}_b = \mathbf{0}\,, \quad T_{sb} = T_{f_b} = -\beta z + T_L\,, \quad p_b = -\rho_f g \alpha \beta \frac{z^2}{2} + \rho_f g \alpha T_L z + cost \right\} \tag{7.6}$$

where $\beta = \frac{T_L - T_U}{d} (> 0)$ is the adverse temperature gradient.

In order to study the stability of m_0, let us introduce the perturbation fields $(\mathbf{u}, \theta, \varphi, \pi)$ to velocity field, fluid temperature field, solid temperature field and pressure field, respectively.

After introducing perturbations to initial data, the following solution of (7.4) arises:

$$\mathbf{v} = \mathbf{u} + \mathbf{v}_b \qquad T_f = \theta + T_{f_b} \qquad T_s = \varphi + T_{sb} \qquad p' = p + p_b \tag{7.7}$$

Once the following dimensionless quantities are defined

$$x_i = x_i^* d, \quad t = t^* \frac{d^2 \rho_f c_f}{\kappa_f}, \quad p = p^* P, \quad u_i = u_i^* U, \quad \theta = \theta^* T', \quad \varphi = \varphi^* T' \tag{7.8}$$

where

$$P = \frac{U \mu_0 d}{K_z}, \qquad U = \frac{\varepsilon \kappa_f}{\rho_f c_f d}, \qquad T' = \beta d \sqrt{\frac{\kappa_f \varepsilon \mu_0}{\beta g \alpha K_z \rho_f^2 c_f d^2}}, \tag{7.9}$$

omitting all asterisks, we obtain the following dimensionless model governing the evolution of perturbation fields:

$$\begin{cases} \dfrac{1}{Va} \mathbf{u}_{,t} = -\nabla p + R\theta \mathbf{k} - f(z) \mathcal{K}^{-1} \mathbf{u} \\ \nabla \cdot \mathbf{u} = 0 \\ \theta_{,t} + \mathbf{u} \cdot \nabla \theta = Rw + \Delta \theta + H(\varphi - \theta) \\ A \varphi_{,t} = \zeta \Delta_1 \varphi + \varphi_{,zz} - H\gamma(\varphi - \theta) \end{cases} \tag{7.10}$$

being $f(z) = e^{c(z - \frac{1}{2})}$, $c = c'd$, $\Delta_1 = \partial_{,xx} + \partial_{,yy}$ and where

$$\begin{aligned} A &= \frac{\rho_s c_s \kappa_f}{\rho_f c_f \kappa_z^s}, \quad \gamma = \frac{\varepsilon \kappa_f}{(1-\varepsilon)\kappa_z^s}, \quad H = \frac{hd^2}{\varepsilon \kappa_f}, \\ R^2 &= \frac{K_z \rho_f^2 c_f d^2 \beta g \alpha}{\mu_0 \varepsilon \kappa_f}, \quad Va = \frac{c_f d^2 \mu_0}{K_z \kappa_f c_a} \end{aligned} \tag{7.11}$$

are diffusivity ratio, weighted conductivity ratio, inter-phase heat transfer coefficient, Rayleigh number and Vadasz number, respectively.

To (7.10) we add the initial conditions:

$$\mathbf{u}(\mathbf{x},0) = \mathbf{u}_0(\mathbf{x}), \quad \theta(\mathbf{x},0) = \theta_0(\mathbf{x}), \quad \varphi(\mathbf{x},0) = \varphi_0(\mathbf{x}), \quad p(\mathbf{x},0) = p_0(\mathbf{x}) \tag{7.12}$$

where $\nabla \cdot \mathbf{u}_0 = 0$, while the boundary conditions are

$$w = \theta = \varphi = 0 \qquad \text{on } z = 0,1. \tag{7.13}$$

Let

$$V = \left[0, \frac{2\pi}{a_x}\right] \times \left[0, \frac{2\pi}{a_y}\right] \times [0,1] \tag{7.14}$$

be the periodicity cell and let us define $(\cdot,\cdot)$ and $\|\cdot\|$ inner product and norm on $L^2(V)$, respectively. Perturbations are assumed to be periodic in x and y directions with periods $\frac{2\pi}{a_x}$ and $\frac{2\pi}{a_y}$, respectively. Moreover, $\forall g \in \{\mathbf{u}, \theta, \varphi, p\}$,

$$g : (\mathbf{x}, t) \in V \times \mathbb{R}^+ \to g(\mathbf{x}, t) \in \mathbb{R}, \;\; g \in W^{2,2}(V) \;\; \forall t \in \mathbb{R}^+$$

and g can be expanded in a Fourier series uniformly convergent in V.

7.3 Linear instability and Chebyshev-tau method

In order to perform the linear instability analysis of m_0, let us consider the linear version of (7.10), i.e.

$$\begin{cases} \dfrac{1}{Va}\mathbf{u}_{,t} = -\nabla p + R\theta\mathbf{k} - f(z)\mathcal{K}^{-1}\mathbf{u} \\ \nabla \cdot \mathbf{u} = 0 \\ \theta_{,t} = Rw + \Delta\theta + H(\varphi - \theta) \\ A\varphi_{,t} = \zeta\Delta_1\varphi + \varphi_{,zz} - H\gamma(\varphi - \theta) \end{cases} \tag{7.15}$$

that can be written as

$$N\frac{\partial}{\partial t}F(\mathbf{x}, t) = MF(\mathbf{x}, t) \tag{7.16}$$

being $F = (u, v, w, \pi, \theta, \varphi)$, N with all zero entries and such that $diag(N) = \left(\frac{1}{Va}, \frac{1}{Va}, \frac{1}{Va}, 0, 1, \frac{A}{\gamma}\right)$ and

$$M = \begin{pmatrix} -\frac{f(z)}{\xi} & 0 & 0 & -\frac{\partial}{\partial x} & 0 & 0 \\ 0 & -\frac{f(z)}{\xi} & 0 & -\frac{\partial}{\partial y} & 0 & 0 \\ 0 & 0 & -f(z) & -\frac{\partial}{\partial z} & R & 0 \\ -\frac{\partial}{\partial x} & -\frac{\partial}{\partial y} & -\frac{\partial}{\partial z} & 0 & 0 & 0 \\ 0 & 0 & R & 0 & \Delta - H & H \\ 0 & 0 & 0 & 0 & H & \frac{\zeta}{\gamma}\Delta_1 + \frac{1}{\gamma} \end{pmatrix} \tag{7.17}$$

It is straightforward to notice that the spatial operator M related to (7.15) is symmetric with respect to L^2-scalar product. As consequence, its spectrum involves only real numbers and the strong version of the principle of exchange of stabilities holds.

Moreover, system (7.15) is autonomous. Hence, we can look for solutions such that

$$\varphi'(\mathbf{x}, t) = \varphi(\mathbf{x})\; e^{\sigma t} \quad \forall \varphi' \in \{w, \theta, \varphi, p\}. \tag{7.18}$$

Substituting (7.18) in (7.15), we get

$$\begin{cases} \dfrac{\sigma}{Va}\mathbf{u} = -\nabla p + R\theta\mathbf{k} - f(z)\mathcal{K}^{-1}\mathbf{u} \\ \nabla\cdot\mathbf{u} = 0 \\ \sigma\theta = Rw + \Delta\theta + H(\varphi-\theta) \\ A\sigma\varphi = \zeta\Delta_1\varphi + \varphi_{,zz} - H\gamma(\varphi-\theta) \end{cases} \tag{7.19}$$

In order to determine the critical threshold of the Rayleigh number for the onset of instability, we focus on the marginal state in (7.19). Accounting for the principle of exchange of stabilities, we set $\sigma = 0$ in (7.19) so that

$$\begin{cases} 0 = -\nabla p + R\theta\mathbf{k} - f(z)\mathcal{K}^{-1}\mathbf{u} \\ \nabla\cdot\mathbf{u} = 0 \\ 0 = Rw + \Delta\theta + H(\varphi-\theta) \\ 0 = \zeta\Delta_1\varphi + \varphi_{,zz} - H\gamma(\varphi-\theta) \end{cases} \tag{7.20}$$

By applying the double curl to $(7.20)_1$ and retaining only the third component, from (7.20) one gets:

$$\begin{cases} \xi R\Delta_1\theta - f'(z)w_{,z} - f(z)(\xi\Delta_1 w + w_{,zz}) = 0 \\ Rw + \Delta\theta + H(\varphi-\theta) = 0 \\ \zeta\Delta_1\varphi + \varphi_{,zz} - H\gamma(\varphi-\theta) = 0 \end{cases} \tag{7.21}$$

where prime denotes ordinary derivative with respect to z.

Because of periodicity of perturbations, unknown fields in (7.21) can be written as:

$$\varphi(x,y,z) = \sum_{n=1}^{+\infty} \bar{\varphi}_n(x,y,z) \qquad \forall\varphi\in\{w,\theta,\varphi\} \tag{7.22}$$

where

$$\Delta_1\bar{\varphi}_n = -a^2\bar{\varphi}_n \tag{7.23}$$

with $a^2 = a_x^2 + a_y^2$.

Now, let us substitute (7.22) in (7.21) and retain only the n-th component. Hence, by denoting $D \equiv \frac{d}{dz}$ and $D^2 \equiv \frac{d^2}{dz^2}$, (7.21) becomes

$$\begin{cases} \left(D^2 - \xi a^2\right) w_n + cDw_n = -f^{-1}(z)\xi a^2 R\theta_n \\ \left(D^2 - a^2 - H\right)\theta_n = -Rw_n - H\varphi_n \\ \left(D^2 - \zeta a^2 - H\gamma\right)\varphi_n = -H\gamma\theta_n \end{cases} \tag{7.24}$$

which will be solved subject to the boundary conditions

$$w = \theta = \varphi = 0 \qquad \text{on } z = 0,1. \tag{7.25}$$

System (7.24) represents an eigenvalue problem of ordinary differential equations, where R is the eigenvalue. Starting from (7.24) one can determine the function $\lambda(a^2)$ which describes how R depends on a^2. As consequence, the critical Rayleigh number for the onset of stationary instability is given by

$$R_L = \min_{a^2 \in \mathbb{R}^+} \lambda(a^2) \tag{7.26}$$

In order to solve the eigenvalue problem (7.24), we employ the Chebyshev-tau method coupled with the QZ algorithm. This numerical procedure takes advantage of the orthogonality of Chebyshev polynomials with respect to the scalar product

$$\langle f, g \rangle = \int_{-1}^{1} \frac{fg}{\sqrt{1-z^2}} dz \qquad f, g \in L^2(-1,1) \tag{7.27}$$

and many of their properties such as a recursive formula for multiplication between two polynomials, i.e.

$$2T_r T_q = T_{r+q} + T_{|r-q|} \tag{7.28}$$

We will not go into further details of this numerical method, but we are going to give the main ideas to carry out this procedure. For more details, interested readers can refer to [65, 97, 98, 99, 100].

Let T_k, $k \in \mathbb{N}$, the k-th Chebyshev polynomial. Solution of (7.24) can be expanded as finite series of Chebyshev polynomials, i.e.

$$w_n = \sum_{k=0}^{N+2} W_k T_k(z), \quad \theta_n = \sum_{k=0}^{N+2} \Theta_k T_k(z), \quad \varphi_n = \sum_{k=0}^{N+2} \Phi_k T_k(z) \tag{7.29}$$

We substitute (7.29) into (7.24) and then we take the inner product with T_k, $k = 0, \ldots, N$, on the weighted Chebyshev polynomial space. In such a way, we manage to write system (7.24) as a generalised eigenvalue problem

$$A\mathbf{x} = RB\mathbf{x} \tag{7.30}$$

where $\mathbf{x} = (W_0, W_1, \ldots, W_N, \Theta_0, \Theta_1, \ldots, \Theta_N, \Phi_0, \Phi_1, \ldots, \Phi_N)^T$,

$$A = \begin{pmatrix} D^2 - \xi a^2 I + cD & 0 & 0 \\ 0 & D^2 - (a^2 + H)I & HI \\ 0 & H\gamma I & D^2 - (\zeta a^2 + H\gamma)I \end{pmatrix} \tag{7.31}$$

and

$$B = \begin{pmatrix} 0 & -\xi a^2 F^* & 0 \\ -I & 0 & 0 \\ 0 & 0 & 0 \end{pmatrix} \tag{7.32}$$

being D^2, D the Chebyshev representation of $\frac{d^2}{dz^2}$ and $\frac{d}{dz}$, respectively, I the identity matrix and F^* the matrix representation of function $f^{-1}(z)$.

For coding purpose, we work with $k = 1, \ldots, N$. Then, the above matrices are $3N \times 3N$, and F^* is $N \times N$. When the exponential function $f^{-1}(z)$ can be well approximated by a second order polynomial, matrix F^* is computed by means of the following recursive formula

$$\begin{aligned}
&F^*_{i,i} = 1 + \frac{c}{2} + \frac{3c^2}{8}, \quad F^*_{i,i+1} = -\frac{c}{2}\left(1 + \frac{c}{2}\right), \\
&F^*_{i,i+2} = \frac{c^2}{8}, \qquad\qquad \text{for } i = 1, \ldots, N-2 \\
&F^*_{i,i-1} = -\frac{c}{2}\left(1 + \frac{c}{2}\right) \quad \text{for } i = 2, \ldots, N \\
&F^*_{i,i-2} = \frac{c^2}{8} \quad \text{for } i = 3, \ldots, N \\
&F^*_{2,1} = -c\left(1 + \frac{c}{2}\right), \quad F^*_{3,1} = \frac{c^2}{4}, \quad F^*_{2,2} = 1 + \frac{c}{2} + \frac{c^2}{2}
\end{aligned} \tag{7.33}$$

The eigenvalue problem (7.30)-(7.32) is then solved by the QZ algorithm which provides eigenvalues with no trouble. In Section 7.5 we show numerical results.

7.4 Optimal nonlinear stability result

This section is devoted to develop a nonlinear stability analysis for the conduction solution m_0, in order to determine sufficient condition for its stability.

We perform the scalar multiplication of $(7.10)_1$ by $\mathbf{u}$, $(7.10)_3$ by θ and $(7.10)_4$ by φ, and then we integrate over the periodicity cell V. The sum of the resulting equations can be written as

$$\frac{d}{dt}E(t) = RI - D \tag{7.34}$$

where

$$\begin{aligned}
&E(t) = \frac{\|\mathbf{u}\|^2}{2Va} + \frac{\|\theta\|^2}{2} + \frac{A\|\varphi\|^2}{2\gamma} \quad \text{Lyapunov Function} \\
&I(t) = 2(\theta, w) \quad \text{Production term} \\
&D(t) = \|\nabla\theta\|^2 + H\|\theta - \varphi\|^2 + \frac{\zeta}{\gamma}\|\nabla_1\varphi\|^2 + \frac{1}{\gamma}\|\varphi_{,z}\|^2 \\
&+ \int_V \left(f(z)\frac{u^2}{\xi} + f(z)\frac{v^2}{\xi} + f(z)w^2\right) dV \quad \text{Dissipation term}
\end{aligned} \tag{7.35}$$

Starting with (7.34), by defining

$$\frac{1}{R_E} = \max_{\mathcal{H}} \frac{I}{D} \tag{7.36}$$

where

$$\mathcal{H} = \{(\mathbf{u},\theta,\varphi) \ : \ w=\theta=\varphi=0 \text{ on } z=0,1; \text{ periodic in } x \text{ and } y \\ \text{directions, with period } \frac{2\pi}{a_x}, \frac{2\pi}{a_y} \text{ respectively; } \nabla\cdot\mathbf{u}=0; \ D<\infty\}, \tag{7.37}$$

we obtain

$$\frac{dE}{dt} = -D\left(1-R\frac{I}{D}\right) \leq -D\left(1-\frac{R}{R_E}\right) \tag{7.38}$$

By employing the Poincaré inequality in $(7.35)_3$, we get

$$D(t) \geq \pi^2\|\theta\|^2 + \frac{\pi^2\zeta^*}{\gamma}\|\varphi\|^2 + \xi^* e^{-\frac{c}{2}}\|\mathbf{u}\|^2 \tag{7.39}$$

being $\xi^* = \min\{1,\xi^{-1}\}$ and $\zeta^* = \min\{1,\zeta\}$. Hence, (7.38)-(7.39) yield the exponential decay of the energy function $E(t)$. In fact, by virtue of (7.39), inequality (7.38) becomes

$$\begin{aligned} \frac{dE}{dt} &\leq -\left(1-\frac{R}{R_E}\right)\left(\pi^2\|\theta\|^2 + \frac{\pi^2\zeta^*}{\gamma}\|\varphi\|^2 + \xi^* e^{-\frac{c}{2}}\|\mathbf{u}\|^2\right) \\ &\leq -\left(1-\frac{R}{R_E}\right) kE(t) \end{aligned} \tag{7.40}$$

where $k = \min\left\{2\pi^2, \frac{2\pi^2\zeta^*}{A}, 2\xi^* e^{-\frac{c}{2}} Va\right\}$, from which

$$E(t) \leq \exp\left\{-k\left(1-\frac{R}{R_E}\right)t\right\} \tag{7.41}$$

By virtue of (7.41), as long as $R < R_E$, perturbation fields on seepage velocity, fluid and solid temperature decay exponentially in time. Thus, we have proved that $R < R_E$ is a sufficient condition for the global nonlinear and exponential stability of the conduction solution m_0.

Now, let us proceed to determine the critical threshold R_E. With this aim, we write the Euler-Lagrange equations by solving the variational problem (7.36), i.e.

$$\begin{cases} R_E\theta\mathbf{k} - \left(f\frac{u}{\xi}, f\frac{v}{\xi}, fw\right) = \nabla\omega \\ R_E w + \Delta\theta + H(\varphi-\theta) = 0 \\ \zeta\Delta_1\varphi + \varphi_{,zz} - H\gamma(\varphi-\theta) = 0 \end{cases} \tag{7.42}$$

where ω is a Lagrange multiplier arising from the incompressibility of $\mathbf{u}$. System (7.42) coincides with (7.20). As consequence, we manage to obtain the coincidence between the global nonlinear stability threshold R_E and the linear instability threshold R_L. As a result, condition $R < R_E$ is not only sufficient, but also necessary for the stability of m_0.

7.5 Numerical results

In the present section, we report results obtained once the generalised eigenvalue problem (7.30) and the subsequent minimum problem (7.26) have been solved. Given the coincidence between linear and nonlinear threshold, we denote by R_c^2 the critical Rayleigh number beyond which thermal convection occurs.

The aim of this section is to highlight the influence of variable viscosity, thermal and mechanical anisotropy, weighted conductivity ratio and interaction coefficient on the onset of convection. Let us remark that, since the interaction heat transfer coefficient H cannot be easily measured, we set a range in which H can vary. According to the choice done in [90, 27], $H \in (10^{-2}, 10^6)$. As consequence, the critical Rayleigh number is plotted as function of H in every picture throughout the section.

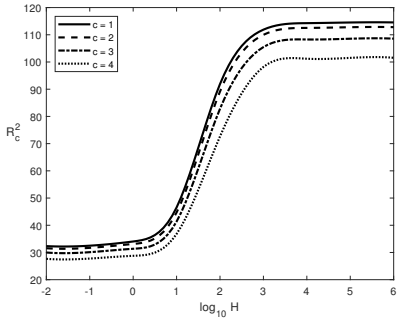

Figure 7.2: Critical Rayleigh number as function of H for different values of c with $\xi = 1.5, \zeta = 5, \gamma = 1$.

	[60]		$H \to \infty$	
c	$a_c^2([60])$	$R_c^2([60])$	a_c^2	$\frac{R_c^2\gamma}{\gamma+1}$
0	9.873	39.478	9.87	39.478
1	10.104	39.220	10.10	39.226
2	10.826	38.357	10.84	38.419
3	12.172	36.681	12.17	36.699
4	14.326	34.005	14.33	34.048
5	17.608	30.336	17.58	30.357

Table 7.1: Comparison between the critical wavenumber $a_c^2([60])$ and the critical threshold $R_c^2([60])$ shown in Table 3 in [60] and the critical wavenumber a_c^2 and the rescaled critical threshold $\frac{R_c^2\gamma}{\gamma+1}$ obtained in the present paper when $H \to \infty$, $\gamma = 1, \xi = 1, \zeta = 1$.

It may be observed that the effect of variable viscosity on the critical Rayleigh number is substantial. As shown in Figure 7.2, as c increases, R_c^2 decreases for

	$H \to \infty$		$H = 100$	
c	a_c^2	$\frac{R_c^2\gamma}{\gamma+1}$	a_c^2	R_c^2
0	9.87	39.478	10.70	72.34
1	10.10	39.226	10.99	71.75
2	10.84	38.419	11.96	70.07
3	12.17	36.699	13.72	66.00
4	14.33	34.048	17.03	60.11
5	17.58	30.357	22.64	52.21

Table 7.2: Comparison between the critical wavenumber a_c^2 and the rescaled critical threshold $\frac{R_c^2\gamma}{\gamma+1}$ obtained when $H \to \infty$ (i.e. LTE regime) and the critical wavenumber a_c^2 and the critical threshold R_c^2 obtained when $H = 100$ (i.e. LTNE regime), with $\gamma = 1, \xi = 1, \zeta = 1$.

every choice of the interaction coefficient H, namely the onset of convection gets easier. This result is physically reasonable and in agreement with what stated in [64], i.e. fluids whose viscosity near the hot boundary is lower than everywhere else in the layer are more likely to become unstable sooner.

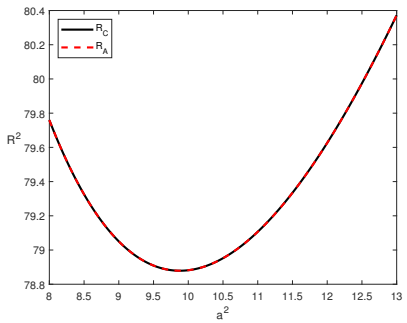

Figure 7.3: Comparison between neutral stability curve R_C (black line) obtained via Chebyshev-tau method set $c = 0$ and neutral stability curve R_A (red dashed line) obtained analytically in [101], where $\xi = 1, \zeta = 1, H = 10^4, \gamma = 1$.

Let us remark that, as $H \to \infty$, fluid and solid phases can be treated as a single phase since they exchange heat so rapidly that they have nearly identical temperature. As consequence, we recover the regime of LTE. Whereas, when $H \to 0$, fluid instability is not affected by the properties of the solid matrix. As pointed out in [12], the respective mathematical problem are identical, except for a rescaling of the Rayleigh number. Table 7.1 shows the coincidence between results delivered in [60] under the assumption of LTE and results obtained in the present paper for $H \to \infty$, after rescaling the Rayleigh number. In addition, one can notice that in

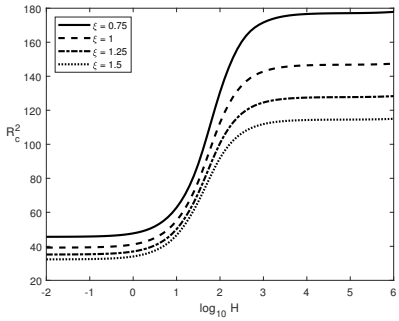

Figure 7.4: Critical Rayleigh number as function of H for different values of ξ with $c = 1, \zeta = 5, \gamma = 1$.

the first line in Table 7.1, where $c = 0$, we recovered the classical Rayleigh number $4\pi^2$ for the Darcy-Benard problem.

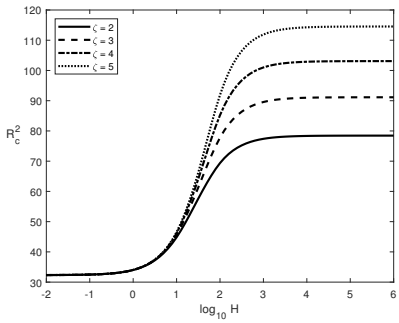

Figure 7.5: Critical Rayleigh number as function of H for different values of ζ with $c = 1, \xi = 1.5, \gamma = 1$.

The decreasing trend of R_c^2 with respect to increasing c, i.e. a higher gradient of viscosity across the layer, depends strongly on H. So, we analyse the behaviour of R_c^2 both for high values of H (for which the LTE regime holds [12]) and for $H = 100$ (for which the LTNE regime holds). In Table 7.2 one can notice that the decreasing trend of R_c^2 is less remarkable for $H \to \infty$ rather than for $H = 100$, even though the critical threshold for the LTE case is always lower than the one in LTNE. Such a result suggests that the effect of variable viscosity on the onset of convection is less intense under the assumption of LTE rather than in the case of LTNE. Similar result has been pointed out in [9].

When $c = 0$, function $f(z) = 1$, i.e. viscosity is constantly equal to μ_0, the value assumed in the middle of the layer. In case of isotropic porous medium, by assuming $c = 0$ we would expect to recover the same results found in [101]. In Figure 7.3 we compare results delivered in the present paper by the Chebyshev-tau method with the analytical expression of the critical Rayleigh number found in

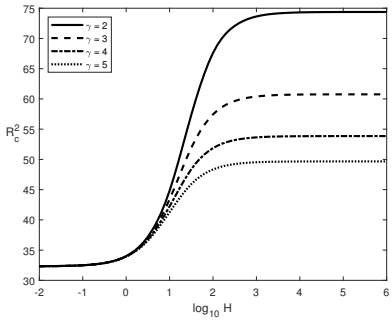

Figure 7.6: Critical Rayleigh number as function of H for different values of γ with $c = 1, \xi = 1.5, \zeta = 5$.

[101]. The two neutral curves are perfectly overlapped. In fact, one can compute the absolute error, which is 1.85×10^{-10} at the most.

In Figure 7.4, the influence of mechanical anisotropy on the critical Rayleigh number is shown. The destabilising effect of increasing permeability on the conduction solution is clear. The Rayleigh number decreases with ξ for any H, in agreement with findings in [90, 27, 14, 102]. This result is physically admissible. Based on definition $(7.2)_1$, increasing ξ is due to an increase in the horizontal permeability K_H, which means that the fluid is allowed to move easier and easier in the horizontal direction. Thus, resistance to fluid motion reduces and the advective transport enhances [26].

On the other hand, solid thermal conductivity has a stabilising effect on m_0, delaying the onset of convection. In Figure 7.5 such a behaviour is evident, specifically for large values of H. If κ_H^s grows, the onset of convection is delayed because the solid matrix easily absorbs heat from the fluid. Actually, when H goes to zero, solid thermal conductivity affects weakly the onset of convection. This result is in agreement with what is found in [90] and it is physically reasonable since small values of H imply that the heat exchange between fluid and solid phases occurs so slowly that the solid matrix does not manage to absorb enough heat to cool down the fluid.

The onset of convection is encouraged by increasing values of the weighted conductivity ratio γ, as shown in Figure 7.6. Increasing values of κ_f lead to an increasing γ, which imply a reduction of R_c^2, i.e. a destabilising effect. This behaviour is expected from a mathematical point of view, since looking at the Rayleigh number definition in $(7.11)_4$ we can notice that R^2 is inversely proportional to κ_f.

7.6 Conclusions

A qualitative study of the onset of convection in a depth-dependent viscosity fluid saturating an anisotropic porous medium in LTNE is performed. A Vadasz-Darcy

model is employed to describe the fluid motion for the problem at stake. We performed the linear instability analysis of the conduction solution as first approach to the problem. That analysis yielded a generalised eigenvalue problem which was solved by means of the Chebyshev-tau method coupled with the QZ algorithm. The energy method has been employed to study the nonlinear stability of the basic state. The optimal result of coincidence between the linear instability threshold and the global nonlinear stability threshold is obtained.

Viscosity decreasing exponentially with depth has a destabilising effect on the onset of convection, leading to lower values of the critical Rayleigh number. In fact, viscosity drag reduces with depth, namely the fluid meets fewer obstacles to its motion. Moreover, comparing results with those ones found under LTE assumption in [60], we can remark that the presence of LTNE makes the influence of variable viscosity more intense. Applications can be found in oil cooling systems in hydraulic units that involve heat exchangers. Within the heat exchanger, maintaining the oil cold is important in order to preserve its characteristics and proper operating conditions. Findings in the chapter show that the effect on the onset of convection of replacing a kind of oil with another with a different law of viscosity is greater under the LTNE hypothesis than under the LTE one. A practical example is given by two oils, i.e. SAE 10W-60 and SAE 0W-30, whose values of kinematic viscosity ν are shown in Table (see [103]). If the aim is to inhibit convection, a greater Rayleigh number is achieved if SEA 0W-30 is preferred to SAE 10W-60.

$T[^\circ C]$	$\nu_{\text{SAE 10W-60}}[mm^2/s]$	$\nu_{\text{SAE 0W-30}}[mm^2/s]$
0	1684.4	550.23
10	831.44	291.93
20	448.10	167.29
40	161.73	66.803

Furthermore, we proved the destabilising effect of both mechanical anisotropy and the weighted conductivity ratio, other than the stabilising effect of thermal anisotropy.

Conclusions

In the present thesis, we took a journey through some main problems of thermal instability in porous media. The undertaken qualitative studies aim to determine the critical value for the characteristic dimensionless parameter (Raylegih number) that captures the physics of the problem. In addition, our aim was to assess the dependence of the critical Rayleigh number on parameters characterising the models. To first approach a stability analysis of the basic steady solution, we performed a linear analysis, which gives information about the fate of small-amplitude disturbances. We managed to obtain the critical threshold of the Rayleigh number for the onset of convection either analytically or via numerical schemes. Specifically, we implemented and employed the Chebyshev-tau method or the shooting method to solve the differential eigenvalue problem arising from the linear analysis. In addition, in order to obtain a sufficient condition for the stability of the steady solution, we needed to perform a nonlinear analysis. This study involves a Lyapunov functional and takes advantage of the Direct Method of Calculus of Variations that ensures the existence of maximum of a functional. Via nonlinear stability analysis, we determined the critical Rayleigh number R_E such that the condition $R < R_E$ is sufficient for the nonlinear stability of the conduction solution. The optimal result that one could get in this respect is the coincidence between the linear and nonlinear thresholds. In case the coincidence is not achieved, a subcritical instability region exists, where we cannot say anything about the future behaviour of perturbations. In the second chapter, with the aid of the weakly nonlinear analysis, we were able to determine under which conditions subcritical instability may occur for the problem at stake. Specifically, we studied the onset of convection in a fluid saturating a horizontal porous layer subject to a downward net mass flow (throughflow). The strength of the throughflow in the dimensionless version is modelled by the Péclet number Pe. We proved the stabilising effect of the downward throughflow on the onset of instability and we determined the threshold for Pe beyond which subcritical instability may occur.

The majority of the thesis is devoted to investigate the onset of convection in porous media under the hypothesis of local thermal nonequilibrium (LTNE). According to this assumption, two different temperatures are defined (one for the fluid phase, one for the solid matrix) implying that two energy balance equations are

needed to close the system involving the Darcy's law and the continuity equation. The LTNE assumption has been widely employed over the last years ever since Banu and Rees [12] studied the problem for the first time.

Throughout the doctoral program, starting from [12], we tried to cover as much as possible a good variety of physical set-ups where thermal convection in porous media may be modelled in LTNE regime. Models studied in the thesis arise to describe practical industrial and engineering situations. Indeed, in these contexts, one aims to remove or storage heat by managing the onset of convection. Ways to achieve this aim involve the usage of man-made porous media that either exhibit anisotropy in mechanical and/or thermal features or are subject to external mechanical agents such as rotations or suctions. More in detail, we have shown how permeability and thermal conductivity of the medium that depend on the direction affect the onset of thermal convection. In particular, we have noticed that horizontal isotropic permeability favours the onset of convection facilitating the fluid motion in the horizontal direction and resulting in wider convective cells. On the other hand, anisotropic thermal conductivity has the opposite effect, given that heat in the fluid is dispersed and absorbed more easily in the solid matrix. Nevertheless, wider periodicity cells arise within the fluid.

As far as anisotropic porous medium is concerned, we studied also the case when permeability and thermal conductivity change value depending on the three directions (full anisotropy). In this setting, when convection takes place, we found that the fluid is divided in so-called convective rolls aligned in x or y directions depending on the ratio between anisotropy parameters. Hence, we proved that full anisotropy leads to bi-dimensional fluid motion.

Moreover, we studied the occurrence of thermal convection in rotating porous media that find many applications in rotating machinery. The action of rotation is described mostly by the Coriolis force that affects the fluid motion in the horizontal direction. Indeed, in our models we proved mathematically the delaying effect of rotation on the onset of convection.

Very interesting topics have been touched when the Cattaneo's law is employed to describe the heat transfer in the solid matrix and when a depth-dependent viscosity fluid saturates the porous medium. The former assumption has been proved to lead to the possibility for oscillatory convection to occur. We proved analytically that steady convection is not affected by the introduction of the thermal inertia term, while oscillatory convection is favoured when the weight of this parameter increases. The latter assumption on the fluid viscosity results in a more easily occurrence of thermal convection. Indeed, we proved that convective cells are more likely to arise in a fluid whose viscosity decreases significantly with temperature.

Bibliography

[1] D. A. Nield and A. Bejan. *Convection in Porous Media*. Springer, New York, 2013.

[2] C. Horton and F. Rogers. Convection Currents in a Porous Medium. *J. of Applied Physics*, 16:367–370, 1945.

[3] E. Lapwood. Convection of a Fluid in a Porous Medium. *Mathematical Proceedings of the Cambridge Philosophical Society*, 44:508–521, 1948.

[4] D. A. S. Rees. The onset of Darcy–Brinkman convection in a porous layer: an asymptotic analysis. *Int. J.of Heat and Mass Transf.*, 45:2213–2220, 2002.

[5] R.A. Wooding. Rayleigh instability of a thermal boundary layer in flow through a porous medium. *J. Fluid Mech.*, 9(2):183–192, 1960.

[6] F.M. Sutton. Onset of convection in a porous channel with net through flow. *Physics of Fluids*, 13(8):1931, 1970.

[7] D. B. Ingham and I. Pop. *Transport Phenomena in Porous Media*. Elsevier, Amsterdam, 2005.

[8] D. A. S. Rees, A. P. Bassom, and P. G. Siddheshwar. Local thermal non-equilibrium effects arising from the injection of a hot fluid into a porous medium. *J. Fluid Mech.*, 594:379–398, 2008.

[9] I. S. Shivakumara, A. L. Mamatha, and M. Ravisha. Effects of variable viscosity and density maximum on the onset of darcy-benard convection using a thermal nonequilibrium model. *Journal of Porous Media*, 13(7):613–622, 2010.

[10] A. M. Hayes, J. A. Khan, A. H. Shaaban, and I. G. Spearing. The thermal modeling of a matrix heat exchanger using a porous medium and the thermal non-equilibrium model. *Int. J. Thermal Sciences*, 47(10):1306–1315, 2008.

[11] B. Straughan. *Convection with Local Thermal Non-equilibrium and Microfluidic Effects*. Springer, 2015.

[12] N. Banu and D. A. S. Rees. Onset of Darcy–Bénard convection using a thermal non-equilibrium model. *Int. J. Heat Mass Transfer*, 45:2221–2228, 2002.

[13] B. Straughan. Global nonlinear stability in porous convection with a thermal nonequilibrium model. *Proc. R. Soc. A*, 462:409–418, 2006.

[14] M. S. Malashetty, I. S. Shivakumara, and S. Kulkarni. The onset of convection

in an anisotropic porous layer using a thermal non-equilibrium model. *Trans. Porous Media*, 60:199–215, 2005.

[15] M. S. Malashetty and M. Swamy. Effect of rotation on the onset of thermal convection in a sparsely packed porous layer using a thermal non-equilibrium model. *Int. J. Heat Mass Transfer*, 53:3088–3101, 2010.

[16] I. S. Shivakumara, J. Lee, A. L. Mamatha, and M. Ravisha. Boundary and thermal non-equilibrium effects on convective instability in an anisotropic porous layer. *Journal of Mechanical Science and Technology*, 25 (4):911–921, 2011.

[17] F. Capone and M. Gentile. Sharp stability results in LTNE rotating anisotropic porous layer. *Int. J. Therm. Sci.*, 134:661–664, 2018.

[18] R. N. Dayananda and I. S. Shivakumara. Impact of Thermal Non-equilibrium on Weak Nonlinear Rotating Porous Convection. *Transp. Porous Media*, 130:819–845, 2019.

[19] P. M. Patil and D. A. S. Rees. Linear Instability of a Horizontal Thermal Boundary Layer Formed by Vertical Throughflow in a Porous Medium: The Effect of Local Thermal Nonequilibrium. *Transp Porous Media*, 99:207–227, 2013.

[20] R. Freitas, P. V. Brandão, L.S. de B. Alves, M. Celli, and A. Barletta. The effect of local thermal non-equilibrium on the onset of thermal instability for a metallic foam. *Physics of Fluids*, 34:034105, 2022.

[21] M. Celli, A. Barletta, and D. A. S. Rees. Local thermal non-equilibrium analysis of the instability in a vertical porous slab with permeable sidewalls. *Transport in Porous Media*, 119(3):539–553, 2017.

[22] M. N. Ouarzazi, S. C. Hirata, A. Barletta, and M. Celli. Finite amplitude convection and heat transfer in inclined porous layer using a thermal non-equilibrium mode. *Int. J. Heat Mass Tran.*, 113:399–410, 2017.

[23] A. Barletta and D. A. S. Rees. Local thermal non-equilibrium analysis of the thermoconvective instability in an inclined porous layer. *International Journal of Heat and Mass Transfer*, 83:327–336, 2015.

[24] N. L. Scott and B. Straughan. A nonlinear stability analysis of convection in a porous vertical channel including local thermal nonequilibrium. *J. Math. Fluid Mech.*, 13:1–10, 2013.

[25] D. A. S. Rees. The effect of local thermal non-equilibrium on the stability of convection in a vertical porous channel. *Transp. Porous Media*, 87:459–464, 2011.

[26] D. R. Hewitt. Vigorous convection in porous media. *Proc. R. Soc. A*, 476, 2020.

[27] S. Govender and P. Vadasz. The effect of mechanical and thermal anisotropy on the stability of gravity driven convection in rotating porous media in the presence of thermal non-equilibrium. *Transp Porous Media*, 69:55–66, 2007.

[28] L. Storesletten. Effects of anisotropy on convection in horizontal and inclined porous layers. *Emerging Technologies and Techniques in Porous Media*, 134:285–306, 2004.

[29] P. A. Tyvand and L. Storesletten. Onset of convection in an anisotropic porous layer with vertical principal axes. *Transport in Porous Media*, 108(3):581–593, 2015.

[30] L. Storesletten and D. A. S. Rees. An analytical study of free convective boundary layer flow in porous media: The effect of anisotropic diffusivity. *Transport in Porous Media*, 27:289–304, 1997.

[31] F. Capone, M. Gentile, and A. A. Hill. Convection problems in anisotropic porous media with nonhomogeneous porosity and thermal diffusivity. *Acta Applicandae Mathematicae*, 122(1):85–91, 2012.

[32] F. Capone, M. Gentile, and A. A. Hill. Anisotropy and symmetry in porous media convection. *Acta Mechanica*, 208(3-4):205–214, 2009.

[33] G. Castinel and M. Combarnous. Critère d'apparition de la convection naturelle dans une couche poreuse anisotrope horizontale. *C. R. Acad. Sci. Paris B*, 278:701–704, 1975.

[34] J. F. Epherre. Critere d'apparition de la convection naturelle dans une couche poreuse anisotrope. *Int. J. of Thermal Sciences*, 14(168):949–950, 1975.

[35] O. Kvernvold and P. A. Tyvand. Nonlinear thermal convection in anisotropic porous media. *J. Fluid Mech.*, 90:609–634, 1979.

[36] C. Cattaneo. Sulla conduzione del calore. *Atti Semin. Mat. Fis. della Università di Modena*, 3:3, 1948.

[37] D. D. Joseph and L. Preziosi. Heat Waves. *Review of Modern Physics*, 61(1):41–73, 1989.

[38] N. J. Pilgrim, W. Batty, R. W. Kelsall, and C. M. Snowden. Nanoscale electrothermal co-simulation: compact dynamicmodels of hyperbolic heat transport and self-consistent device Monte Carlo. *Microelectron. J.*, 35:823–830, 2004.

[39] T. Ruggeri and I. Muller. *Rational Extended Thermodynamics*. Springer, 1998.

[40] T. Ruggeri and M. Sugiyama. *Classical and Relativistic Rational Extended Thermodynamics of Gases*. Springer, 2021.

[41] T. Ruggeri. Can constitutive relations be represented by non-local equations? *Quarterly of Applied Mathematics LXX*, 3:597–611, 2012.

[42] B. Straughan and F. Franchi. Benard convection and the Cattaneo law of heat conduction. *Proceedings of the Royal Society of Edinburgh*, 96A:175–178, 1984.

[43] B. Straughan. Porous convection with Cattaneo heat flux. *Int. J. Heat Mass Transf.*, 53:2808–2812, 2010.

[44] F. Capone and J. A. Gianfrani. Onset of convection in LTNE Darcy–Brinkman anisotropic porous layer: Cattaneo effect in the solid. *Int.*

J. of Non-Linear Mech., 139:103889, 2022.

[45] B. Straughan. Exchange of stability in Cattaneo–LTNE porous convection. *Int. J. of Heat and Mass Transf.*, 89:792–798, 2015.

[46] B. Straughan. Porous convection with local thermal non-equilibrium temperatures and with Cattaneo effects in the solid. *Proc. R. Soc. A*, 469:20130187, 2013.

[47] M. Hema, I. S. Shivakumara, and M. Ravisha. Double diffusive LTNE porous convection with Cattaneo effects in the solid. *Heat Transfer*, 49(6):3613–3629, 2020.

[48] M. Hema and I. S. Shivakumara. Impact of Cattaneo law of heat conduction on an anisotropic Darcy-Bénard convection with a local thermal nonequilibrium model. *Thermal Science and Engineering Progress*, 2020.

[49] I. S. Shivakumara, M. Ravisha, CO Ng, and V. L. Varun. A thermal nonequilibrium model with Cattaneo effect for convection in a Brinkman porous layer. *Int. J. Non-Linear Mech.*, 2015.

[50] F. Capone and R. De Luca. The effect of the Vadasz number on the Onset of Thermal Convection in Rotating Bidispersive Porous Media. *Fluids*, 5(4):173, 2020.

[51] F. Capone, R. De Luca, and M. Gentile. Coriolis effect on thermal convection in a rotating bidispersive porous layer. *Proceedings of the Royal Society A: Mathematical, Physical and Engineering Sciences*, 476(2235), 2020.

[52] S. Govender. Coriolis effect on the stability of centrifugally driven convection in a rotating anisotropic porous layer subjected to gravity. *Transport in porous media*, 67(2):219–227, 2007.

[53] E. Palm and P. A. Tyvand. Thermal convection in a rotating porous layer. *J. of Applied Mathematics and Physics (ZAMP)*, 35, 1984.

[54] P. Vadasz. Coriolis effect on gravity-driven convection in a rotating porous layer heated from below. *Journal of Fluid Mechanics*, 376:351–375, 1998.

[55] P. Vadasz. Heat transfer and fluid flow in rotating porous media. In *Developments in Water Science*, volume 47, pages 469–476. Elsevier, 2002.

[56] P. Vadasz. *Fluid flow and heat transfer in rotating porous media*. Springer, 2016.

[57] P. Vadasz. Instability and convection in rotating porous media: A review. *Fluids*, 4(3):147, 2019.

[58] K. E. Torrance and D. L. Turcotte. Thermal convection with large viscosity variations. *J. Fluid Mech.*, 47 (1):113–125, 1971.

[59] L. Richardson and B. Straughan. A nonlinear energy stability analysis of convection with temperature dependent viscosity. *Acta Mechanica*, 97:41–49, 1993.

[60] B. Straughan. Stability Criteria for Convection with Large Viscosity Variations. *Acta Mechanica*, 61:59–72, 1986.

[61] D. R. Kassoy and A. Zebib. Variable viscosity effects on the onset of convection in porous media. *Physics of Fluids*, 18:1649, 1975.

[62] J. R. Booker. Thermal convection with strongly temperature-dependent viscosity. *J. of Fluid Mech.*, 76(4):741–754, 1976.

[63] P. J. Tackley. Effects of strongly variable viscosity on three-dimensional compressible convection in planetary mantles. *J. of Geophysical Research*, 101:3311–3333, 1996.

[64] J. M. Straus and G. Schubert. Thermal Convection of Water in a Porous Medium: Effects of Temperature- and Pressure-Dependent Thermodynamic and Transport Properties. *Journal of Geophysical Research*, 82 (2), 1977.

[65] B. Straughan. *The Energy Method, Stability and Nonlinear Convection*. Springer, New York, 2004.

[66] D. D. Joseph. Variable Viscosity Effects on the Flow and Stability of Flow in Channels and Pipes. *Physics of Fluids*, 7:1761, 1964.

[67] E. Palm, T. Ellingsen, and B. Gjevik. On the occurrence of cellular motion in Bénard convection. *J. of Fluid Mech.*, 30(4):651–661, 1967.

[68] K. R. Rajagopal, G. Saccomandi, and L. Vergori. Stability analysis of the Rayleigh–Bénard convection for a fluid with temperature and pressure dependent viscosity. *Zeitschrift für angewandte Mathematik und Physik volume*, 60:739–755, 2009.

[69] B. Straughan. Sharp global nonlinear stability for temperature-dependent viscosity convection. *Proc. R. Soc. Lond. A*, 458:1773–1782, 2002.

[70] J. I. Diaz and B. Straughan. Global stability for convection when the viscosity has a maximum. *Continuum Mechanics and Thermodynamics*, 16(4):347–352, 2004.

[71] F. Capone and M. Gentile. Nonlinear stability analysis of convection for fluids with exponentially temperature-dependent viscosity. *Acta Mechanica*, 107:53–64, 1994.

[72] F. Capone and M. Gentile. Nonlinear stability analysis of the Bénard problem for fluids with a convex nonincreasing temperature depending viscosity. *Continuum Mechanics and Thermodynamics volume*, 7:297–309, 1995.

[73] S. Thangam and C. F. Chen. Stability analysis on the convection of a variable viscosity fluid in a infinite vertical slot. *Physics of Fluids*, 29:1367, 1986.

[74] L. E. Payne and B. Straughan. Unconditional Nonlinear Stability in Temperature-Dependent Viscosity Flow in a Porous Medium. *Studies in Applied Mathematics*, 105:59–81, 2000.

[75] L. Richardson and B. Straughan. Convection with temperature dependent viscosity in a porous medium: nonlinear stability and the Brinkman effect. *Atti della Accademia Nazionale dei Lincei. Classe di Scienze Fisiche, Matematiche e Naturali. Rendiconti Lincei. Matematica e Applicazioni, Serie 9*, 3:223–230, 1993.

[76] J. N. Flavin and S. Rionero. *Qualitative estimates for partial differential equations: an introduction*. CRC Press, Florida, 1996.

[77] G. P. Galdi and S. Rionero. *Weighted Energy Methods in Fluid Dynamics and Elasticity*. Springer, Berlin, 1985.

[78] G. J. M. Pieters and C. J. Van Duijn. Transient growth in linearly stable gravity-driven flow in porous media. *European Journal of Mechanics-B/Fluids*, 25(1):83–94, 2006.

[79] D. A. S. Rees and A. Mojtabi. The effect of conducting boundaries on weakly nonlinear Darcy–Bénard convection. *Transport in Porous Media*, 88(1):45–63, 2011.

[80] D. A. S. Rees and A. Barletta. Three-dimensional convective planforms for inclined Darcy–Bénard convection. *Fluids*, 5(2):83, 2020.

[81] D. A. S. Rees and A. P. Bassom. The inclined Wooding problem. *Transp. Porous Media*, 125:465–482, 2018.

[82] E. Palm, J. E. Weber, and O. Kvernold. On steady convection in a porous medium. *J. of Fluid Mech.*, 54:153–161, 1972.

[83] B. Bidin and D. A. S. Rees. Pattern selection for Darcy–Bénard convection with local thermal nonequilibrium. *Int. J. of Heat and Mass Transf.*, 153:119539, 2020.

[84] P.G. Drazin. *Introduction to Hydrodynamic Stability*. Cambridge University Press, 2002.

[85] D. A. S. Rees. The onset and nonlinear development of vortex instabilities in a horizontal forced convection boundary layer with uniform surface suction. *Transp. Porous Media*, 77:243–265, 2009.

[86] F. Capone, M. Gentile, and J. A. Gianfrani. Optimal Stability Thresholds in Rotating Fully Anisotropic Porous Medium with LTNE. *Transp. Porous Media*, 139:185–201, 2021.

[87] S. Chandrasekhar. *Hydrodynamic and hydromagnetic stability*. Courier Corporation, 2013.

[88] B. Straughan. Anisotropic bidispersive convection. *Proceedings of the Royal Society A: Mathematical, Physical and Engineering Sciences*, 475(2227), 2019.

[89] P. A. Tyvand and L. Storesletten. Onset of convection in an anisotropic porous medium with oblique principal axes. *J. Fluid Mech.*, 226:371–382, 1991.

[90] F. Capone and J. A. Gianfrani. Thermal convection for a Darcy-Brinkman rotating anisotropic porous layer in local thermal non-equilibrium. *Ricerche di Matematica*, 2021.

[91] I. S. Shivakumara, A. L. Mamatha, and M. Ravisha. Local thermal non-equilibrium effects on thermal convection in a rotating anisotropic porous layer. *Applied Mathematics and Computation*, 259:838–857, 2015.

[92] M. S. Malashetty, M. Swamy, and S. Kulkarni. Thermal convection in a rotating porous layer using a thermal nonequilibrium model. *Physics of Fluids*,

19:054102, 2007.

[93] N. C. Papanicolaou, C. I. Christov, and P. M. Jordan. The influence of thermal relaxation on the oscillatory properties of two-gradient convection in a vertical slot. *Eur. J. Mech. B Fluids*, 30:68–75, 2011.

[94] M. S. Malashetty, I. S. Shivakumara, and S. Kulkarni. The onset of Lapwood–Brinkman convection using a thermal non-equilibrium model. *Int. J. Heat and Mass Transfer*, 48:1155–1163, 2005.

[95] A. Postelnicu and D. A. S. Rees. The onset of Darcy–Brinkman convection in a porous layer using a thermal nonequlibrium model-part i: stress-free boundaries. *Int. J. Energy Res.*, 27:961–973, 2003.

[96] F. Capone and J. A. Gianfrani. Natural convection in a fluid saturating an anisotropic porous medium in LTNE: effect of depth-dependent viscosity. *Acta Mechanica*, pages 1–14, 2022.

[97] J. J. Dongarra, B. Straughan, and D. W. Walker. Chebyshev tau-QZ algorithm methods for calculating spectra of hydrodynamics stability problems. *Applied Numerical Mathematics*, 22:399–434, 1996.

[98] B. Straughan and D. W. Walker. Two very accurate and efficient methods for computing eigenvalues and eigenfunctions in porous convection problems. *J. Comput. Phys.*, 127:128–141, 1996.

[99] D. Bourne. Hydrodynamic stability, the Chebyshev tau method and spurious eigenvalues. *Continuum Mech. Thermodyn.*, 15:571–579, 2003.

[100] F. Capone, M. Gentile, and A. A. Hill. Penetrative convection in a fluid layer with throughflow. *Ricerche Mat.*, 57:251–260, 2008.

[101] D. A. S. Rees and I. Pop. Local thermal nonequilibrium in porous medium convection. *Transport Phenomena in Porous Media III (ed. Ingham, Pop)*, pages 147–173, 2005.

[102] A. Barletta and M. Celli. Effects of anisotropy on the transition to absolute instability in a porous medium heated from below. *Physics of Fluids*, 34:024105, 2022.

[103] Anton Paar. Viscosity of engine oil. https://wiki.anton-paar.com/it-it/olio-motore/, 2022.